

Concentration and derivatisation in silicone rubber traps for  
gas chromatographic trace analysis of aldehydes

**Concentration and derivatisation in silicone rubber traps for  
gas chromatographic trace analysis of aldehydes**

MARIA JOSÉ FERNANDES

BY

**MARIA JOSÉ FERNANDES**

Submitted in partial fulfilment of the requirements for the degree of

**Master of Science**

**Chemistry**

in the Faculty of Natural & Agricultural Science

University of Pretoria

Pretoria

July 2001

# **Concentration and derivatisation in silicone rubber traps for gas chromatographic trace analysis of aldehydes**

BY

**MARIA JOSÉ FERNANDES**

Promoter

Prof Dr E R Rohwer

Submitted in partial fulfilment of the requirements for the degree of MSc, Chemistry  
in the Faculty of Natural & Agricultural Science

University of Pretoria

Pretoria

South Africa

## **SUMMARY**

Low molecular mass aldehydes, such as formaldehyde (HCHO) and acrolein, are introduced into the environment through incomplete fuel combustion and tobacco smoke. Indoors, formaldehyde is emitted mainly by Urea Formaldehyde (UF)-resin treated furniture. These aldehydes have long been suspected carcinogens and for this reason several methods exist to monitor them. The methods that can most effectively and selectively pre-concentrate aldehydes involve in-situ derivatisation. Unfortunately, the derivatising agents as well as their associated solvents or adsorbents, are responsible for problems encountered with these methods. A

recently developed method using Solid Phase MicroExtraction (SPME), introduced polydimethylsiloxane as the absorbent for the derivatising agent, with promising results. However, this method is not ideal for field sampling.

In our study, the use of the silicone rubber trap, developed in our laboratory, as a pre-concentrating device for volatile aldehydes in the air, was investigated. The silicone rubber is saturated with the dynamic headspace of O-(2,3,4,5,6-PentaFluoroBenzyl) Hydroxyl Amine (PFBHA). Carbonyl compounds are pre-concentrated, by reaction with the sorbed PFBHA, to form the stable oxime-derivative. The oxime-derivatives are then thermally desorbed, cryogenically focussed and analysed using Gas Chromatography-Mass Spectrometry and Gas Chromatography-Flame Ionisation Detection.

The reaction efficiency of HCHO with PFBHA was experimentally determined to be between 75% to 95%. Breakthrough of the HCHO-Oxime did not occur even after a collection volume of 3 litres. Our detection limit for HCHO is restricted by the HCHO-oxime impurity in the PFBHA blank. The minimum detected HCHO concentration was 0.1ppm. Lower detection limits for acetaldehyde, acrolein and crotonal were obtained as they are absent in the PFBHA blank. They were 0.035ppm, 0.057ppm and 0.064ppm respectively for a collection volume of 10ml, and s/n of 3. The trap was also tested on real gaseous indoor and outdoor air samples and headspace analysis of beer.

Derivatisation on a silicone rubber trap is a promising technique. The simpler method for coating the trap with PFBHA reduces sample preparation time. The silicone rubber is inert, and after thermal desorption is immediately reusable. Analysis of the traps can easily be automated, and the sampling set-up is inexpensive, convenient and portable for fieldwork.

# Konsentrering en derivatisering in silikoonrubber-opvangers vir gaschromatografiese spooranalise van aldehyede

DEUR

**MARIA JOSÉ FERNANDES**

Promotor

Prof Dr E R Rohwer

Ingehandig in deelse bereik van die behoeftes vir die graad MSc, Chemie

in die Fakulteit Natuur- & Landbouwetenskappe

Universiteit van Pretoria

Pretoria

Suid-Afrika

## SAMEVATTING

Lae-molekulêremassa aldehyede, soos formaldehyd (HCHO) en akroleïen, word vrygestel in die omgewing deur onvolledige verbrandingsprosesse en deur tabak-rook. Binnemuurs, word formaldehyd hoofsaaklik vrygestel deur Ureum-Formaldehyd (UF) - hars behandelde meubels. Hierdie aldehyede is lankal verdagte karsinogene, daarom bestaan daar 'n verskeidenheid metodes om hulle te monitor. Die beste metodes wat aldehyede effektief en selektief prekonsentreer maak gebruik van *in-situ* derivatisering. Probleme word egter ondervind met die derivatiseringsmiddels asook hul geassosieerde oplosmiddels en adsorbeërs. 'n



Nuwe, baie belowende metode wat SoliedeFaseMikroEkstraksie (SFME) gebruik, stel polidimetielsiloksaan bekend as die absorbeerder vir die derivatiseringsreagens. Ongelukkig is hierdie metode minder geskik vir monsterneming buite die laboratorium.

In ons studie word die gebruik van silikoonrubber-opvangers, wat in ons laboratorium ontwikkel is, vir die prekonsentrasie van vlugtige aldehyede in lug ondersoek. Die silikoonrubber word versadig met die dinamiese dampruim van O-(2,3,4,5,6-PentaFluoroBenziel)HydroksielAmien (PFBHA). Karbonielverbindings word gekonsentreer, deur reaksie met die geabsorbeerde PFBHA, om stabiele oksiem-derivate te vorm. Die oksiem-derivate word daarna termies gedesorbeer, gefokus deur afkoeling en geanaliseer deur middel van gaschromatografie en gaschromatografie-massaspektrometrie.

Eksperimenteel is vasgestel dat die reaksie van HCHO met PFBHA tussen 75% en 95% volledig verloop. Geen deurbraak van die HCHO-oksiem het na 'n versamelvolumen van 3 liter plaasgevind nie. Die detekselimiet vir HCHO was beperk deur die HCHO-oksiem onsuiverheid in die PFBHA. Die minimum waarneembare HCHO-konsentrasie was 0.1dpm. Laer detekselimiete is moontlik vir asetaldied, akroleien en krotonaldied omdat hul reaksieprodukte nie teenwoordig was in die PFBHA reagens nie. Hul detekselimiete was 0.035dpm, 0.057dpm en 0.064dpm onderskeidelik vir 'n versamelvolumen van 10ml (s/n 3). Die opvanger is ook getoets met werklike binne- en buitemuur lugmonsters en bier-dampruim.

Derivatisering in silikoonrubber-opvangers is 'n belowende tegniek. 'n Makliker metode om die opvanger met PFBHA te bedek verminder die hoeveelheid monstervoorbereidingstyd. Die silikoonrubber is inert en na termiese desorpsie is dit dadelik herbruikbaar. Analiese van die opvangers kan maklik geoutomatiseer word

en die monsternemingstelsel is goedkoop, gerieflik en draagbaar vir monsterneming buite die laboratorium.

My skoenste geselede to.

Dr. J. J. L. van der Merwe, for his guidance, advice and support during the preparation of this dissertation.

Dr. J. J. L. van der Merwe, for his guidance, advice and support during the preparation of this dissertation.

Dr. J. J. L. van der Merwe, for his guidance, advice and support during the preparation of this dissertation.

Dr. J. J. L. van der Merwe, for his guidance, advice and support during the preparation of this dissertation.

Dr. J. J. L. van der Merwe, for his guidance, advice and support during the preparation of this dissertation.

Dr. J. J. L. van der Merwe, for his guidance, advice and support during the preparation of this dissertation.

Dr. J. J. L. van der Merwe, for his guidance, advice and support during the preparation of this dissertation.

Thank you

Maris

## ACKNOWLEDGEMENTS

My sincerest gratitude to:

Professor Egmont Rohwer, for his guidance, support and continuous encouragement (and at least five solutions to every problem).

Mr Anthony Hasset, for his good humour and technical assistance with all the instrumentation used throughout this project.

Mr Robin Muir, for making all the glass devices used in this project. Mr Leon Engelbrecht and Mr Reggie Dumas for their technical assistance and Mr David Masemula, for tirelessly replacing gas bottles and liquid nitrogen.

The National Research Fund and the University of Pretoria for financial support.

My colleagues and friends in research especially; André Venter, Anita Botha, Andreas Landman and Isabel Ricco for their advice, support and encouragement.

My Parents and Family, who have given me the opportunity to go further and supported me every step of the way.

Alexander Whaley, for proof reading my thesis. For his readiness to help with anything and everything at anytime. For his continuous encouragement and support.

*Thank you*

*Maria*

# CONTENTS

	Page
SUMMARY	i
SAMEVATTING	iii
ACKNOWLEDGEMENTS	vi
CONTENTS	vii
ABBREVIATIONS	x
LIST OF TABLES	xiii
LIST OF FIGURES	xiv
CHAPTER 1 INTRODUCTION	1
1.1 Background	1
1.2 Our Approach	6
1.3 Arrangement and Presentation	7
CHAPTER 2 METHODS FOR DETERMINING ALDEHYDES IN AIR	8
2.1 Introduction	8
2.2 Direct Reading Methods	8
2.3 Indirect Reading Methods	9
2.3.1 Non-Chromatographic Methods	9
2.3.1.1 Colorimetric Methods	9
2.3.1.2 Polarographic Methods	12
2.3.2 Chromatographic Methods	13
2.3.2.1 Ion Chromatography	13
2.3.2.2 Capillary Electrophoresis (CE)	14
2.3.2.3 Direct Gas Chromatographic Methods	14
2.3.3 Derivatisation and Chromatographic Separation	16
2.3.3.1 Hydrazones	16
2.3.3.2 Oximes	19
2.3.3.3 Cyclisation Reactions	22
2.4 Conclusion	26
CHAPTER 3 SAMPLE PREPARATION TECHNIQUES	27
3.1 Introduction	27
3.1.1 Dynamic Headspace Sampling	28



	Page
3.2 Adsorption	28
3.2.1 Solid Phase Extraction (SPE)	30
3.2.2 Breakthrough Volume	31
3.3 Cryo-trapping	33
3.4 Absorption	33
3.4.1 Impingers and Bubblers	34
3.4.2 Denuders	34
3.4.3 Polymeric Sorbents	35
3.4.3.1 Open Tubular Traps (OTT)	36
3.4.3.2 The Multichannel Silicone Rubber Trap (MCT)	37
3.4.3.3 Packed Silicone Beds	38
3.4.3.4 Solid Phase MicroExtraction (SPME)	38
3.5 Recovery	41
3.5.1 Solvent Extraction	41
3.5.2 Thermal Desorption	42
 CHAPTER 4 GAS STANDARDS	 43
4.1 Introduction	43
4.2 Static Methods	43
4.3 Dynamic Methods	44
4.3.1 Permeation Methods	45
4.3.2 Diffusion Methods	48
4.4 Experimental	50
4.5 Conclusion	61
 CHAPTER 5 INSTRUMENTATION	 62
5.1 Thermal Desorption-Cryogenic Trapping Unit (TCT)	62
5.2 Gas Chromatograph (GC)	63
5.3 Flame Ionisation Detector (FID)	65
5.4 The Mass Spectrometer (MS)	69
 CHAPTER 6 IN-SITU DERIVATISATION	 73
6.1 In-situ Derivatiation	73
6.1.1 Selecting a Derivatizing Reagent	73
6.1.2 The Silicone Rubber Trap	74
6.2 Identification of the Reagent and Oxime-Products	78

ABBREVIATIONS		Page
6.3	The Derivatising Reagent	85
6.3.1	Loading the Reagent onto the Silicone Rubber Trap	85
6.3.2	Loading from an Aqueous solution of Reagent	85
6.3.3	Reagent Purity	88
6.3.4	Loading from the Pure Reagent	89
6.3.5	Reagent Loading Repeatability	90
6.4	Thermal Desorption-Cryogenic Focussing	95
6.5	Reaction Efficiency	97
6.6	Reagent Depletion <i>versus</i> Breakthrough Volume	104
6.7	Conclusion	106
CHAPTER 7	TESTING THE SILICONE RUBBER TRAP ON REAL SAMPLES	108
7.1	Introduction	108
7.2	Experimental	108
7.3	Results and Discussion	110
7.3.1	Air Samples	110
7.3.2	Headspace Beer Samples	113
7.4	Conclusion	115
CHAPTER 8	CONCLUSION	129
	REFERENCES	132
APPENDIX 1	Table 3.1 Comparison of adsorbents	142
APPENDIX 2	Calculation of Gas Concentrations	144
APPENDIX 3	PFBHA-Aldehyde Reaction Schemes	147
APPENDIX 4	EI-Mass Spectra of PFBHA Aldehyde-Oximes	149

## ABBREVIATIONS

N	=	number of plates
ACGIH	=	American Conference of Governmental Industrial Hygienists
%RSD	=	Percentage Relative Standard Deviation
amu	=	atomic mass units
BEA	=	N-(BenzylEthanol) Amine
CH <sub>3</sub> CHO	=	Acetaldehyde
DNPH	=	2,4-DiNitroPhenylHydrazine
DNSH	=	Dansylhydrazine
DVB	=	DiVinylBenzene
ECD	=	Electron Capture Detector
EI	=	Electron Impact
EPA	=	Environmental Protection Agency
FID	=	Flame Ionisation Detector
GC	=	Gas Chromatography
HCHO	=	Formaldehyde
HID	=	Helium Ionisation Detector
HMP	=	2-HydroxyMethylPiperidine
HPLC	=	High Performance Liquid Chromatography
HSSE	=	Headspace Sorptive Extraction
ITD	=	Ion Trap Detector
k	=	capacity factor
K	=	distribution coefficient
LC-MS	=	Liquid Chromatography - Mass Spectrometry
LLE	=	Liquid-Liquid Extraction
MCT	=	MultiChannel Trap
MS	=	Mass Spectrometry
UV	=	Ultraviolet

N	=	number of plates
NIOSH	=	National Institute for Occupational Safety and Health
NIST	=	National Institute for Standards and Technology
NPD	=	Nitrogen-Phosphorus Detector
OSHA	=	Occupational Safety and Health Administration
OTT	=	Open Tubular Traps
PDMS	=	PolyDiMethylSiloxane
PEL	=	Permissible Exposure Limit
PFBHA	=	O-(2,3,4,5,6-PentaFluoroBenzyl) Hydroxyl Amine
PFPH	=	O-(2,3,4,5,6-PentaFluoroPhenyl) Hydrazine
PLOT	=	Packed Layer Open Tubular
ppb	=	part-per-billion
ppm	=	part-per-million
PTFE	=	PolyTetraFluoroEthylene
SIM	=	Selected Ion Monitoring
SPE	=	Solid Phase Extraction
SPME	=	Solid Phase MicroExtraction
STEL	=	Short Term Exposure Limit
s / n	=	Signal - to - noise ratio
TCD	=	Thermal Conductivity Detector
TCPH	=	2,4,6-TriChloroPhenylHydrazine
TCT	=	Thermal Desorbtion - Cryogenic Trapping unit
TIC	=	Total Ion Chromatogram
TSD	=	Thermionic Specific Detection
TWA	=	Time Weighted Average
UF	=	Urea - formaldehyde
UV	=	Ultra-Violet

## LIST OF TABLES

VOC	=	Volatile Organic Compound
$V_b$	=	breakthrough volume
WCOT	=	Wall-Coated Open Tubular
WHO	=	World Health Organisation



## LIST OF TABLES

	Page
Table 1.1: Indoor Personal Exposure Limits (PEL) for airborne formaldehyde [3,4]	2
Table 3.1: A comparison of various adsorbents [19,71-75,79,82]	141
Table 4.1: Summary of gas standard devices prepared and results obtained	53
Table 5.1: Contributions to the Effective Carbon Number (ECN) [120,122]	67
Table 6.1: Instrumentation Parameters	77
Table 6.2: EI-Mass Spectra for PFBHA-aldehyde derivatives [17,22,50]	81
Table 6.3: The variation in the ratio of the isomer peaks of acetal, acrolein and crotonal-oximes	103
Table 6.4: Determination of minimum detectable concentrations for acetaldehyde, acrolein and crotonal	104
Table 7.1: Quantitation of collected real samples for formaldehyde (HCHO) analysis	116
Table 7.2: Quantitation of collected real samples for acetaldehyde (CH <sub>3</sub> CHO) analysis	117

## LIST OF FIGURES

	Page
Figure 2.1: Reaction scheme for Purpald® reagent with an aldehyde or ketone [29]	11
Figure 2.2: Reaction scheme for bisulphite with an aldehyde [30]	14
Figure 2.3: Reaction scheme for the conversion of an aldehyde to an alkane [16]	14
Figure 2.4: Reaction scheme for the reduction of an aldehyde to an alcohol [31]	15
Figure 2.5: Reaction scheme for 2,4-DNPH with an aldehyde [20,37-45]	17
Figure 2.6: Reaction scheme for DNSH with an aldehyde [46]	18
Figure 2.7: Reaction scheme for PFPH with an aldehyde [47,48]	18
Figure 2.8: Reaction scheme for TCPH with an aldehyde [49]	19
Figure 2.9: Reaction scheme for first, benzylhydroxylamine with an aldehyde. Second methoxy amine with an aldehyde [8]	20
Figure 2.10: Reaction scheme for PFBHA with an aldehyde [50]	22
Figure 2.11: Reaction scheme for ethanolamine with an aldehyde [8,21]	22
Figure 2.12: Reaction scheme of 2-HMP with an aldehyde [23,58-60]	23
Figure 2.13: Reaction scheme of cysteamine with an aldehyde [8,61,62]	24
Figure 2.14: Reaction scheme for formaldehyde with aqueous ammonia [63]	24

	Page
Figure 2.15: Reaction scheme for Dimedon with an aldehyde [64]	25
Figure 2.16: Hantzsch reaction scheme [65-66]	26
Figure 3.1: Flow diagram of sample preparation techniques for gaseous organic compounds	27
Figure 3.2: Steps involved in the SPE technique [76]	30
Figure 3.3: Liquid-phase extraction devices [82]	33
Figure 3.4: Cross-sections of various trap configurations using 100% Polydimethylsiloxane	36
Figure 3.5: A commercial SPME device from Supelco [87]	40
Figure 4.1: Aldehyde gas standard devices	50
Figure 4.2a*: Mass loss curves for the aldehyde diffusion gas standards prepared * acrolein mass loss curve not shown, as diffusion was too rapid.	54
Figure 4.2b#: Mass loss curves for the aldehyde type 1 permeation gas standards # acrolein mass loss not shown, as permeation was too rapid	54
Figure 4.2c**: Mass loss curves for the aldehyde type 2 permeation gas standards ** no butanal and benzaldehyde gas standards of this type were prepared	55
Figure 4.2d: Mass loss curves for the formaldehyde gas standards	56
Figure 4.3: Dilution system for the gas standard	57
Figure 4.4: T-piece split	58

	Page
Figure 4.5: Reconstructed Ion Chromatogram using m/z 181 of SPME-PFBHA coated fibre exposed to aldehyde diffusion gas standards (type 3)	60
Figure 4.6: Reconstructed Ion Chromatogram using m/z 181 of SPME-PFBHA coated fibre exposed to aldehyde permeation gas standards (type 1)	61
Figure 5.1: The 2 main phases in the TCT 4020 thermal desorption unit	63
Figure 5.2: A Hewlett Packard Flame Ionisation Detector [119]	65
Figure 5.3: Estimating Effective Carbon Numbers for PFBHA and the HCHO-Oxime	68
Figure 5.4: A Quadrupole Mass Spectrometer [125,126]	71
Figure 5.5: A Gas Chromatograph (GC) coupled to an Ion Trap Detector (ITD), having an external ion source [125]	72
Figure 6.1: The suggested mechanism for the reaction of an aldehyde with PFBHA	75
Figure 6.2: In-situ derivatisation on the silicone rubber trap	76
Figure 6.3: GC-FID chromatogram of a desorbed silicone rubber trap	78
Figure 6.4: Overlaid TIC of SPME-PFBHA coated fibre exposed to pure aldehyde	79
Figure 6.5: A. Obtained EI-Mass Spectrum for PFBHA B. NIST library EI-Mass Spectrum for PFBHA	80
Figure 6.6: A. Obtained EI-Mass Spectrum for HCHO-Oxime B. NIST library EI-Mass Spectrum for HCHO-Oxime	80

	Page
Figure 6.7: A. Obtained EI-Mass Spectrum for the acetaldehyde-oxime B. NIST library EI-Mass Spectrum for the acetaldehyde-oxime	82
Figure 6.8: Formation of the pentafluorotropylium ion $m/z$ 181 [50,125]	82
Figure 6.9: McLafferty rearrangement of the butanal-oxime to form $m/z$ 239 [130]	83
Figure 6.10: Mechanism for the formation of $m/z$ 250 from 2-alkenal-oximes, Where $R' = H$ (acrolein) and $CH_3$ (crotonal) [130]	83
Figure 6.11: Set-up for loading headspace from aqueous reagent	85
Figure 6.12: GC-ITD MS Total Ion Chromatogram of PFBHA (loaded from aqueous headspace) and 30sec sampling of a 5ppm HCHO atmosphere	86
Figure 6.13: ITD EI-Mass Spectrum of the formaldehyde-oxime	87
Figure 6.14: Comparison of HCHO-Oxime in PFBHA (aq) and PFBHA(s)	89
Figure 6.15: Set-up for loading headspace from the pure reagent	89
Figure 6.16: GC-FID chromatogram of the PFBHA reagent, headspace collected from the pure solid for 10min at 5ml/min	91
Figure 6.17: The depletion of PFBHA headspace from an aqueous solution	92
Figure 6.18: The depletion of PFBHA headspace from the pure reagent	92
Figure 6.19: Peak area of PFBHA and HCHO-oxime with increasing loading volume at 5 and 10ml/min collection flow rates	94
Figure 6.20: The depletion of PFBHA from the silicone trap with exposure to nitrogen at a flow rate of 10ml/min	94



	Page
Figure 6.21: Optimisation of the thermal desorption of dodecane (C <sub>12</sub> ) from a silicone trap	96
Figure 6.22: Collection of a 5.98ppm HCHO atmosphere at 10ml/min over time	98
Figure 6.23: Determination of reaction efficiency of 5.98ppm HCHO with PFBHA	98
Figure 6.24: Collection of a 0.1ppm HCHO atmosphere at 10ml/min over time	99
Figure 6.25: Determination of reaction efficiency of 0.1ppm HCHO with PFBHA	99
Figure 6.26: GC-FID chromatogram obtained for the collection of 3, 1.5 and 2.5 ppm acetal, acrolein and crotonal respectively, for 10min at a flow rate of 10ml/min	102
Figure 6.27: Determination of reaction efficiency of 3ppm acetal, 1.5ppm acrolein and 2.5ppm crotonal with PFBHA	101
Figure 6.28: Determining the breakthrough volume of the HCHO-oxime onto the second trap	105
Figure 7.1: GC-FID chromatogram of an air sample from a newly-carpeted laboratory	118
Figure 7.2: GC-FID chromatogram of an air sample from a poorly ventilated office	119
Figure 7.3: GC-FID chromatogram of an air sample from a parking lot	120
Figure 7.4: GC-FID chromatogram of parking lot air sample without PFBHA <i>in-situ</i> derivatisation	121

	Page
Figure 7.5: GC-FID chromatogram of an air sample from a bar filled with tobacco smoke	122
Figure 7.6: GC-FID chromatogram of the indoor air of a new car	123
Figure 7.7: GC-FID chromatogram of the indoor air of an 11 year old car	124
Figure 7.8: GC-FID chromatogram of Castle Lager headspace sample	125
Figure 7.9: GC-FID chromatogram of Black Label Beer headspace sample from trap 2	126
Figure 7.10: GC-FID chromatogram of Windhoek Light beer headspace sample	127
Figure 7.11: A. GC-FID chromatogram of Castle Lager headspace sample without PFBHA in-situ derivatisation B. GC-FID chromatogram of Castle Lager headspace sample with PFBHA in-situ derivatisation (figure 7.8)	128

## CHAPTER 1

### INTRODUCTION

#### 1.1 BACKGROUND

The increased pollution of the environment has generated a need for the continuous improvement of existing methods and for the development of new, reliable and sensitive methods for air, water and soil quality control.

Volatile aldehydes in air such as formaldehyde, acetaldehyde and acrolein have received attention as hazardous air pollutants. Formaldehyde (HCHO) is classified by the Environmental Protection Agency (EPA), the American Council of Governmental Industrial Hygienists (ACGIH), the National Institute of Occupational Safety and Health (NIOSH) and the Occupational Safety and Health Administration (OSHA) as a probable human carcinogen [1,2].

Airborne concentrations of HCHO above 0.1 ppm can cause irritation of the eyes, the nose and throat, the upper respiratory tract and the lacrimation glands [1,2,5,6]. It is also thought that HCHO can cause nausea, dizziness and lethargy at levels as low as 50 ppb [7].

Aldehydes are present in exhaust gases due to incomplete combustion of hydrocarbons and in photo-oxidation processes occurring in the atmosphere [8].

Sasol has recently added alcohol to their fuel [9], which has the advantage of reducing particulates, carbon monoxide and nitrous oxide emissions. However, this measure leads to an increase in aldehyde emissions, in particular formaldehyde and acetaldehyde [10-12].

This problem, however, is not localised to our external environment. Since people in developed countries spend up to 90% of their time indoors, exposure to air pollutants in the indoor environment can be high. In the 1970's, concerns were raised that certain organic compounds found in non-industrial buildings could cause health problems similar to those of Sick Building Syndrome [4,13]. As a result, formaldehyde has been the most widely studied compound in indoor air. Average HCHO levels in office buildings range from 10 ppb to 78 ppb. Several studies point to formaldehyde predisposing children to respiratory tract infections. 1 to 2% of children exposed to 60-120ppb HCHO at home may develop asthma; with an increased likelihood if also exposed to tobacco smoke [4]. Concentrations of formaldehyde were found to be 10 or more times higher indoors than outdoors [4]. Tobacco smoke, combustion gases from gas appliances, disinfectants and water based paints [4,14] release formaldehyde indoors. The main culprits however, are products manufactured using urea-formaldehyde (UF) resins including particleboard used in flooring and furniture, hardwood plywood panelling and UF-foam insulation [1,4,7,13,15]. Table 1.1 lists the Permissible Exposure Limits (PEL) for airborne HCHO in the workplace (indoors).

Table 1.1 Indoor Personal Exposure Limits (PEL) for airborne formaldehyde [3,4].

	PEL	STEL	CEILING
OSHA	0.75ppm <sup>#</sup>	2ppm <sup>##</sup>	0.5ppm <sup>*</sup>
NIOSH	0.016ppm		0.1ppm
ACGIH			0.3ppm
WHO		0.1ppm <sup>**</sup>	

<sup>#</sup> Time Weighted Average (TWA) over 8 hours.

<sup>##</sup> Short Term Exposure Limit (STEL) during 15 min period.

<sup>\*</sup> action level measured over 8 hours.

<sup>\*\*</sup> 30 min average.

Acetaldehyde also causes irritation of the eyes, nose and throat. However, acetaldehyde is usually handled in industry under closed systems, as it is an explosive hazard. In industry exposure to acetaldehyde is not known to be continuous or at high levels, hence the recommended threshold limit for acetaldehyde is 100ppm with a Short Term Exposure Limit (STEL) of 150ppm [6].

Higher aliphatic aldehydes, such as propanal and butanal, are typically components of the exhaust of internal combustion engines. They are characterised by a lower general toxicity and as such, no exposure limits have been set for them [6].

The toxicity of the aliphatic aldehydes generally decreases as the chain length increases [6].

Acrolein and crotonal, are acute eye and respiratory irritants. The toxicity of these aldehydes is enhanced by the presence of the double bond. The threshold limit for acrolein is 0.1ppm with a STEL of 0.3ppm for 15min. Crotonal is ten times less toxic than acrolein, hence the threshold limit of 2ppm [6].

Thus increasing awareness of the effects that certain aldehydes, particularly formaldehyde, can have on human health, indicates a need to be able to detect and quantify the level of aldehydes in the environment, both indoor and outdoor.

Research into the determination of formaldehyde in air, still continues despite the several methods already developed. Although detection of exposure limits can be reached with these methods, they prove tedious and time consuming.

With the aim that no sample preparation be required, methods for analysing aldehydes directly would be ideal, but they make use of bulky and complicated instrumentation. Although direct analysis of HCHO gas, using Gas Chromatography (GC) would also be ideal, we are hampered by the fact that common detectors in GC like the Flame Ionisation Detector (FID) and the Thermal Conductivity Detector (TCD) lack sensitivity for this compound [16]. Mass Spectrometry for low masses, such as



30amu for HCHO, would not show sufficient sensitivity either, as this mass falls in the same mass region as air (nitrogen 28 amu and oxygen 32 amu).

Similarly, the detection of acetaldehyde particularly in beer is also difficult, yet important to monitor, as acetaldehyde and other carbonyl compounds are known to contribute to the stale flavour in beer [17]. Acetaldehyde has a mass of 44 amu coinciding with that of carbon dioxide (CO<sub>2</sub>), which is prevalent in both beer and air. In addition, a high vapour pressure and polarity make acetaldehyde a difficult compound to pre-concentrate on non-polar sorbents. Chromatography on non-polar thin film stationary phases often leads to co-elution of acetaldehyde with the ethanol in the beer.

Indirect methods using derivatising reactions remove these detection and concentration difficulties, while introducing new ones. Problems encountered are determined principally by the sample preparation techniques used. These involve the pre-concentration device, the derivatising reagent and the desorption method.

The collection of gaseous samples in impingers and bubblers is not very portable and convenient for field-work. Hence, much attention has been given to tubes packed with sorbents, where the gaseous sample can be sucked through the tube using a portable pump.

Indirect methods make use typically of the following procedure: The derivatising reagent either coats the sorbent or is present in solution. In the former case, formaldehyde gas reacts with the reagent on the surface of the sorbent. The product is often extracted from the sorbent or solution using a solvent. The extract is then concentrated to a small volume by evaporation and injected into the instrument for analysis. However, the use of toxic solvents is undesirable. Dilution of the product to be analysed, results in a decrease in sensitivity since only a tiny portion of the extract is finally transferred onto the column. An alternative product transfer method is

desired. Thermal desorption of the entire contents of the sorbent trap directly onto the column eliminates the above-mentioned concerns.

Adsorbents unfortunately are known to have several disadvantages. They possess active sites, which allow for chemical reactions with the sorbed analytes being analysed, or in this case, the reagent being used for derivatisation. Tenax, for example, is known to release benzaldehyde as one of its thermal degradation products, thereby making it unsuitable for use in benzaldehyde analysis [18]. Some compounds may be irreversibly adsorbed on the sorbent, especially polar compounds on carbon sorbents [19]. Additionally, sorbents must undergo several steps of pre-treatment before being packed into collection tubes. After the analysis, the sorbent must once again undergo several reconditioning and preparation steps before it can be re-used. This entire process becomes time consuming. Thus, the ideal sorbent should be chemically inert, thermally stable and immediately reusable.

Polydimethylsiloxane or silicone rubber, has recently become popular as a liquid-like sorbent [18]. Analytes dissolve into the phase as they would in a solution. The silicone adsorbent has a larger capacity or concentration range for which the partition isotherm is linear. For adsorbents once all available sites are occupied by a monolayer, the adsorbent shows less retention for any further analytes entering the trap (non-linear partition isotherm). Thermal degradation of the silicone, during thermal desorption, produces polysiloxane compounds with reproducible retention times. In addition, these compounds are easily distinguished by their Electron Impact (E.I) mass spectral fragments. After thermal desorption, the silicone rubber is ready for use again.

Several derivatising reagents have been used for the reaction with HCHO and other low molecular mass aldehydes. By far the most popular reagent is 2,4-

DiNitroPhenylHydrazine (DNPH). HCHO is collected on a sorbent or in an impinger containing the reagent, followed by solvent extraction and separation by High Performance Liquid Chromatography (HPLC) with Ultra Violet (UV) detection. HPLC cannot match the desired resolution, speed of analysis, compound identification and quantification of Gas Chromatography (GC). 2,4-DNPH however, is not suitable for use in GC analysis either, as it requires high temperatures to be volatilised (which may decompose the derivative) and regular cleaning of the inlet liner [11,20,21]. Recently, in-situ derivatisation of HCHO, using a SPME fibre coated with O - (2,3,4,5,6-PentaFluoroBenzyl) HydroxylAmine (PFBHA), analysed with GC-FID or Gas Chromatography – Electron Capture Detection (GC-ECD), showed promising results [22]. The method uses a Polydimethylsiloxane (PDMS) – divinylbenzene (DVB) polymer fibre as the sorbent for PFBHA. Formaldehyde again, as with other adsorbents, reacts on the surface of the fibre. As long as the PFBHA remains minimally consumed, the oxime formation rate is limited by the HCHO concentration. The method is ideal for grab sampling and as a passive sampler for time weighted averaging in indoor air analysis. Oximes, in general are volatile and ideal for analysis using GC. The SPME fibre is desorbed directly in the hot inlet of the GC and no special desorption equipment is required. SPME fibres however are fragile and expensive. A more rugged sampling system is required, that would allow many samples to be taken in the field before being transported to the laboratory. Hence, the possibility of performing in-situ derivatisation on our silicone rubber traps using PFBHA, which show a number of advantages over SPME, was investigated.

## 1.2 OUR APPROACH

Sampling methods are required that (1) reduce the complexity and cost of the sampling system involved (2) reduce the experimental uncertainties/errors (3) lower

the limit of detection for formaldehyde in the outdoor environment [23].

On this basis, our research was carried out to find a pre-concentration method for formaldehyde gas and other aldehydes, which could fulfil the above requirements using the Silicone rubber traps developed in our laboratories [24-27] in combination with Gas Chromatography – Flame Ionisation Detection (GC-FID) and Gas Chromatography – Mass Spectrometry (GC-MS).

Our aim is (1) to prepare stable gas standards of volatile aldehydes. (2) Select and load a derivatising reagent onto our silicone rubber traps in a convenient, repeatable manner. (3) Demonstrate the efficient pre-concentration of the aldehyde gas standards on the reagent-coated silicone rubber trap. (4) Quantitatively recover and analyse the contents of the trap. (5) Demonstrate *in-situ* derivatisation on our silicone rubber traps with real gaseous indoor and outdoor air samples and headspace analysis of beer.

### 1.3 ARRANGEMENT AND PRESENTATION

Chapter 2 will introduce the methods already available for the determination of formaldehyde and other aldehydes in air. Chapter 3 follows with sample preparation focussing on pre-concentration devices and techniques. Preparation of aldehyde gas standards is described in chapter 4. The instrumentation is briefly discussed in chapter 5. The characteristics of the trap in terms of completeness of reaction on the absorbent, trapping efficiency and complete transfer onto the column are examined in chapter 6. The application of the trap on real gaseous samples is shown in chapter 7.

## CHAPTER 2

### METHODS FOR DETERMINING ALDEHYDES IN AIR

#### 2.1 INTRODUCTION

Several reviews have been written on the various methods for the measurement of aldehydes in the environment [8,11,21]. These methods may be classified into two groups namely direct and indirect methods. Direct methods analyse the aldehydes during collection and therefore show great potential as the risk of sample contamination is greatly reduced. However, the cost and complexity of the instrumentation, as well as the properties of aldehydes make these methods, on the whole, unsuitable. Indirect methods, on the other hand, utilise these properties to improve ease of detection. Indirect methods analyse the aldehydes after they have been collected by some means. A brief summary of these methods that have been developed follows.

#### 2.2 DIRECT READING METHODS

These methods give immediate results. Long-Path Fourier Transform Infrared Spectroscopy and differential absorption in the near UV region from a high pressure Xenon lamp, has been applied to the detection of formaldehyde. However, long optical paths are required (meters to kilometres) to obtain sensitivities of a few ppb. The laser fluorescence technique, with the aid of a photomultiplier, can monitor aldehyde concentrations as low as 40ppb. A tuneable diode laser may be used to monitor



formaldehyde in air at the 1-2ppb level, using hourly data averaging. An electrochemical fuel detector can instantaneously determine formaldehyde over the 0.3-5ppm range. Most of these methods require expensive, complex equipment and highly skilled operators. Several other direct reading methods have also been developed, but show poor sensitivity [11].

A novel reactive passive sampler monitoring card system was developed for on-site determination of formaldehyde in air. Formaldehyde diffuses through a polymeric membrane and reacts with a chemically impregnated sorbent layer. A colour-change is produced which is proportional to the exposure amount. Its working range is between 0.1 and 2ppm[28].

## **2.3 INDIRECT READING METHODS**

### **2.3.1 NON-CHROMATOGRAPHIC METHODS**

#### **2.3.1.1 COLORIMETRIC METHODS**

These methods rely on absorption spectrophotometry. The reaction product's absorbance can be measured and related to the concentration of the aldehyde collected, using Beer's Law. A brief introduction to some colorimetric methods follows.

## **CHROMOTROPIC ACID METHOD**

Formaldehyde is collected on an adsorbent trap, or in an impinger containing either distilled water or a bisulphite solution. Chromotropic acid (4,5-dihydroxynaphthalene-2, 7-disulphonic acid), followed by concentrated sulphuric acid is then added to the extracted formaldehyde solution. A violet-coloured product forms, and its absorbance is measured at 580nm. Unfortunately, long collection times are required. Interferences from compounds such as phenols, ethanol, high mass alcohols and olefins inhibit the reaction, leading to negative bias in the results. The detection limit has been improved to 0.3-0.03 ppm, by changing the collection medium, the collection device, reaction temperature and storage [11,21]. NIOSH Method 3500[1] uses this technique, which has a working range of 0.02 to 4 ppm in an 80L air sample.

## **PARAROSANILINE METHOD**

This method shows a two-fold increase in sensitivity over the chromotropic acid method. An impinger containing a sodium sulphite solution is used to collect formaldehyde. Sodium tetrachloromercurate and pararosaniline are added to the solution producing a purple-coloured product, which can also be determined spectrophotometrically at 560nm. Interferences from propanal, acrolein and acetaldehyde cause a positive bias in the results at 5ppm and above. In addition, the use of the toxic mercurate salt was not desired so the method was modified to exclude the salt. The modified method is sensitive to temperature, at the same time gaining interference from hydrogen cyanide, sulphite ion, hydroxylamine and sulphur dioxide. This method was also used to analyse formaldehyde collected on molecular sieve sorbent tubes. A disadvantage of these

tubes, however, is the decrease in breakthrough volume for HCHO as the water in the environment increases. The detection limit was found to be 0.03ppm[11,21]

### PURPALD® REAGENT

Purpald® also known as 4-amino-3-hydrazino-5-mercapto-1,2,3-triazole, is a new reagent for the sensitive and specific spectrophotometric test for aldehydes. The reagent reacts with both aldehydes and ketones, as shown in figure 2.1. However, only the aldehyde-product can be oxidised to give the conjugated, purple-coloured, bicyclic ring system determined at 532 nm and 549 nm. The working ranges are 0.5 - 5ppm HCHO or 5 - 20 ppm HCHO after suitable dilution [29].

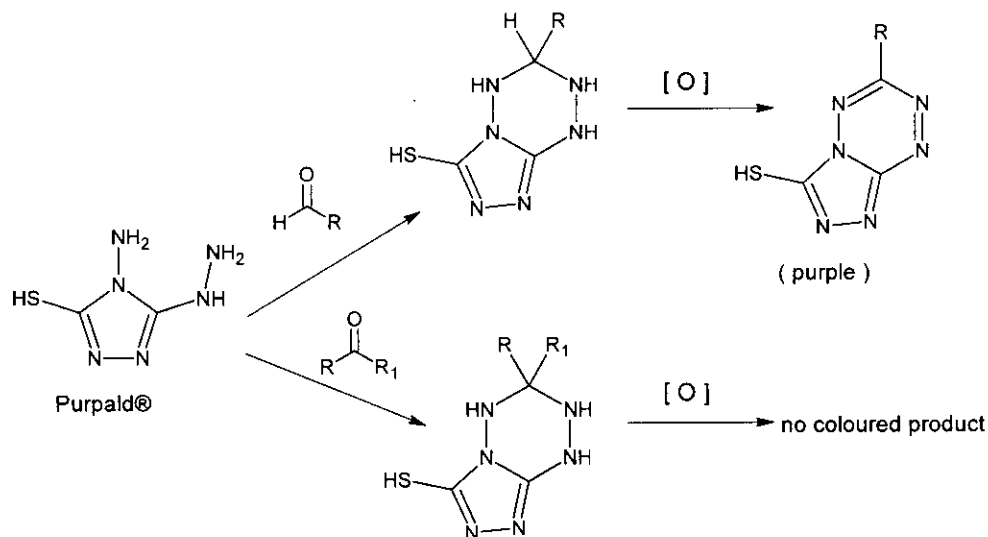


Figure 2.1 Reaction scheme for Purpald® reagent with an aldehyde or ketone [29].

### **3-METHYL-2-BENZOTHAZOLONE HYDRAZONE (MBTH) METHOD**

Formaldehyde reacts *in-situ* when it is collected in an impinger containing a 0.05% MBTH aqueous solution. Ferric chloride and acid are added to this product forming a blue cationic dye, which can be determined spectrophotometrically. This method's sensitivity is reported to be 30ppb formaldehyde in air. The dye is unstable after 4 hours. Other aldehydes collected will cause a positive interference. Aromatic amines, amino heterocyclics, azo dyes, stilbenes and Schiff bases may interfere by also reacting with MBTH [11,21]. The method is normally used for sum total aldehyde level determination.

#### **2.3.1.2 POLAROGRAPHIC METHODS**

##### **GIRARD T METHOD**

A bubbler filled with Girard T reagent (Trimethylammoniohydrazide chloride) is used to collect the formaldehyde. The formaldehyde-hydrazide reaction affords a hydrazone, which is then determined by Polarography. Other volatile aldehydes also collected cause interference in the analysis. The reported limit of quantitation is 0.3ppm[21]

##### **HYDRAZINE METHOD**

Formaldehyde collected in a bubbler filled with aqueous methanol is allowed to react with hydrazine. Differential Pulse Polarography at a dropping mercury electrode is used to selectively determine the formaldehyde hydrazone. Even though the detection limit is as

low as 0.01ppm, the sample collection set-up is not very portable, limiting its use to the lab [21].

## **2.3.2 CHROMATOGRAPHIC METHODS**

### **2.3.2.1 ION CHROMATOGRAPHY**

#### **OXIDATIVE CHARCOAL TUBE METHOD**

Formaldehyde is collected and partially oxidised to formate, on an oxidant-coated sorbent. Aqueous hydrogen peroxide is used to extract the formate, which is then determined by ion chromatography. Collected samples are not stable for more than 5 days. The method shows a limit of quantitation of 0.03ppm[21].

#### **PULSED AMPEROMETRIC DETECTION**

Aldehydes in solution are separated on a cation exchange resin in the potassium form, and are then detected electrochemically by oxidation with a platinum electrode. Detection limits range between 1 and 3ppm, though no application to airborne aldehydes has been made [11].

### 2.3.2.2 CAPILLARY ELECTROPHORESIS (CE)

Current applications involve substituted benzaldehydes, which react in-column with sodium bisulphite to produce charged complexes, which can be separated using CE [30].

The reaction scheme is shown in figure 2.2.

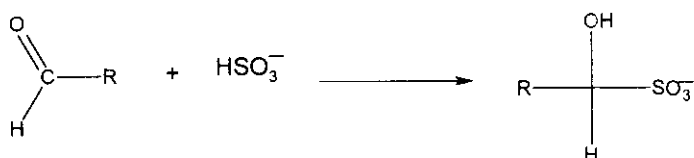


Figure 2.2 Reaction scheme for bisulphite with an aldehyde [30].

### 2.3.2.3 DIRECT GAS CHROMATOGRAPHIC METHODS

Whole air samples are injected onto a Porapak Q pre-column, hydrocarbons are not collected and pass through. This allows the aldehydes (C2-C5) collected to be diverted to another Porapak Q column followed by a "methanizer" where they are converted to their corresponding alkanes. Detection is with an FID, providing a method sensitivity of 0.3-0.08ppm[11]. Similarly, formaldehyde, acetaldehyde, and other volatile gases in a non-corrosive gas matrix, are converted to methane and ethane, respectively, using a nickel coated catalyst in a hydrogen atmosphere, and analysed using an FID, shown in figure 2.3. A detection limit of 0.1ng for formaldehyde and 0.06ng for acetaldehyde was obtained [16].

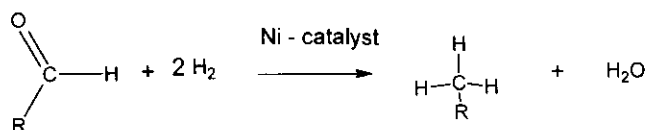


Figure 2.3 Reaction scheme for the conversion of an aldehyde to an alkane [16].



Carbonyl compounds have also been efficiently reduced to their corresponding alcohol, by sodium borohydride (NaBH<sub>4</sub>), shown in figure 2.4, followed by GC on porous polyaromatic resin beads and FID detection [31].

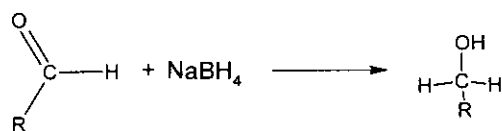


Figure 2.4 Reaction scheme for the reduction of an aldehyde to an alcohol [31].

A helium ionisation detector (HID) was used for the direct analysis of formaldehyde (HCHO) in the ppb-ppm range. The HID shows a marked increase in sensitivity over the FID for HCHO. However, due to the HID's large response to water in the air, the number of samples that can be analysed using the HID are limited as it takes 40min to fully elute the water isothermally before the next sample can be analysed [32].

Various adsorbents have been used to collect aldehydes, followed by either solvent extraction or thermal desorption with cryogenic focussing. Emphasis is placed on the GC column and detector used. Formaldehyde may, at the nanogram level, interact with the stationary phases of certain WCOT columns to form dimers and trimers [16]. Analysis of free carbonyls on commonly used GC-columns suffers from overlapping by dominant hydrocarbons. A new PLOT column (CP-LOWOX), which separates the interfering hydrocarbons, was successfully applied in the separation of semi-volatile aldehydes (C<sub>6</sub>-C<sub>11</sub>) pre-concentrated on various sorbents, thermally desorbed and analysed on an FID/MS [33]. A mixture of 10 short chain aldehydes were separated within 1 minute on inert spherical silica particles encapsulated with polyethylenimine (PEI) with CO<sub>2</sub> as the mobile phase, under solvating gas chromatography conditions [34]. C<sub>2</sub>-C<sub>5</sub> aldehydes were trapped on a pre-column cold trap, heated from -183°C to 120°C in 3.5 minutes and analysed simultaneously by 4 detectors [35]. Cryogenic trapping was also used in the

dynamic headspace analysis of volatile reaction products during the curing of urea-formaldehyde (UF) coatings [36].

### 2.3.3 DERIVATISATION AND CHROMATOGRAPHIC SEPARATION

*In-situ* derivatisation of aldehydes has several advantages over direct aldehyde analysis. Special storage is no longer required, because the aldehydes are stabilised as their derivatives. Background and interferences are reduced by the specific selective nature of the chemical reaction. Special detectors can be used since the derivative now has enhanced detectability. Use of *in-situ* derivatisation for the measurement of aldehydes has been studied extensively. Two common methods involve the reaction of a carbonyl with a hydrazine to form a hydrazone, or with an amine to yield an oxime.

#### 2.3.3.1 HYDRAZONES

##### 2,4-DINITROPHENYLHYDRAZINE (DNPH)

Formaldehyde has been collected in an impinger [37] and bubbler [38] containing DNPH, on DNPH coated sorbents [39-41], DNPH coated glass fibre [20], sintered glass [42] and PDMS SPME fibre [43]. HCHO reacts *in-situ* with the DNPH solution to form the 2,4-Dinitrophenylhydrazone chromophore which can be determined using HPLC with UV detection or GC-ECD/MS/FID/TSD [20,40,43]. The reaction takes place under strongly acidic conditions. Although this reagent has been used with GC analysis, removal of excess DNPH is required prior to injection (which leads to column and detector deterioration) [11,20,21], and frequent cleaning of the inlet liner [10]. High oven

temperatures are required because of the low volatility of the derivative [8]. Hence, HPLC-UV is favoured for this method, being both sensitive and easy to implement [10,11,21]. This technique is employed as a standard method for formaldehyde determination by the EPA, (EPA-TO11)[1], and NIOSH, (Method 2016)[3]. To further enhance the resolution and detection of an HPLC, a new detection method using Diode Array Ultraviolet Spectroscopy and Atmospheric Pressure Negative Chemical Ionisation Mass Spectrometry for liquid chromatography was introduced. The set-up showed a significant increase in resolution (34 carbonyls) and sensitivity in the ppb range [44]. Figure 2.5 shows the reaction scheme.

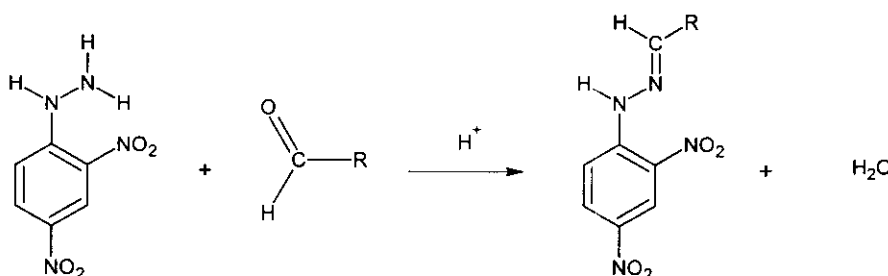


Figure 2.5 Reaction scheme for 2,4-DNPH with an aldehyde [20, 37-45].

#### **DANSYLHYDRAZINE (DNSH) – (1-Dimethyl-aminonaphthalene-5-sulfonylhydrazine)**

Schmied, et.al, developed a method for determining aldehydes and ketones simultaneously by derivatisation on silica gel coated with DNSH. The reaction scheme is shown in figure 2.6. The reaction is highly efficient and allows for collection flow rates of 2L/min. After collection, the hydrazones are extracted and separated by HPLC with fluorescence detection. DNSH was purified before each use. Detection limits are in the picogram range [46].

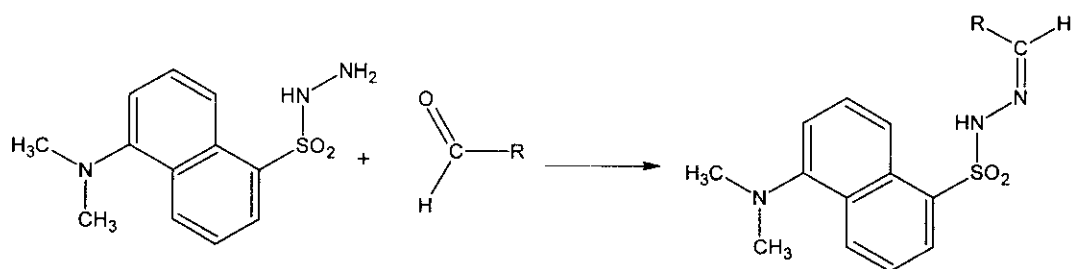


Figure 2.6 Reaction scheme for DNSH with an aldehyde [46].

### O- (2,3,4,5,6-PENTAFLUOROPHENYL) HYDRAZINE (PFPH)

The hydrazine's detectability using ECD is enhanced by the pentafluoro-moiety. At this stage, the reagent has only been used in the study of lipid peroxidation in which volatile carbonyl compounds are formed [47,48]. Stashenko et al [47] heated a vegetable oil sample in a test tube and added PFPH solution. After the carbonyls reacted at room temperature with the PFPH, they were extracted into non-polar phases using either LLE or SPE. The extracts were analysed by GC-FID/ECD/MS-SIM. Detection limits of  $10^{-14}$  and  $10^{-12}$  mol/ml per aldehyde were obtained using ECD and MS-SIM respectively. More recently, using the same concept used by Pawliszyn [22], a SPME fibre was used to pre-concentrate carbonyls using *in-situ* derivatisation on a PFPH coated PDMS/DVB fibre which, following desorption in the GC inlet, was analysed by GC with ECD to obtain a detection limit of 10-90 fmol [48]. The reaction scheme is shown in figure 2.7 below.

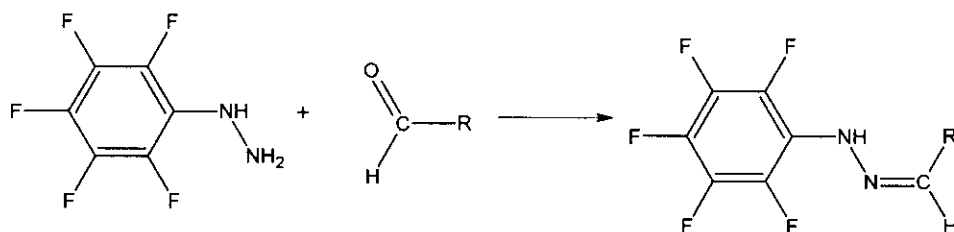


Figure 2.7 Reaction scheme for PFPH with an aldehyde [47,48].

## 2,4,6-TRICHLOROPHENYLHYDRAZINE (TCPH)

This reagent was introduced to reduce the problems experienced using 2,4-DNPH and GC analysis. An octadecyl silica cartridge impregnated with TCPH was used to collect HCHO. Thereafter the cartridge was held at 100°C for 6 min to allow for complete reaction. The cartridge is eluted with acetonitrile followed by GC-ECD analysis. Detection limits are determined by the blank, in the case of HCHO the limit of detection is 0.1ppb in 10L, while other carbonyls have even lower limits. An ozone scavenger had to be used to eliminate the interference of ozone above 300ppb[49]. The reaction scheme is shown in figure 2.8 below.

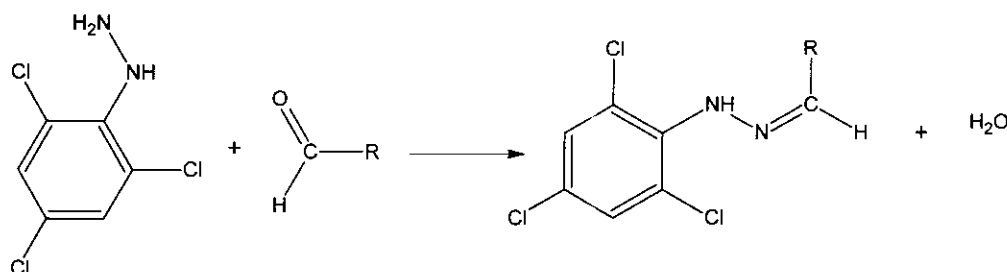


Figure 2.8 Reaction scheme for TCPH with an aldehyde [49].

### 2.3.3.2 OXIMES

Oximes are ideal for GC analysis due to their volatility, providing good separation, while the reaction conditions are mild, unlike those for hydrazone formation [8]. Typical amine reagents used in HCHO derivatization reactions followed by GC analysis are discussed below.

## BENZYLHYDROXYLAMINE AND METHOXYAMINE

Benzylhydroxylamine and Methoxyamine can be applied to automobile exhaust and stationary source analysis. The reagents however, are not suitable for ambient air measurements since their reaction with low molecular mass aldehydes yield volatile products, hence detection limits were not reported for benzyloximes. Figure 2.9 shows the reaction scheme for benzylhydroxylamine with an aldehyde, and the scheme for methoxyamine with an aldehyde. The carbonyls were collected on silica gel, eluted with water, derivatised with benzylhydroxylamine and analysed using GC-NPD. Derivatives were well separated and could be detected to the picogram level. O-Methyloximes provided detection limits of 40ppb for aldehydes in air. For the determination of unsaturated aldehydes, particularly acrolein and crotonal, their respective O-methyloximes and benzyloximes are brominated and analysed using GC-ECD. The brominated acrolein methyloxime was detected at 0.5ppb in a 40L air sample [8].

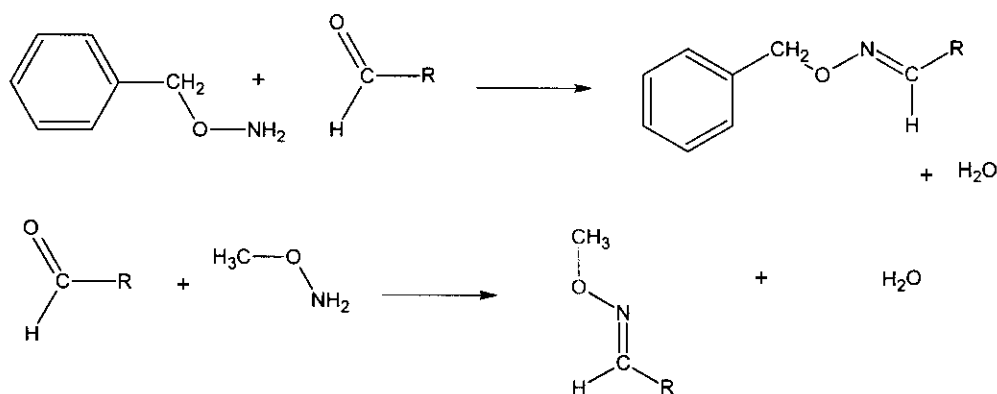


Figure 2.9 Reaction scheme for first, benzylhydroxylamine with an aldehyde. Second, methoxy amine with an aldehyde [8].



## O -(2,3,4,5,6-PENTAFLUOROBENZYL) HYDROXYLAMINE (PFBHA)

This reagent is ideal for the determination of trace amounts of volatile aldehydes in air samples [8]. The oximes that are formed are volatile and stable to high temperatures allowing for GC analysis. All the oximes have a common base peak of  $m/z$  181, which allows for easy identification with Mass Spectrometry [50]. The reagent has been used typically for determining aldehydes in drinking water with Electron-Capture Detection (ECD) [51] (EPA method 556) and Mass Spectrometry (MS) [50] as well as in beer [17], Cognac [52] and vegetable oils [53]. Recently PFBHA has also been used for indoor air and headspace sample analysis. C-18 silica gel cartridges coated with PFBHA were used to determine aldehydes in air emitted by vegetation as terpene oxidation products. After elution of the derivatives with hexane, a 50L air sample provided a detection limit of 2ppb using GC-MS [54]. Wu and Que Hee [55] developed a dynamic personal air sampler consisting of Tenax-GC solid sorbent coated with PFBHA, which was eluted with hexane and analysed by GC-MS. The detection limit for acrolein was 0.025ppm. Later, Wu and Que Hee [56] developed a passive sampler by applying the same concept. Martos and Pawliszyn introduced the use of a SPME PDMS/DVB fibre, for the *in-situ* derivatisation of HCHO. The headspace of an aqueous PFBHA solution coats the fibre, which is then exposed to the HCHO atmosphere or headspace of a sample. The fibre is then desorbed in the inlet of a GC oven. The technique is excellent for grab sampling and time weighted averaging for indoor air. Detection limits were as low as 15 ppb using GC-FID [22,57]. Figure 2.10 shows the reaction scheme.

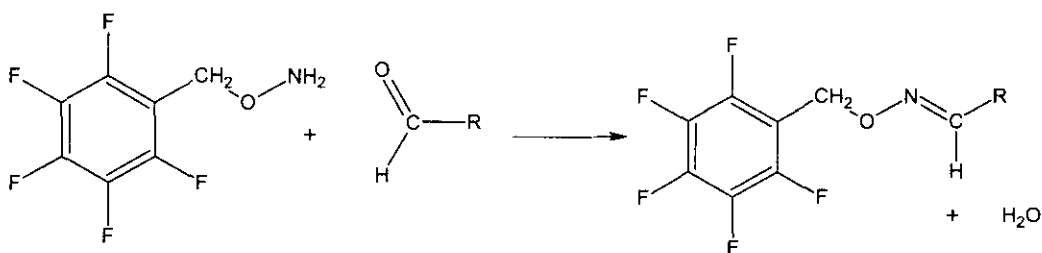


Figure 2.10 Reaction scheme for PFBHA with an aldehyde [50].

### 2.3.3.3 CYCLISATION REACTIONS

#### N - (BENZYLETHANOL) AMINE (BEA) -COATED SORBENT TUBE METHOD

Formaldehyde and most carbonyl compounds react rapidly with secondary aminoethanols to form the cyclic oxazolidine derivative, as shown in figure 2.11. Formaldehyde was collected on BEA coated Chromosorb sorbent. The derivative was extracted with isooctane and separated using GC-FID. Detection was in the range of 0.55-4.71mg/m<sup>3</sup> [8]. The method lacks sensitivity caused by the low sampling rate required to ensure derivative formation, and high blank levels. Thus, the reagent is not suitable for ambient air analysis. The use of a Nitrogen specific detector enhances sensitivity slightly. Acid gases/mists will react with the BEA and convert it to the ammonium salt, resulting in lower BEA reagent availability [21].

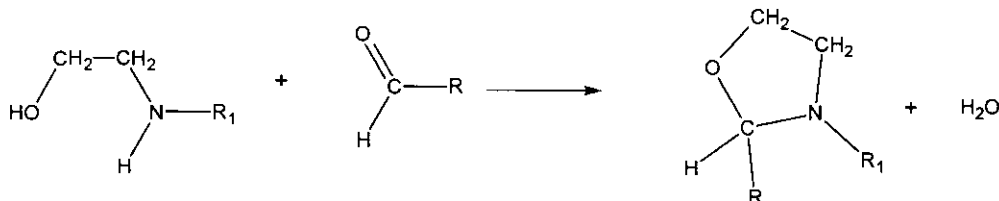


Figure 2.11 Reaction scheme for ethanolamine with an aldehyde [8,21].

## 2-HYDROXYMETHYLPYPERIDINE (HMP)

Kennedy, et al. determined acrolein in air by pre-concentration on a XAD-2 sorbent tube coated with 2-HMP. Acrolein forms a bicyclo-oxazoline, which can then be determined by Gas Chromatography - Nitrogen Specific Detection (GC-NSD) in the 0.13-1.5 mg/m<sup>3</sup> range [58]. Formaldehyde can also be determined by conversion to hexahydrooxazolo [3,4-a] pyridine in a denuder tube coated with 2-HMP (with a back-up tenax sorbent tube). Figure 2.12 shows the reaction scheme. Recovery can be done by thermal desorption followed by GC-MS analysis for which the limit of detection is in the range of 0.03 to 0.51 mg/m<sup>3</sup> [23]. NIOSH uses this technique for the determination of formaldehyde and acrolein in air (Method 2541) with a detection range of 0.3-20mg/m<sup>3</sup> [59], as well as aldehyde screening (Method 2539)[60] using GC –FID/MS detection.

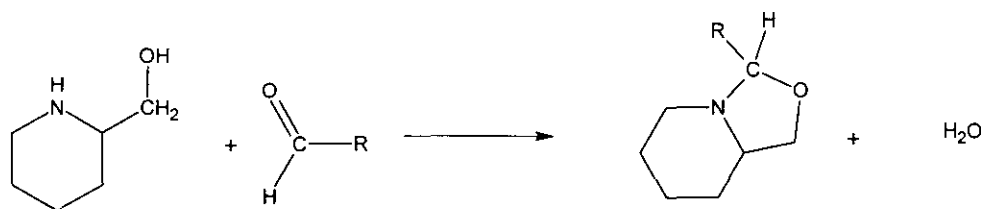


Figure 2.12 Reaction scheme of 2-HMP with an aldehyde [58-60,23].

## CYSTEAMINE (2-AMINOETHANETHIOL)

Cysteamine reacts readily with carbonyl compounds at room temperature and neutral pH. However, it does not react with  $\beta$ -unsaturated aldehydes such as acrolein and crotonaldehyde. Unlike certain derivatising reagents, no cis-trans isomers of the reaction product are formed making quantitation easier [8]. This reagent has been used in the determination of volatile carbonyl compounds in cigarette smoke [61] and automobile exhausts [62]. The smoke/exhaust is collected in a vessel containing an aqueous

solution of cysteamine. The carbonyl compound is converted to the thiazolidine as shown in figure 2.13, followed with analysis by GC with NPD. Detection limits are in the picogram range.

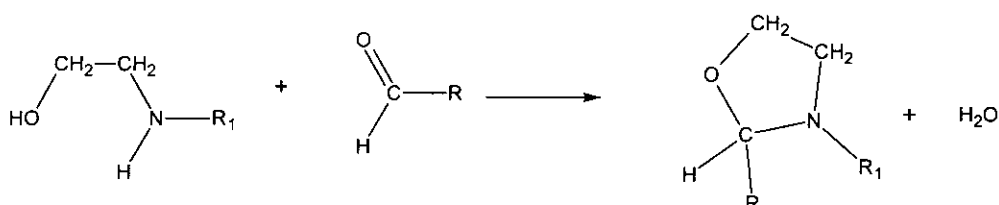


Figure 2.13 Reaction scheme of cysteamine with an aldehyde [8,61,62].

## AMMONIA

Formaldehyde is collected on a silica gel sorption cartridge that was coated with polyethylene glycol (PEG-400), to increase the polarity of the adsorbent. The pre-concentrated HCHO is extracted using aqueous ammonia, which HCHO reacts exclusively with to form a hexamethylenetetramine, shown in figure 2.14, which is analysed using GC-FID. Detection limits fall in the same range as for the use of 2,4-DNPH, but with the use of thermionic detection, the limit can improve [63].

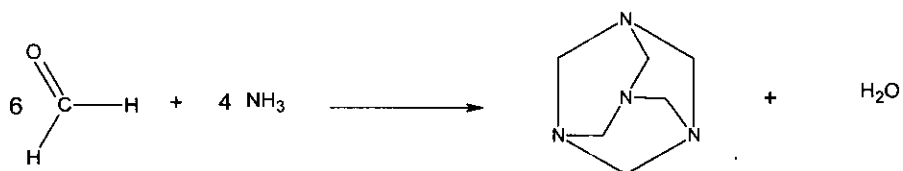


Figure 2.14 Reaction scheme for formaldehyde with aqueous ammonia [63].

### ACETYLACETONE OR DIMEDONE (5,5-DIMETHYL-1, 3 -CYCLOHEXANDION)

Aldehydes in air were determined by pumping air through a bubbler to which dimedone, ethanol and piperidine are added. An extensive sample workup consisting of washing, refluxing for 20 minutes, a triple extraction with diethyl ether and drying leads to an extract, which is analysed by GC-ECD. This method, unlike the 2,4-DNPH for GC method, can separate o-, m- and p-tolualdehyde as well as acrolein, propanal and acetone which are poorly separated by HPLC. The detection limit for acrolein was 80pg and benzaldehyde was 17pg[64]. Figure 2.15 shows the reaction scheme.

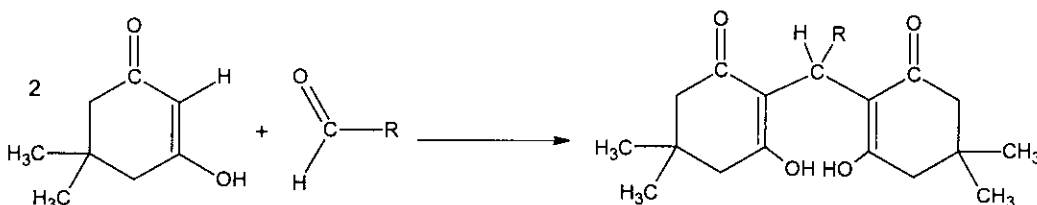


Figure 2.15 Reaction scheme for Dimedon with an aldehyde [64].

The reaction of the dimedon reagent above with HCHO in the presence of ammonia is otherwise known as the Hantzsch reaction. The reaction scheme is shown in figure 2.16. Formaldehyde has been simultaneously derivatised in, and extracted by CO<sub>2</sub> supercritical fluid using the Hantzsch reaction [65]. LC-MS has also been used to determine the derivatives of the Hantzsch reaction. An advantage of this reaction is that only the product exhibits fluorescent properties. Problems with increasing fluorescence in the reagent blank were experienced [66].

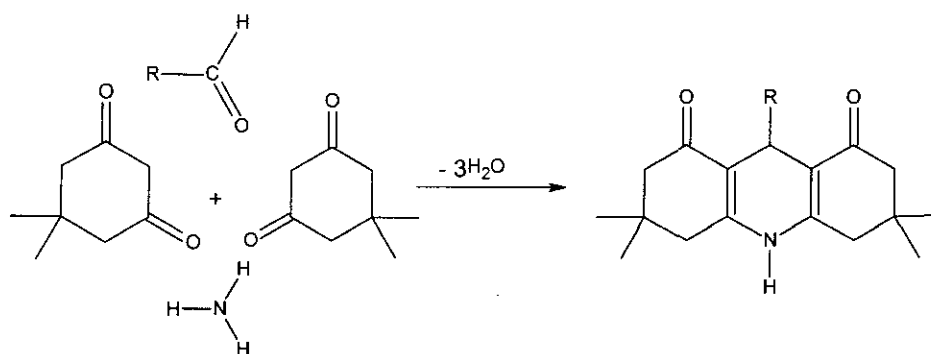


Figure 2.16 Hantzsch reaction scheme [65-66].

## 2.4 CONCLUSION

Despite all the available methods, not one of them can satisfy all the criteria for concurrent aldehyde analysis. The need for a field method, which is cheap, sensitive, selective and most importantly simple, is greater than ever.



## CHAPTER 3

### SAMPLE PREPARATION TECHNIQUES

#### 3.1 INTRODUCTION

Samples, which require analysis, are often too dilute, too complex or incompatible with the chromatographic system. Hence, some form of sample preparation is essential before any instrumental analysis. Ideally, sample preparation should require minimal effort and expense. Moreover, minimal sample preparation will decrease the amount of experimental uncertainty in the results obtained. Due to the nature of our research, we will only discuss those techniques concerned with the pre-concentration of gaseous volatiles from air. The flow diagram below shows a brief summary of the techniques commonly used.

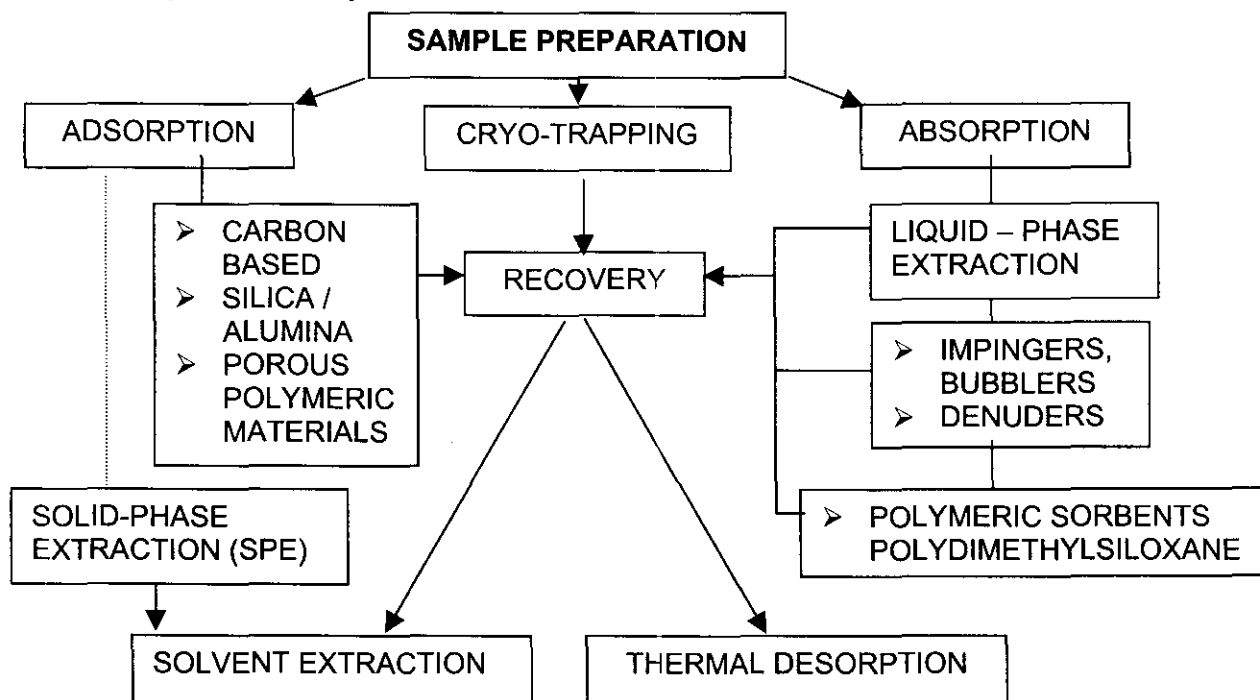


Figure 3.1 Flow diagram of sample preparation techniques for gaseous organic compounds.

### 3.1.1 DYNAMIC HEADSPACE SAMPLING

This technique is described here as it is used in our study to load our derivatising reagent and for analysing acetaldehyde in beer. Dynamic headspace sampling employs the continuous removal of the headspace vapours from a solid/liquid matrix, followed by collection on a trap such as a cryo-trap, solid phase extraction device or ad/absorbents [67-70].

The recovery (R) of analyte, from the dynamic headspace onto the trap can be described by the equation [67-70]:

$$R = 1 - \exp [-Ft / KV_L + V_G] \quad (3.1)$$

Where F is the stripping gas flow rate, t is the stripping time, K the gas-liquid partition coefficient,  $V_L$  is the sample volume and  $V_G$  the volume of gas passed through the liquid in time t. This equation was derived based on the assumption that the system is in thermodynamic equilibrium, no breakthrough occurs on the trap (i.e. a closed loop), the liquid matrix is involatile and the partition coefficient is independent of concentration [67-70].

### 3.2 ADSORPTION

Adsorption is a physical process occurring on the surface of adsorbents. As analytes are retained on active surfaces on the sorbent, the amount of adsorption that occurs is related to the available surface area of the sorbent, which in turn is related to the porosity of the material. The rate of adsorption is determined by the structure of both the micropores and the molecules moving into the pores [71]. Table 3.1 in Appendix 1 lists the more common types of sorbents used for pre-concentration, as well as their structure, uses, surface areas and pore diameters, advantages and disadvantages.

Adsorption tubes are prepared by packing the sorbent into glass tubes, of varying sizes depending on the application.

When choosing a sorbent for pre-concentration, it is not only important to see how well compounds are adsorbed that is, their retention, but also how easily they can be recovered.

Carbon-based adsorbents are cheap, all purpose pre-concentration sorbents.

However, desorption of the sorbates (particularly polar compounds) may prove difficult and water accumulation is high, making them unsuitable for thermal desorption with cryogenic focusing [19].

Porous polymers are typically used for pre-concentrating high molecular mass and non-volatile compounds such as pesticides. They are popular because they are relatively inert, have large surface areas and are hydrophobic. They also allow for collection of large sample volumes (100L) at high flow rates [73]. However, their general disadvantages include the displacement of VOC's especially by CO<sub>2</sub> [19], and the irreversible adsorption of certain compounds, such as amines [19]. Furthermore oxidation, hydrolysis and polymerisation of the sample may occur [19]. Except for Tenax, these adsorbents are thermally unstable above 250°C, which makes them unsuitable for thermal desorption as this leads to artefact formation [19]. At the same time, sorbents are not reusable after solvent desorption. Careful purification, which usually involves Soxhlet extraction with high purity solvents, of these sorbents is compulsory before they can be used for trace analysis [19]. Finally, porous polymers are more expensive than the charcoals.

All solid sorbents are ideally suited to trapping a particular series of compounds. In an attempt to trap a wider range of compounds, multi-layered traps, which utilise the best features of each adsorbent, have been prepared [74,75]

Sorbents used with solvent extraction are usually silica gel, activated charcoal,

Anasorb 747, carboxens (carbonised porous polymers), porous polymers and carbon

molecular sieves. Those used in sampling with thermal desorption include Tenax, Chromosorb 106, Graphitised carbons and carbon molecular sieves [71].

### 3.2.1 SOLID-PHASE EXTRACTION (SPE)

Solid-Phase Extraction (SPE) is not, traditionally, a technique used for pre-concentrating gaseous compounds. However, it has been included in the discussion because it has been used, predominantly, as a reagent coated sorbent [46,49,54] for derivatisation, and for the extraction of the derivatised products formed during liquid extraction [47].

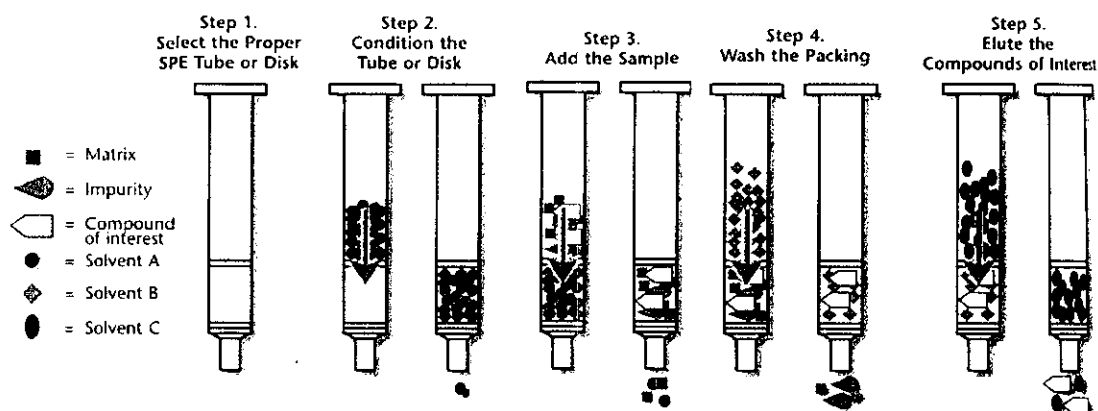


Figure 3.2. Steps involved in the SPE technique [76].

The SPE device is depicted in Figure 3.2. The SPE cartridge consists of a packed adsorbent column between two fritted plastic/metal disks in a polypropylene open syringe barrel [76].

Unlike LLE, which involves the partitioning of the analyte between two immiscible phases, SPE involves the partitioning of the analyte between a solid and a liquid phase. The analyte is extracted when its affinity for the solid phase is greater than for liquid phase. Later, the analyte is removed by extraction with a solvent for which the analyte has a greater affinity.

The liquid phase is passed through the cartridge by suction or positive pressure (e.g. gravity or gas pressure from a syringe).

Retention is caused by the intermolecular forces experienced between the analyte, the active sites on the sorbent-surface and the liquid phase [77].

Common sorbents used for SPE are based on silica gel with a modified surface.

According to the chemical groups bonded to the silica, the phases are classified as non-polar, polar or ion-exchangers.

Octadecyl surface phases (C18) are used for the reverse-phase extraction of non-polar compounds in aqueous solution. The shorter octyl phases (C8), are used to extract medium polarity compounds, while silica gel and alumina oxides are used for extracting polar compounds [78].

SPE is simple, requires less solvent and time than LLE, and it is easily automated.

However, it becomes a bit tedious with all the steps required to prepare the sorbent and then extract the analyte, as depicted in figure 3.2. Also, the packing quality varies from cartridge to cartridge [47].

To overcome problems encountered with the SPE cartridges, disk devices have been developed. They are either membranes or sorbents that have been packed into circular disks 0.5mm thick and 4 to 96mm in diameter. The sample processing rates are faster than those of the SPE columns and the small diameter disks are ideal for processing smaller samples [47].

### **3.2.2 BREAKTHROUGH VOLUME**

Breakthrough volume is a measure of the retention of an analyte on a sorbent i.e. retention capability. Tubes that are packed with ad/absorbents can be regarded as chromatographic columns, operating under frontal analysis conditions with a constant concentration of analyte. The analyte will continue to be ad/absorbed in the trap until it reaches its breakthrough volume ( $V_b$ ). This is usually when 5% of the initial

concentration of the analyte has started to elute from the trap. Therefore, the maximum sampling volume or breakthrough volume ( $V_b$ ), is described by Raymond and Guiochon [79] as:

$$V_b = V_r \times ( 1 - ( 2 / \sqrt{N} ) ) \quad (3.2)$$

Where  $V_r$  is the retention volume and  $N$  the number of plates of the trapping column. However, for short “columns” which have a low number of plates ( $N$ ), Lövkvist and Jönsson [80], have suggested a more realistic model for breakthrough volume, which can be described by:

$$V_b = V_r \times ( a_0 + ( a_1 / N ) + ( a_2 / N^2 ) )^{-1/2} \quad (3.3)$$

Where  $a_0$ ,  $a_1$  and  $a_2$  are coefficients for different values of the breakthrough level  $b$  described as [80]:

$b$  = total amount of analyte eluted from trap / total amount of analyte sampled

$b$  can vary from 0.1, 1, 2 to 10%, the popular value being 5%.

Baltussen et al [81], have applied this theory for breakthrough volume at 5%, on their silicone packed beds, giving:

$$V_b = V_0 \times ( 1+k ) \times ( 0.9025 + ( 5.360 / N ) + ( 4.603 / N^2 ) )^{-1/2} \quad (3.4)$$

Where  $V_0$  is the trap dead volume and  $k$  the capacity factor.



### 3.3 CRYO-TRAPPING

Volatile compounds can be trapped at temperatures lying far below their boiling points. This is usually achieved by collecting whole air samples through a steel tube or capillary, which is cooled by using either liquid nitrogen or carbon dioxide. To increase the condensing surface, the tubes are packed with an inert material possessing a high surface area such as glass wool or beads. The tube is then heated ballistically to a suitable injection temperature and the analytes are transferred onto the column. Unfortunately this set-up is not always sufficiently portable for field work, and extra care must be taken when sampling in humid environments as pre-concentrated water will freeze and block the trap [19].

### 3.4 ABSORPTION

Absorption is synonymous with dissolution and partitioning. In this process, the analyte will dissolve into a liquid where it is retained until it is thermally desorbed or preferentially extracted into a different solvent for which the analyte has a greater affinity.

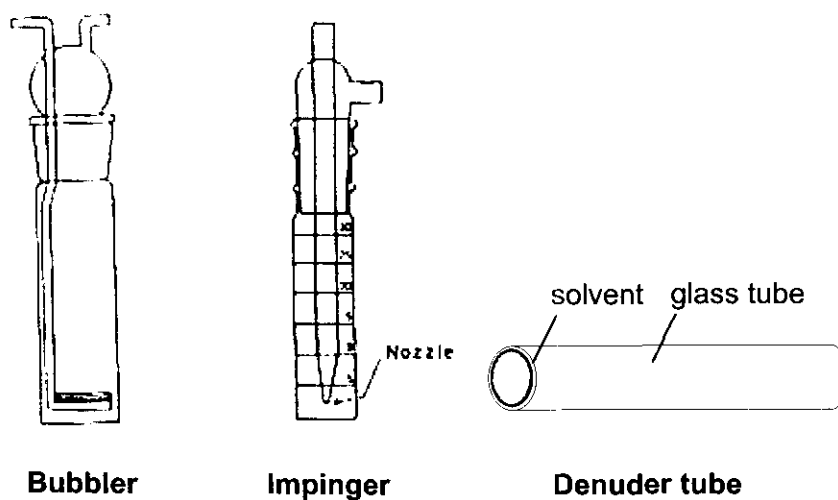


Figure 3.3. Liquid-phase extraction devices[82].

### 3.4.1 IMPINGERS AND BUBBLERS

Special devices such as impingers and bubblers are used to disperse sampled gas in a solvent, see Figure 3.3. The finely divided gas bubbles rise from the bottom of the vessel, allowing for more contact between the gas bubbles and the solvent as the bubbles move toward the surface. In the case of reactive compounds such as formaldehyde, a derivatising reagent is included with the solvent to improve the extraction efficiency and simultaneously provide a more stable compound [82]. Adjusting the temperature of the solvent may also improve extraction. These devices are often used for sampling of gases from industrial stacks and automobile exhausts. However, large sample volumes are required, which may involve the use of large pumps and the devices themselves are clumsy to wear. Due to the large volumes of solvent used there is also a dilution factor present and an additional concentrating step is required [18,82].

### 3.4.2 DENUDEERS

Denuders are open glass tubes that have been coated on the inside with a thin layer of solvent as in Figure 3.3. Air is sucked through the tube where the analyte gas, present in the air is extracted into the solvent. Unlike impingers and bubblers, higher collection flow rates may be used and the extract is more concentrated because of the smaller volume of solvent used [18]. Impingers and denuders have the advantage that any appropriate solvent can be used to trap a desired compound.

### 3.4.3 POLYMERIC SORBENTS

Adsorbents, LLE and SPE techniques, are undesirable because they carry contaminants into the final extracted sample, along with the analytes of interest, producing a high background in the analysis. Recently, polydimethylsiloxane (silicone) has emerged as an alternative to adsorbents and organic solvents used for pre-concentration [22,24-27,81,86,87,92-98].

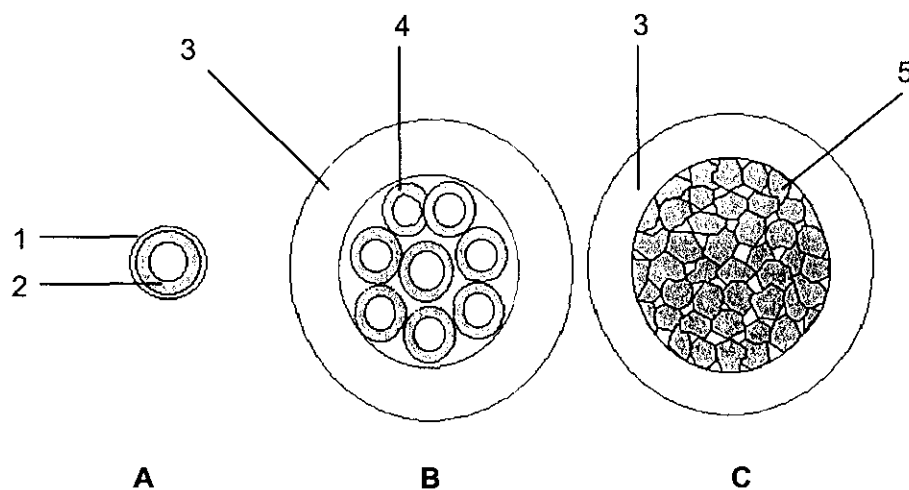
Polydimethylsiloxane is a non-polar, homogeneous liquid stationary phase used in GC capillary columns, generally known as SE-30, DB-1 or HP-1 columns. Just as the sample mixture injected onto a GC column will partition between the mobile and stationary phases leading to a separation of components, so too, will gaseous mixtures in air partition into silicone. The retention of the analytes from air in the trap is determined by their breakthrough volume, as previously discussed. The trapped contents in the silicone can then be extracted using a solvent [83] or by thermal desorption [25,81].

Apart from being inert, the silicone “fluid” is thermally stable (150-250°C) under oxygen-free conditions [78]. The advantage of thermally desorbing the silicone lies in its immediate reusability. In addition, all the silicone degradation peaks reveal repeatable retention times as well as easily identifiable Electron Impact (EI) mass spectral fragments. The main volatile silicone degradation products are methylcyclsiloxanes, with the most abundant of these being hexamethylcyclotrisiloxane (D3) followed by gradually decreasing amounts of the higher molecular mass cyclic siloxanes (D4, D5, D6...)[85].

Unfortunately, as we know that “like-dissolves-like”, polar compounds will be virtually unretained on a non-polar phase. Hence modified polymers e.g. polymethylacrylates etc. [86-88] have been developed in an attempt to increase the polarity of the stationary phase. However, these polymers no longer exhibit a dissolution process,

but rather an adsorptive process with all associated disadvantages and particularly high backgrounds during thermal desorption [86].

Due to the remarkable properties of silicone, it has been widely used, leading to several possible configurations as described below, and depicted in figure 3.4 and 3.5.



**A - Ultra Thick Film Open Tubular Trap**  
**B - Multichannel Silicone Rubber Trap**  
**C - Silicone Packed Bed Trap**

- 1 – Wide bore capillary column.
- 2 – Silicone rubber tube  $d_r$  145  $\mu\text{m}$ .
- 3 – Glass tube (60mm o.d. 40mm i.d. length~16cm).
- 4 – Multiple silicone rubber tubes (0.63mm o.d. 0.3 mm i.d.) arranged in parallel.
- 5 – Pulverised Silicone rubber particles.

Figure 3.4. Cross-sections of various trap configurations using 100% polydimethylsiloxane.

### 3.4.3.1 OPEN TUBULAR TRAPS (OTT)

Grob and Habich [89] introduced the use of OTTs to overcome the problems experienced due to incomplete transfer of desorbed analytes from packed column traps onto GC capillary columns. The difference in flow rates, obtained when moving from a packed column to a capillary column, was eliminated by using the OTT, which

has similar dimensions to a capillary column. Various coatings, ranging from activated charcoal to SE30, were used inside the OTTs for the pre-concentration of various compounds [83,89-92]. This also led to the development of ultra thick film OTTs, by Blomberg and Roeraade [93,94], and Burger et al [92,95]. Blomberg and Roeraade used dynamic coating techniques requiring special instrumentation, whereas Burger's technique is easier to prepare. A single 1m long silicone rubber tube is inserted into a fused silica capillary, to provide a film thickness of 145 $\mu$ m. The silicone tube needs to be first stretched and immersed into liquid nitrogen. In this way it is sufficiently manageable to be inserted into the capillary, figure 3.4A. The capillary then fits into a modified GC where it can be thermally desorbed onto another GC column for analysis. However, the OTTs show limited sampling capacity and can only operate under low sampling flow rates (10ml/min).

#### **3.4.3.2 THE MULTICHANNEL SILICONE RUBBER TRAP (MCT)**

Ortner and Rohwer developed the multichannel silicone rubber trap [72]. It is based on the same principle as the open tubular traps developed by Burger et al [95]. However, instead of one long silicone rubber tube inside a fused silica capillary, the trap is made more compact by having several shorter lengths of silicone rubber tubes arranged in parallel inside a glass tube, depicted in figure 3.4B. This makes the trap suitable for desorption in a conventional desorption unit. The trap exhibits a low pressure drop, allowing for collection at high flow rates, particularly of non-volatile compounds. However, to improve the extraction of semi-volatile analytes into the silicone [24,26] it is operated under low sampling flow rates (15ml/min) to increase the number of plates (N). The MCT has also been applied to the analysis of aqueous samples [25,27].

### 3.4.3.3 PACKED SILICONE BEDS

Baltussen et al [81,86,96-98] packed a glass tube with equally sized particles of pulverised 100% polydimethylsiloxane, shown in figure 3.4.C. As this method of packing allows for a low-pressure drop over the trap along with turbulent flow, high sampling flow rates (500ml/min) can be used. These packed beds have successfully been applied to the analysis of organic acids, PAHs and nitro-PAHs from air [96], for characterisation of natural gas [81], monitoring nicotine in air [98], and amines, pesticides and PAHs in aqueous samples [86,97]. An added benefit of these traps is that breakthrough volumes can be calculated and predicted based on the retention of analytes on an SE-30 column [81].

### 3.4.3.4 SOLID PHASE MICROEXTRACTION (SPME)

The SPME technique is in principle a solventless liquid-extraction, developed by Pawliszyn [87]. The SPME device resembles a syringe. A 1cm long thin polymeric fibre, normally silicone, is attached to the tip of the syringe plunger, which can be retracted into the syringe barrel, as depicted in figure 3.5[99]. This device is practical for piercing septa and exposing only the fibre to a hot GC inlet, vial etc.

Unlike the other pre-concentration techniques, which are typically dynamic because they involve a flowing stream of gas passing over the sorbent, SPME is a static sampling technique.

The fibre is exposed either to the headspace of a sample or immersed in a liquid sample in a sealed vial for a precise period of time. The analytes will partition into the liquid phase until a distribution-equilibrium has been reached. This process usually takes between 2-30min. Equilibrium can be attained more rapidly in headspace SPME than in immersion SPME, as the analytes can diffuse more rapidly towards the

fibre. This extraction step is equivalent to one theoretical plate (N). From the equation below [87,99], it can be seen that the amount extracted (n), is directly proportional to the concentration of the analyte in the sample ( $C_o$ ).

$$n = \frac{K_{fs} V_f V_s C_o}{K_{fs} V_f + V_s} \quad (3.5)$$

Where  $K_{fs}$  is the distribution coefficient between the fibre and sample.  $V_f$  is the volume of the fibre,  $V_s$  is the sample volume and  $C_o$  the initial concentration of the analyte in the sample [87,99]. Consequently, trace analysis of analytes having a small partition coefficient ( $K_{fs}$ ) will require sensitive instrumentation.

As for solvent extraction, the extraction efficiency can be improved by adjusting the pH, temperature, fibre ("solvent") polarity, fibre thickness, salt content and agitation. Various SPME fibre coatings, of differing thickness, have been developed by forming copolymers with the silicone (e.g. PDMS/DVB for non-polars), adding adsorbent material to the coating (e.g. Carbowax/PDMS), or by using a different polymer (e.g. polyacrylate for polar compounds). However, these variations do not exhibit dissolution properties as described for the liquid silicone polymer above [99].

In addition, when the analyte is too volatile or unstable derivatisation techniques can be used. This is done by coating the fibre with derivatising reagent followed by reaction with the analyte (*in-situ* derivatisation) [22,43]. SPME is suitable for the analysis of large sample volumes, as shown by equation (3.6), taken from (3.5) where  $V_s \gg K_{fs} V_f$  [87,99],

$$n = K_{fs} V_f C_o \quad (3.6)$$



As the amount extracted by the fibre is independent of the sample volume, the thickness of the fibre plays a larger role. Compounds with a low  $K_{fs}$ , are efficiently extracted by using a thicker fibre and vice versa.

After extraction, the fibre is conveniently thermally desorbed in a hot GC inlet during the splitless mode.

For precision and to save time, reproducible fibre exposure time, desorption time, vial size, sample volume and other sampling parameters are much more important than obtaining full equilibration between fibre and analyte.

This sample preparation technique has become popular because it is simple, rapid, solventless and has demonstrated low detection limits. However, the fibre has proven fragile and is easily destroyed if not handled with care. Also, depending on the sample complexity and desorption conditions, the fibre may not be reusable due to memory effects. Under ideal conditions, the fibre assembly can provide 50-100 extractions [99].

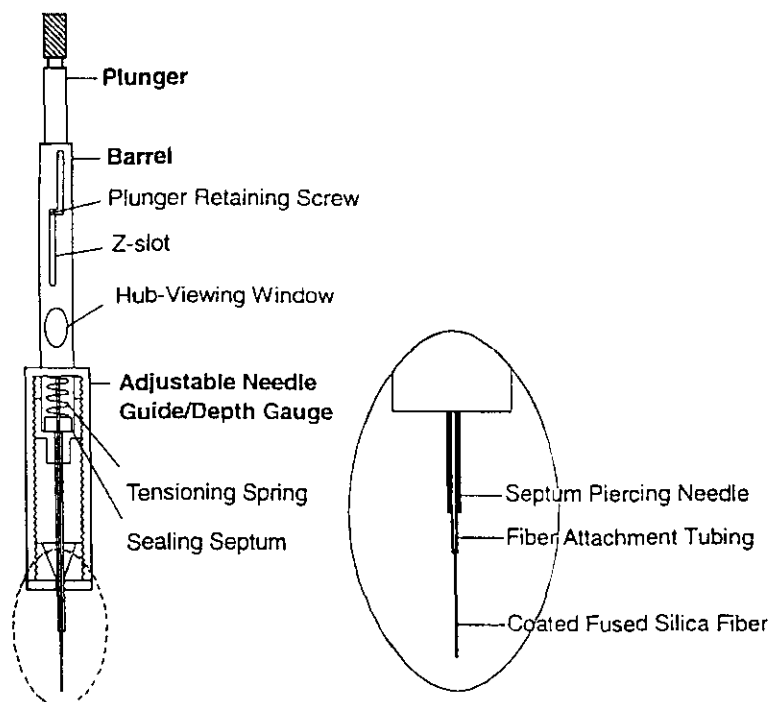


Figure 3.5. A commercial SPME device from Supelco [87].

A similar approach called Headspace Sorptive Extraction (HSSE) [100] uses a small glass rod coated with a large amount of polydimethylsiloxane (50mg). This is used similarly to the SPME fibre by exposure to headspace samples, except it is thermally desorbed in an automated thermal desorber. In addition, HSSE shows increased sensitivity over SPME as the volume of absorbent ( $V_t$ ) is much larger.

### **3.5 RECOVERY**

#### **3.5.1 SOLVENT EXTRACTION**

This technique is otherwise known as liquid-liquid extraction [72,82]. A solvent can be used to isolate analytes from a liquid sample or from a solid, in our case the sorbents. The technique relies on a distribution of the analyte between two immiscible phases. For acids and bases the distribution coefficient ( $K = C_{\text{solvent}} / C_{\text{sample}}$ ) is easily affected by the pH of the solution and in this way the extraction can be made more selective. In general, the principle that “like-dissolves-like” is applied. Polar analytes will dissolve into polar solvents and non-polar analytes into non-polar solvents. The sample solution is shaken up with an equal amount of solvent in a separation funnel. When the 2 phases separate, the desired fraction is collected. The extraction efficiency increases with the number of extractions. Because the final fraction still contains a large amount of solvent, an extra step is required to concentrate the extract before it can be analysed. Analytes with small  $K$ 's or large sample volumes require continuous extraction or counter current extraction to achieve a complete separation [72,82]. Overall, this is a simple but time-consuming technique and the general trend is to move away from these methods. In addition, the large volumes of high purity solvents required for such extractions are toxic and expensive.

Recently, these disadvantages were minimised with the introduction of liquid-liquid micro-extractions. Typically, 1ml of solvent is added to 10ml of sample in a vial and the extract can be injected without further pre-concentration.

### 3.5.2 THERMAL DESORPTION

Thermal desorption is the process through which the analytes on a sorbent are removed by heat energy. During this process, the analytes are transferred onto the chromatographic column. However, it is common to have a refocusing step before transfer onto the column. Usually, a second trap is cooled, using either liquid nitrogen or CO<sub>2</sub> gas, to sub-ambient temperatures ranging from 0°C to –100°C. This second trap is heated ballistically after desorption, in order to transfer the analytes in a narrow plug onto the column. A description of the instrument used for thermal desorption is given in chapter 5.

Thermal desorption has several advantages over solvent extraction. The main one being the removal of the dilution effect. With solvent extraction only a small fraction of the entire extract is injected for analysis. In addition, thermal desorption requires no expensive high purity solvents or labour to perform the liquid extractions as automated thermal desorption units allow for the desorption of several traps overnight. Disadvantages include the occasional blocking of the cryogenic trap. Although this can be prevented by avoiding the use of hydrophilic sorbents. In addition, instrumentation and use of large quantities of liquid nitrogen becomes expensive [18,19].

## CHAPTER 4

### GAS STANDARDS

#### 4.1 INTRODUCTION

In order to determine unknown quantities of formaldehyde and other aldehydes in the environment, it is important to test the method on controlled aldehyde atmospheres. Although there are commercial formaldehyde gas standards available, several methods for their generation in a laboratory do exist [101-104,23,32,39,40].

The gas standard used should provide stable, accurate, reproducible and controllable concentrations of the aldehyde studied, at the part-per-million (ppm) and part-per-billion (ppb) levels. It should be simple and ensure that sufficient amounts of the standard will always be available.

There are two types of methods for generating gas standards namely, static and dynamic methods [101,105-107].

#### 4.2 STATIC METHODS

Static methods [101,105-107] involve the addition of a known amount of pure analyte gas or vapour to a known volume of diluent gas (nitrogen or purified air) into a closed container, e.g. Teflon bags [22,55], stainless steel cylinders or glass

vessels [32,108]. Mixing of diluent and pure gas then occurs. Although this method is simple and inexpensive, losses of the analyte may occur due to adsorption and condensation on the walls of the container. Leaks can occur and pressure changes will exert an effect on the final concentration. Only limited volumes can be prepared, and poor accuracy arises with the introduction of a small volume of analyte into a dilution gas. Because of these difficulties static methods are not suitable for the preparation of low concentration gas standards of polar analytes.

### **4.3 DYNAMIC METHODS**

Dynamic methods [101,105-107] provide a constant concentration of analyte gas over a long period of time. They involve the continuous addition of analyte gas or vapour, having a known generation rate, into a flowing stream of diluent gas with a known flow rate. Once an equilibrium has been reached, these methods have an advantage over static methods. Losses due to adsorption or condensation against the walls are now negligible, since all surfaces are coated with the analyte. Additionally, a wide dynamic range can be obtained by varying the concentrations. These methods also provide flexibility of collection volumes and flow rates used. The main disadvantage is that the equipment used for this set-up is more elaborate and expensive.

Dynamic methods can be divided into 2 groups namely permeation and diffusion methods [101,105-107].

#### 4.3.1 PERMEATION METHODS

In this method the idea is to mix a small known volume of the analyte gas or vapour, which passes through the membrane of a permeation device, with a known volume of diluent gas [23,39,40,101,105-107,109-113].

The permeation device normally consists of a PolyTetraFluoroEthylene (PTFE, Teflon®) tube, which is sealed on both ends with Teflon plugs or glass beads, after the analyte gas, liquid or solid is introduced. Teflon is chosen for the construction of the device, because it is chemically inert. After a certain period, if the temperature is held constant, the vapour will continuously permeate through the membrane of the tube at a constant rate. A standard mixture can then be obtained if the permeation tube is immersed in a flowing stream of a purge gas, with a known flow rate.

At equilibrium, the permeation rate( $r$ ) of the analyte gas through a membrane is given by [101,105,107]:

$$r = DS ( P_1 - P_2 ) ( A / d ) \quad (4.1)$$

Where  $D$  is the diffusion coefficient,  $S$  is the solubility constant,  $P_1$  and  $P_2$  are the partial pressures of the permeant gas on the two sides of the membrane,  $A$  is the membrane area and  $d$  is the membrane thickness.

By using the Arrhenius equation, the permeation coefficient,  $B$ , for a particular gas can be expressed as [101,105,107]:

$$B = DS = B_0 e^{(-E_p / RT)} \quad (4.2)$$

Where  $E_p$  is the permeation activation energy,  $R$  is the gas constant and  $T$  is the absolute temperature of the membrane.

The following equation can now be obtained by substituting equation 4.2 into equation 4.1 [101,105,107]:

$$r = B_0 e^{(-E_p/RT)} (P_1 - P_2) (A/d) \quad (4.3)$$

As shown by this equation, the permeation rate is proportional to the area and membrane material type and inversely proportional to the thickness of the membrane.

To maintain a 1% accuracy in the permeation rate, it is necessary to control the temperature of the permeation tube to within  $\pm 0.1^\circ\text{C}$ , since it can be seen from equation 3 that the permeation rate varies logarithmically with the inverse temperature ( $1/T$ ) [101,109].

Quite often the above constants are not available to allow prediction of the permeation rate. However, a gravimetric method exists which can also be used to determine the permeation rate. In an environment where the temperature is constant, and a flowing stream of diluent gas is present, the mass loss of the tube is equal to the mass of permeating analyte. The mass loss of the permeation tube must be weighed at room temperature to the nearest 0.01mg. Several measurements will allow the construction of a mass *versus* time graph. The first few points that deviate from the straight line are excluded as these indicate that a steady state has not been reached. The slope of the straight line best fitting the points obtained provides the permeation rate, which can also be described by the following equation [101,109]:



$$r = W / t \quad (4.4)$$

where  $W$  is the mass loss (g) over the time interval  $t$  (min).

Errors in the concentration are generated when the permeation rate is not accurately determined. Since the permeation rate is dependant on the temperature, it remains very important that during calibration the temperature remains constant to within 0.1°C. The tube should always be used at that calibration temperature [101,109].

Permeation methods used to generate formaldehyde gas standards have been used previously [23,39,40,101]. One method involves the thermal depolymerisation of paraformaldehyde or  $\alpha$ -polyoxymethylene inside the permeation tube [23,39,40,101]. Thermal depolymerisation occurs when the permeation tube is inserted into a glass gas-tight chamber, which is then placed inside a system where the temperature can be controlled at 80°C, e.g. in a thermostated oven or oil bath. There is an inlet for the purging and dilution gas, which allows the gas to be conditioned to the same temperature before entering the chamber. At this stage the dilution gas mixes with the permeated formaldehyde in the chamber and forms a standard gaseous mixture [23,101]. Another method involves the generation of formaldehyde inside a permeation cell. Paraformaldehyde is loosely packed into a gas-tight glass or stainless steel cell with quartz wool. A PTFE permeation tube is placed inside the cell, with one end connected to the purge gas flow and the other end to the mixing chamber. The temperature of the cell was controlled as above. Formaldehyde diffuses into

the teflon tube where it mixes with the diluent gas, then moves on into the chamber. The formaldehyde concentration is monitored over time by a UV spectrometer. Once the concentration (absorbance) over time becomes constant, the standard can be used. In this method, the formaldehyde concentration is inversely proportional to the total flow rate of the diluent gas [101].

It should be noted that, at moderate temperatures, formaldehyde can decompose into carbon monoxide and hydrogen, particularly when in contact with metal surfaces. Hence a modification of this method was made using a silicone membrane and thermally depolymerising  $\alpha$ -polyoxymethylene therein [101,103].

#### 4.3.2 DIFFUSION METHODS

Gas standards are most commonly prepared via diffusion methods [58,101,105-107]. These methods involve the maintenance of a saturated vapour pressure in a reservoir and diffusion through a capillary tube into a stream of purging gas to make a mixture of known concentration. Diffusion of the vapours through the capillary tube will occur at a constant rate, if the tube geometry and temperature remain constant. If it can be assumed that the concentration of the vapour generated at the upper part (mixing chamber) of the diffusion tube is nearly zero and the lower part (reservoir) is saturated, then the following equation can be used to describe the diffusion rate  $r$ , in grams per second [101,105-107,114].

$$r = ( DMPA / RTL ) \ln [ P / ( P - P_v ) ] \quad (4.5)$$

$D$  is the diffusion coefficient ( $\text{cm}^2/\text{s}$ ) at pressure  $P$  (atm) and temperature  $T$  (K).  $M$  is the molecular mass (g/mol).  $P$  is the pressure at the open end of the capillary

tube (atm),  $A$  is the cross-sectional area of the diffusion path ( $\text{cm}^2$ ) and  $R$  is the gas constant ( $\text{cm}^3 \cdot \text{atm} / \text{mol} \cdot \text{K}$ ).  $T$  (K) is the absolute temperature of the diffusion cell,  $L$  is the length of the diffusion path (cm) and  $P_v$  is the partial pressure of the diffusion vapour (atm) at the temperature  $T$ . From this equation, it can be seen that the diffusion rate is dependent on the geometry of the diffusion path, pressure and temperature.

Diffusion methods have been used to generate formaldehyde gas standards [101,114-116]. One method uses a diffusion cell made of pyrex glass consisting of a reservoir and a long-neck capillary tube. The desired concentration range is obtained by varying the dimensions of the diffusion tube, the temperature of the system and the flow rate of the diluent gas. The paraformaldehyde, or trioxane [102], thermally depolymerises in the reservoir to form the formaldehyde vapour, which diffuses through the tube into the mixing chamber where it mixes with the purging gas flowing above the opening of the capillary tube. The diffusion coefficients can be obtained from literature and the diffusion rate can be calculated using equation 4, and alternatively, calibration of the diffusion tube can be done gravimetrically, as for the permeation tube [101]. Lower concentrations of formaldehyde can be obtained by diluting the gas mixture again further downstream [101].

#### 4.4 EXPERIMENTAL

Gas standards of selected saturated aldehydes, namely formaldehyde, acetaldehyde, propionaldehyde (propanal) and butyraldehyde (butanal) were prepared as well as a few unsaturated aldehyde gas standards of acrolein, crotonaldehyde and benzaldehyde.

A diffusion and permeation tube was prepared, to provide a high and low concentration respectively for each compound, and also to determine which generation method provided the more stable standard.

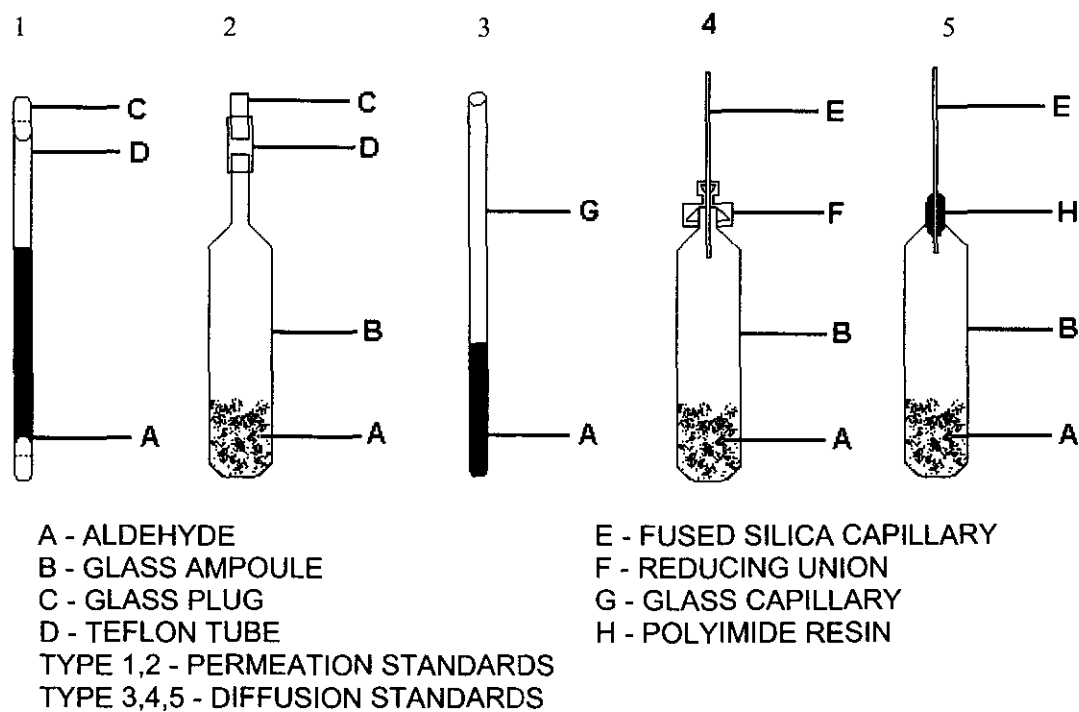


Figure 4.1. Aldehyde gas standard devices.

The diffusion standards, see figure 4.1, type 3, were prepared by placing a certain amount of a compound into a glass capillary tube, sealed at one end only. Formaldehyde gas had to be prepared at a higher temperature, so it was handled separately from the other aldehydes. All the diffusion standards, excluding formaldehyde, were then collectively placed in a closed glass container, having an inlet and outlet, where nitrogen gas could flow over the open-ends of the capillary tubes, allowing diffusion of the aldehydes to occur over the length of the capillary. Diffusion rates were determined by measuring the mass loss of each capillary over a time period. The entire set-up, excluding that for formaldehyde, was placed under a fume hood as several of these compounds are toxic by inhalation [6], and simultaneously this kept the temperature constant.

Permeation standards, see figure 4.1, type 1, were prepared by placing a certain amount of aldehyde into a thin-walled teflon tube, which is then sealed at both ends with pieces of sealed glass capillary. All the permeation tubes, excluding formaldehyde, are placed in a glass tube, large enough to allow nitrogen to flow over the PTFE surfaces of each tube as for the diffusion standards. The permeation rate was also determined gravimetrically, as above.

The diffusion and permeation tubes for the preparation of the formaldehyde gas standard were placed in a GC oven, thermostated at 80.05°C, allowing simultaneously, for the thermal depolymerisation of paraformaldehyde and preventing the repolymerisation of liberated formaldehyde. The permeation tube for formaldehyde was prepared as for the other aldehydes, figure 4.1, type 1. The diffusion tube was prepared differently, see figure 4.1, type 4. A 1/16 " to 1/4" reducing union was fitted to a glass vessel consisting of a reservoir and short

1/4" neck. A length of fused silica capillary was inserted into the union and held in place with a column ferrule. Since the diffusion rate is dependent on the diffusion path length and cross-sectional area, the diffusion rate could be varied by changing the length and/or bore of the fused silica capillary.

Mass loss versus time graphs were plotted for each device, see Figure 4.2.a,b. From the slope of the curves it could be seen that the aldehyde diffusion and permeation tubes made did not provide low enough mass loss rates. How would it be possible to lower the mass loss rate? Firstly, of the two generation methods the permeation tubes provided the lower mass loss rate. Secondly, it could be possible to modify the permeation device. From equation 1, the permeation rate is directly proportional to the area of the membrane ( $A$ ) and inversely proportional to the thickness of the membrane ( $d$ ). With this in mind, it was decided to decrease the area through which the aldehyde could permeate by decreasing the length of the tube, see figure 4.1, type 2. For acrolein, which has an extremely high mass loss rate, we decided to use a thick-walled teflon membrane, which increases the term,  $d$  (membrane thickness), resulting in a proportional decrease in permeation rate,  $r$ , as seen from equation 4.3. Results obtained are shown in Figure 4.2c. Since these permeation standards were larger in size they could no longer be inserted into the glass tube with the nitrogen blowing through it. They were placed, instead, in an impinger type device. Table 4.1, shows a summary of the results obtained for all the gas standards prepared.

Table 4.1 - Summary of gas standard devices prepared and results obtained

	ACETALDEHYDE			PROPANAL			BUTANAL	
type	3	1	2	3	1	2	3	1
length (cm)	9			9			9	
I.D (mm)	1.2	1.6	1.6	1.2	1.6	1.6	1.2	1.6
wall width (mm)	-	0.25	0.25	-	0.25	0.25	-	0.25
mass loss (ng/min)	<b>40</b>	<b>60</b>	<b>40</b>	<b>100</b>	<b>30</b>	<b>7</b>	<b>40</b>	<b>10</b>
r <sup>2</sup>	0.9744	0.9563	0.9922	0.9956	0.9921	0.989	0.9899	0.9806

	ACROLEIN				CROTONAL			BENZALDEHYDE	
type	3	1	1	2	3	1	2	3	1
length (cm)	9	5	4	1	9	5	1	9	5
I.D (mm)	1.2	1.6	1.6	1.6	1.2	1.6	1.6	1.2	1.6
wall width (mm)	-	0.25	1.6	1.6	-	0.25	0.25	-	0.25
mass loss (ng/min)	<b>4000</b>	<b>300</b>	<b>90</b>	<b>20</b>	<b>900</b>	<b>100</b>	<b>30</b>	<b>50</b>	<b>9</b>
r <sup>2</sup>	1	0.9947	0.9991	0.997	0.9874	0.9989	0.9902	0.9969	0.9984

	FORMALDEHYDE									
type	4	4	4	4	5	1	1	1	2	
length (mm)	74.25	77.8	84.1	74.5	64.5	54.65	51.2	50	10	
I.D (mm)	0.54	0.32	0.25	0.1	0.1	4.55	1.6	1.6	1.6	
wall width (mm)	-	-	-	-	-	0.25	0.25	1.6	1.6	
mass loss (ng/min)	<b>400</b>	<b>100</b>	<b>80</b>	<b>200</b>	<b>400</b>	<b>600</b>	<b>200</b>	<b>80</b>	<b>10</b>	
r <sup>2</sup>	0.9991	1	0.9943	0.9825	1	0.9956	0.9908	0.997	1	

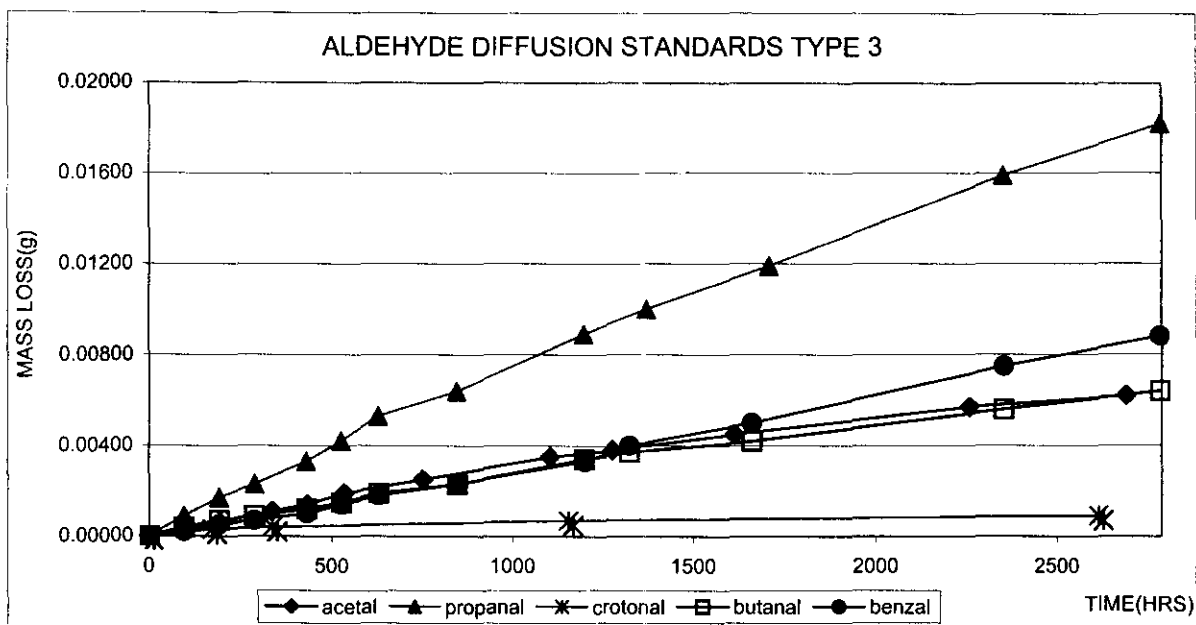


Figure 4.2 a\* - Mass loss curves for the aldehyde diffusion gas standards prepared.  
\* Acrolein mass loss curve not shown, as diffusion was too rapid.

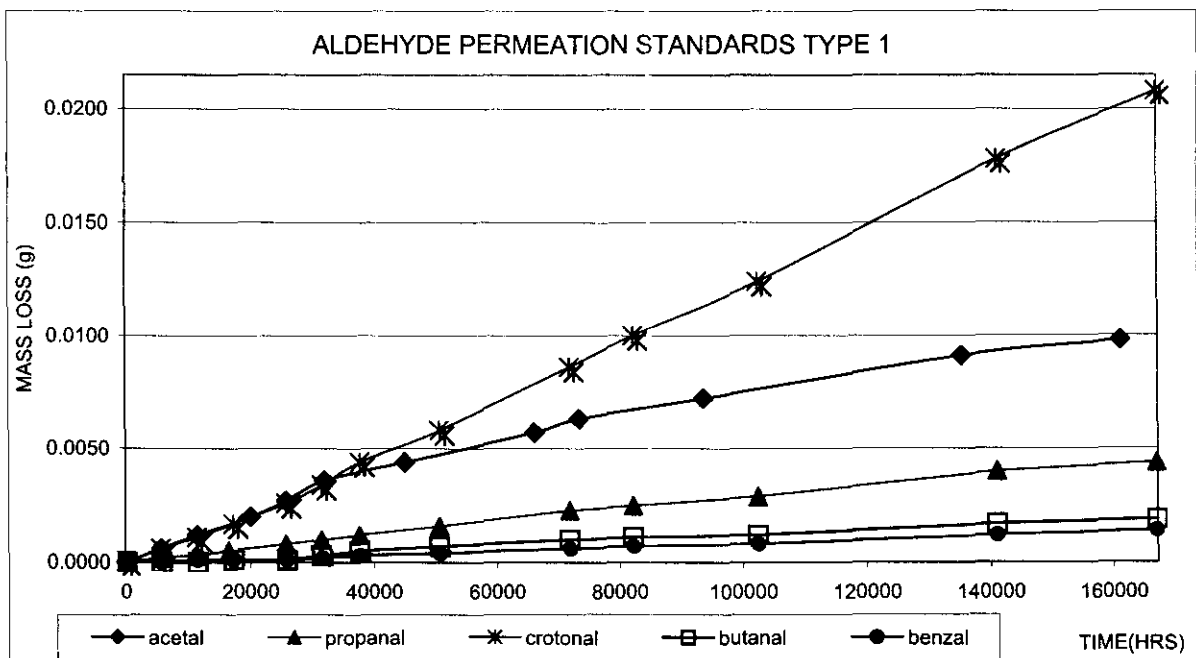


Figure 4.2 b# - Mass loss curves for the aldehyde type 1 permeation gas standards.  
# Acrolein mass loss curve not shown, as permeation was too rapid.



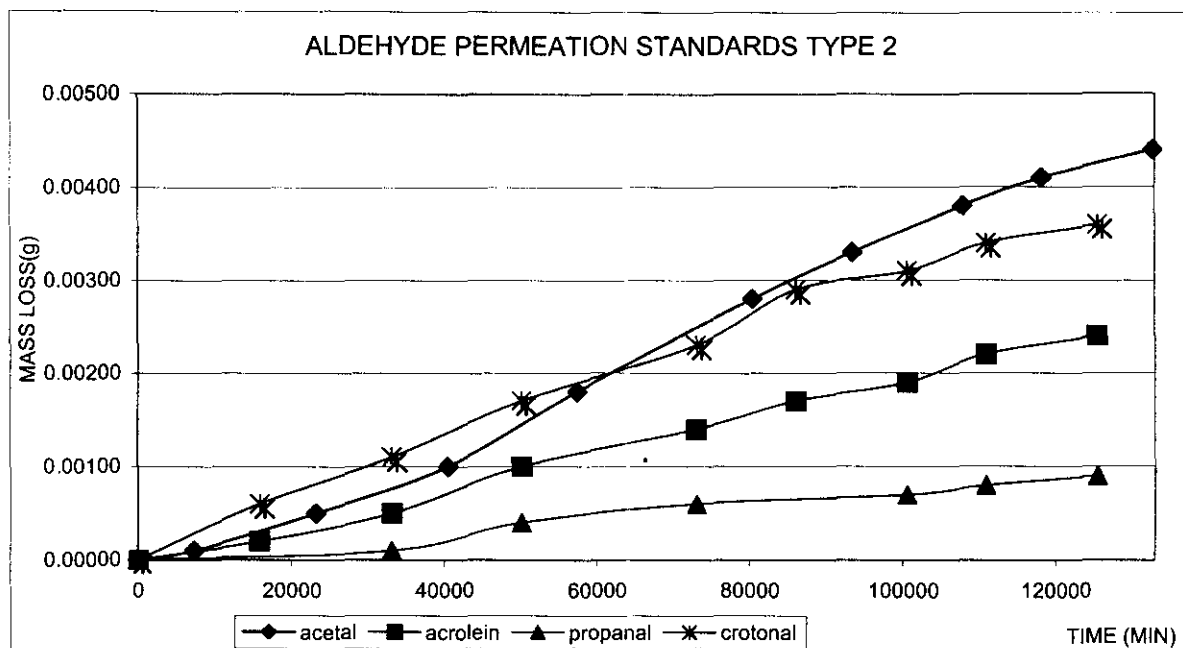


Figure 4.2 c\*\* - Mass loss curves for the aldehyde type 2 permeation gas standards.  
\*\* No butanal and benzaldehyde gas standards of this type were prepared.

The formaldehyde gas standards mass loss rates were too high (400 - 100 ng/min) to be used without an additional dilution step. The mass loss curves for the HCHO gas standards prepared are shown in figure 4.2.d. A diffusion standard with a longer length of fused silica capillary was attempted, but proved too cumbersome and delicate to be inserted into the PTFE vessel used at the time. For the HCHO diffusion vessel (Table 4.1,type 4), a proportional decrease in diffusion rate had already been observed for the change from the 0.54mm (400ng/min) to the 0.25 mm i.d capillary (80ng/min). This trend was expected to continue when moving from the 0.25mm i.d fused silica capillary to the 0.1mm i.d fused silica capillary, but this was not the case. Most likely, the ferrule around the narrow bore capillary was not leak-tight. Polyimide resin (Figure 4.1,type 5) was used as an alternative to the column- nut and ferrule in order to obtain a leak tight seal. A diffusion rate of 400ng/min indicated that this was not achieved.

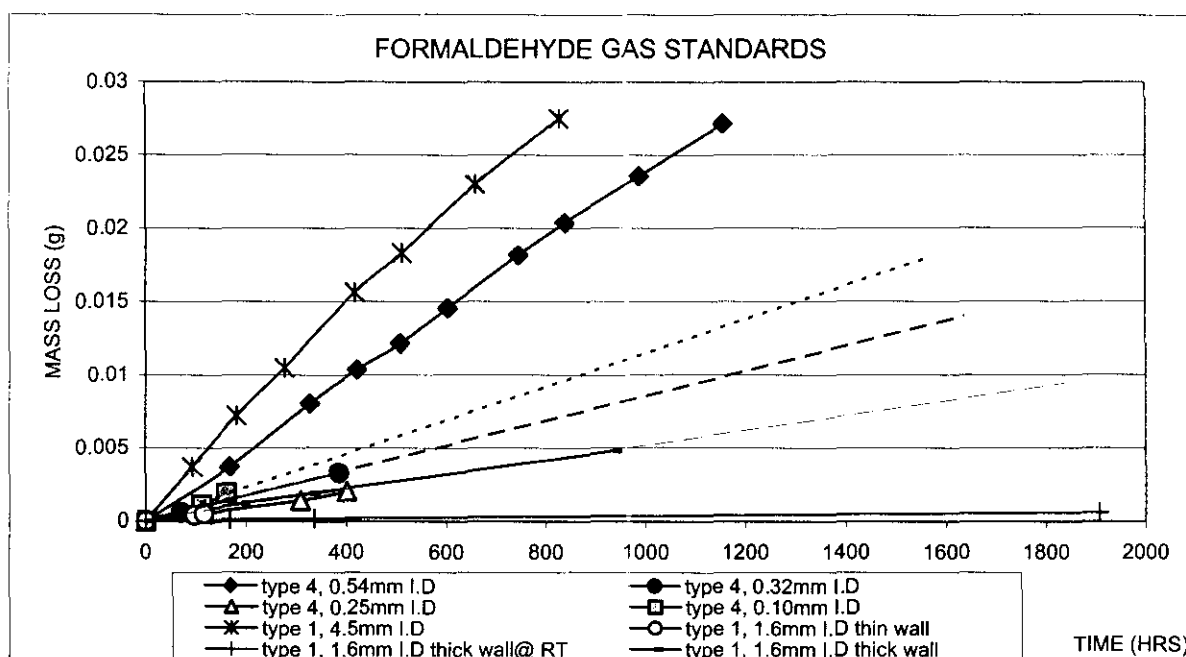
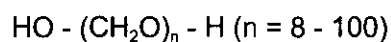


Figure 4.2 d - Mass loss curves for the formaldehyde gas standards.

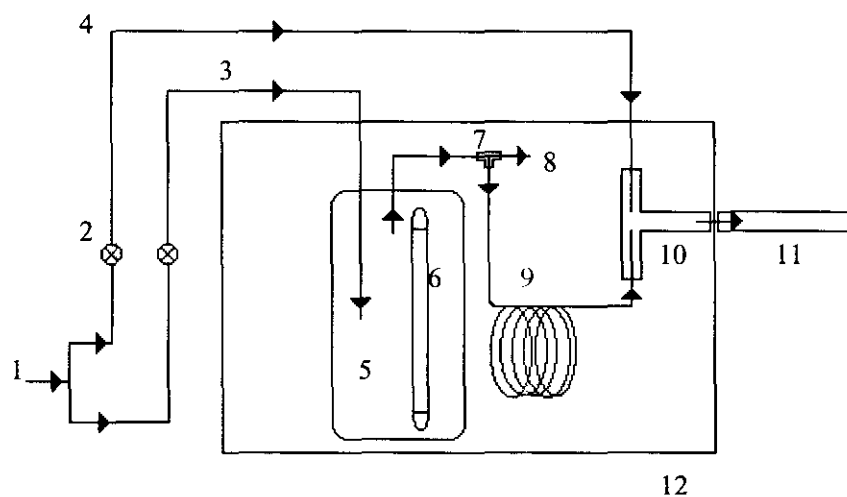
It was then decided to substitute the thin-walled HCHO permeation device (200ng/min), with a thick-walled membrane, figure 4.1, type 1. This provided a mass loss of 50ng/min, but as yet was not low enough. The only alternative remaining was to use a lower temperature.

As Paraformaldehyde is a polymer built up with formaldehyde monomers,



it was then considered that perhaps it was not necessary to fully depolymerise the paraformaldehyde, but rather to use its vapour pressure at room temperature instead, which is well above atmosphere. HCHO, however polymerises easily at temperatures below 80°C, it will not repolymerise between 80°C and 100°C [15]. Now assuming that the HCHO concentration is low enough once it has permeated through the membrane, repolymerisation should theoretically not be

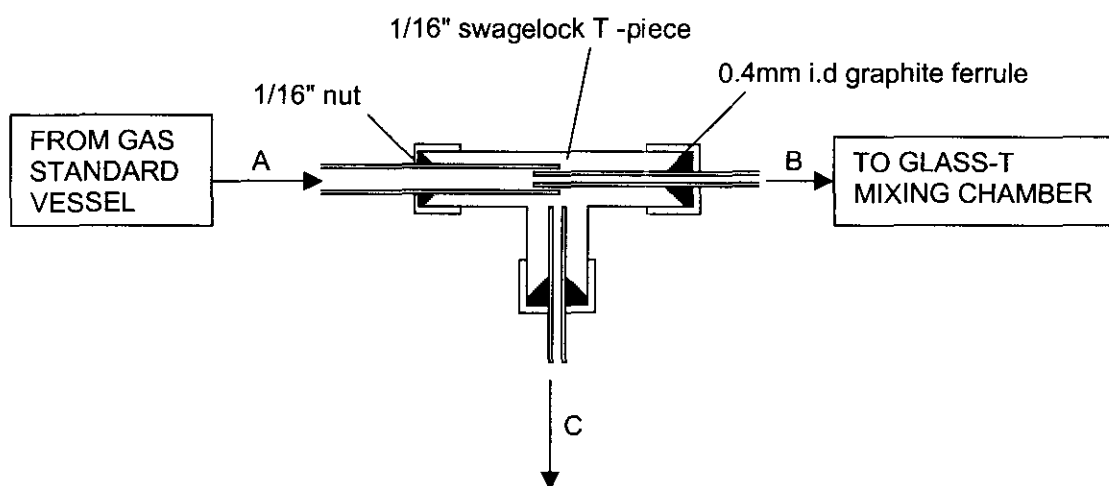
able to take place at lower temperatures. With this assumption, the thick-walled permeation tube (figure 4.1, type 2) was calibrated at room temperature and provided a mass loss of 10ng/min which was ideal. With time, however, it was discovered that there was no longer any mass loss even though the paraformaldehyde was still clearly present. While the HCHO permeated through the membrane, it managed to concentrate in the membrane and repolymerise. All the pores were thereby blocked, making it impermeable to any further HCHO moving through. The low temperature method thus had to be abandoned. A description of all the HCHO gas standards prepared as well as their mass loss rates are summarised in Table 4.1.



- 1 - HIGH PURITY NITROGEN GAS
- 2 - MASS FLOW CONTROLLERS
- 3 - PURGE GAS
- 4 - DILUENT GAS
- 5 - GLASS VESSEL
- 6 - GAS STANDARD
- 7 - T-PIECE SPLIT
- 8 - SPLIT VENT
- 9 - RESTRICTOR
- 10 - GLASS T-PIECE
- 11 - SILICONE RUBBER TRAP
- 12 - GC - OVEN

Figure 4.3. Dilution system for the gas standard.

Since no attempted gas standard for HCHO could reliably provide low enough concentrations, it was decided to include a dilution system. Figure 4.3, shows the set-up arranged to fit inside a GC-oven so that the temperature of all the components could be maintained at 80°C. If the temperature were to fall below 80°C, HCHO could repolymerise and deposit as the polymer onto the cooler surfaces. A 100 ng/min HCHO permeation standard was placed inside a closed glass vessel. A 74:1 split ratio then provided a 1.33ng/min HCHO atmosphere.



A - 0.54mm i.d F.S capillary, 30 ml/min

B - 2m 0.25mm i.d F.S capillary, RESTRICTOR 0.4 ml/min

C - 1cm 0.25mm i.d F.S capillary, SPLIT VENT 29.6 ml/min

Figure 4.4. T-piece split.

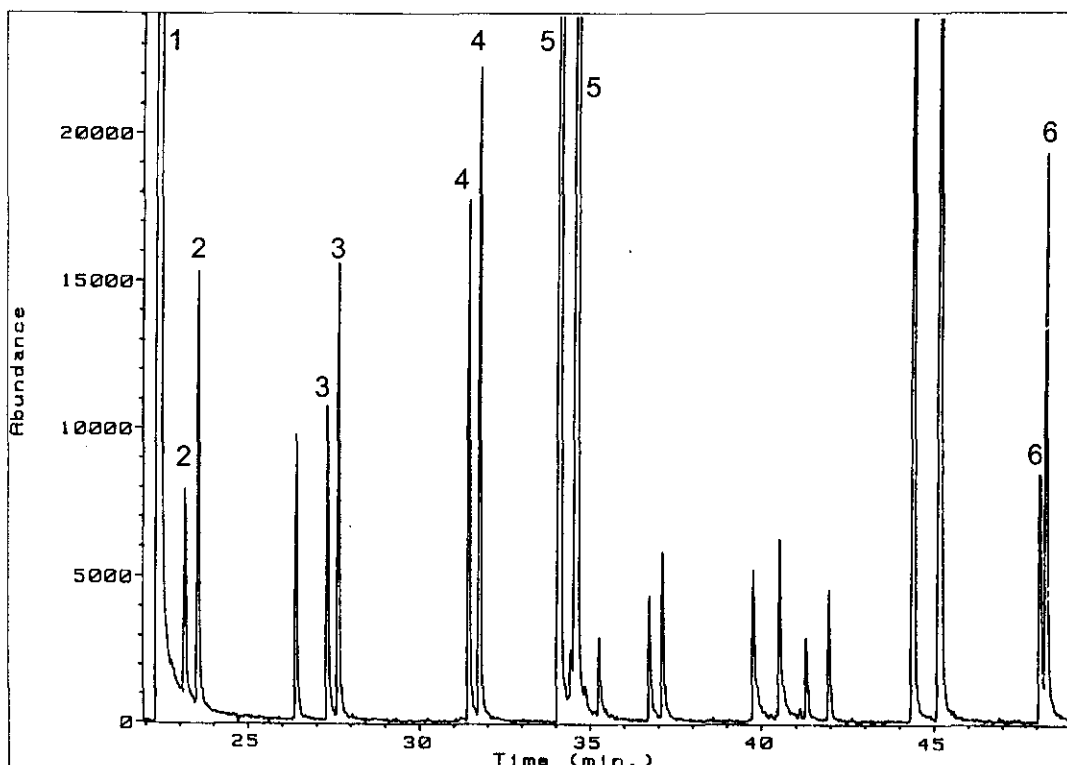
The split was prepared using a 1/16 " swagelock T-piece and 2 differing lengths of 0.25mm i.d. fused silica capillary. Figure 4.4 shows the inside of the T-piece. The 2m long 0.25mm i.d fused silica capillary was inserted into the wider bore (0.54mm i.d) capillary leading from the glass vessel which contained the

standard. The 2m length of fused silica capillary served as a restrictor so that the bulk of the flow was split through the 1cm fused silica capillary (inserted on the third leg of the T-piece). The split ratio is dependant on the lengths of the two 0.25mm i.d fused silica capillaries. The longer the length of the split vent capillary, the smaller the split ratio. In addition, the shorter the length of restrictor capillary the smaller the split ratio. The flow rate through the split had to be set before the diluting flow could be added. The restrictor length was then inserted into a 4mm i.d glass T-piece where it joined up with the diluting flow entering from the other end. The gas mixture could then be collected at the exit of the glass T-piece on the outside of the GC-oven. A 1/4" swagelock union was used at the exit to allow for easy collection with the trap.

The concentration of the HCHO atmosphere could be changed by adjusting the dilution flow. A diluting flow of 10ml/min provided a concentration of 0.1ppm. Appendix 2 demonstrates the calculation method used to determine aldehyde gas concentrations.

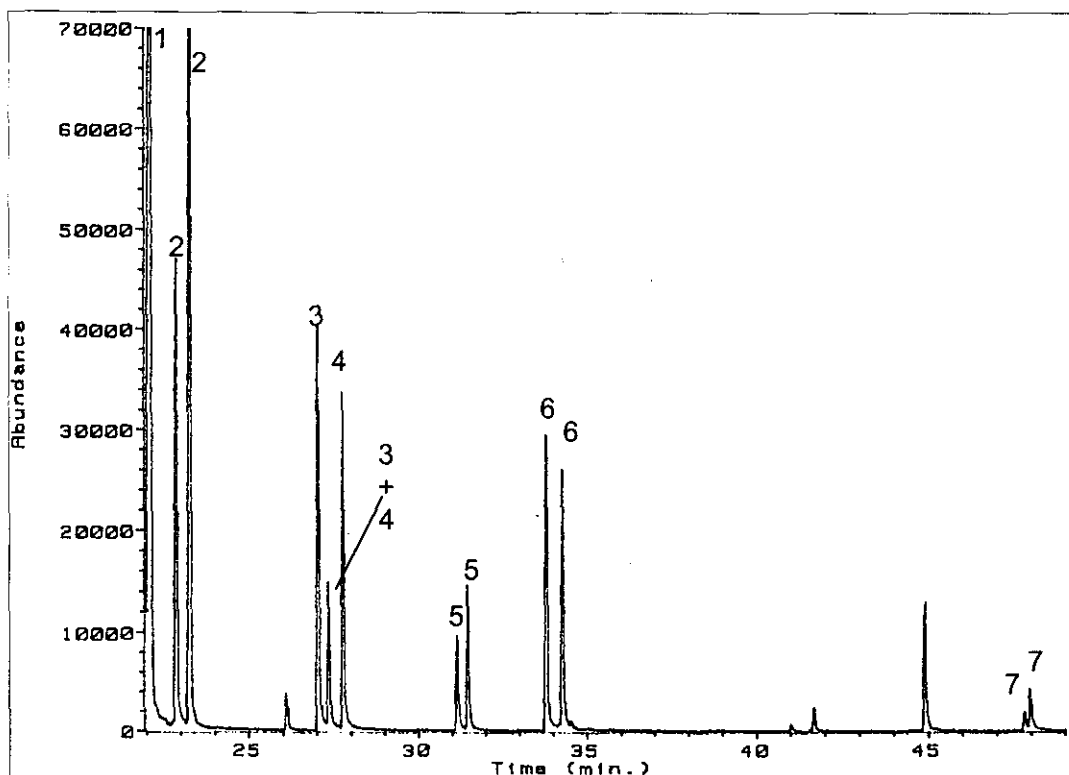
The diffusion and permeation (type 1) aldehyde standards (excluding HCHO) were tested using a 100% PDMS SPME fibre. See table 4.1 for their respective mass loss rates. The fibre was exposed to the dynamic headspace of a 10g/L PFBHA aqueous solution for 2 min. Thereafter the fibre was exposed to the diffusion standards for 5 min, desorbed at 250°C in the HP 5890 GC-inlet. Instrument parameters are listed in table 6.1. The temperature program used was 30°C/5min ramped at 3°/min to 180°C then ramped again at 50°/min to 280°C and held there for 4 min. The permeation standards were tested similarly, except the fibre was exposed to the standards for 10min. Figure 4.5 and 4.6

show the Reconstructed Ion Chromatograms using  $m/z$  181, for the diffusion and permeation aldehyde gas standards respectively. The oxime products could be identified based on an earlier study discussed in section 6.2. From these chromatograms we could clearly see that the gas standards were functioning. Notice that the acrolein-oxime was not detected from the diffusion standards sampled, upon further inspection the acrolein diffusion tube was empty.



- |                  |                   |                       |
|------------------|-------------------|-----------------------|
| 1. PFBHA         | 2. Acetal-oxime   | 3. Propanal-oxime     |
| 4. Butanal-oxime | 5. Crotonal-oxime | 6. Benzaldehyde-oxime |

Figure 4.5. Reconstructed Ion Chromatogram using  $m/z$  181 of SPME-PFBHA coated fibre exposed to aldehyde diffusion gas standards (type 3).



- |                  |                   |                       |                   |
|------------------|-------------------|-----------------------|-------------------|
| 1. PFBHA         | 2. Acetal-oxime   | 3. Propanal-oxime     | 4. Acrolein-oxime |
| 5. Butanal-oxime | 6. Crotonal-oxime | 7. Benzaldehyde-oxime |                   |

Figure 4.6. Reconstructed Ion Chromatogram using  $m/z$  181 of SPME-PFBHA coated fibre exposed to aldehyde permeation gas standards (type 1).

#### 4.5 CONCLUSION

We have successfully prepared stable and continuous gas standards for formaldehyde, acetaldehyde, acrolein, propanal, crotonal, butanal and benzaldehyde. A dilution set-up allowed lower concentrations of the formaldehyde gas standard to be obtained.

## CHAPTER 5

### INSTRUMENTATION

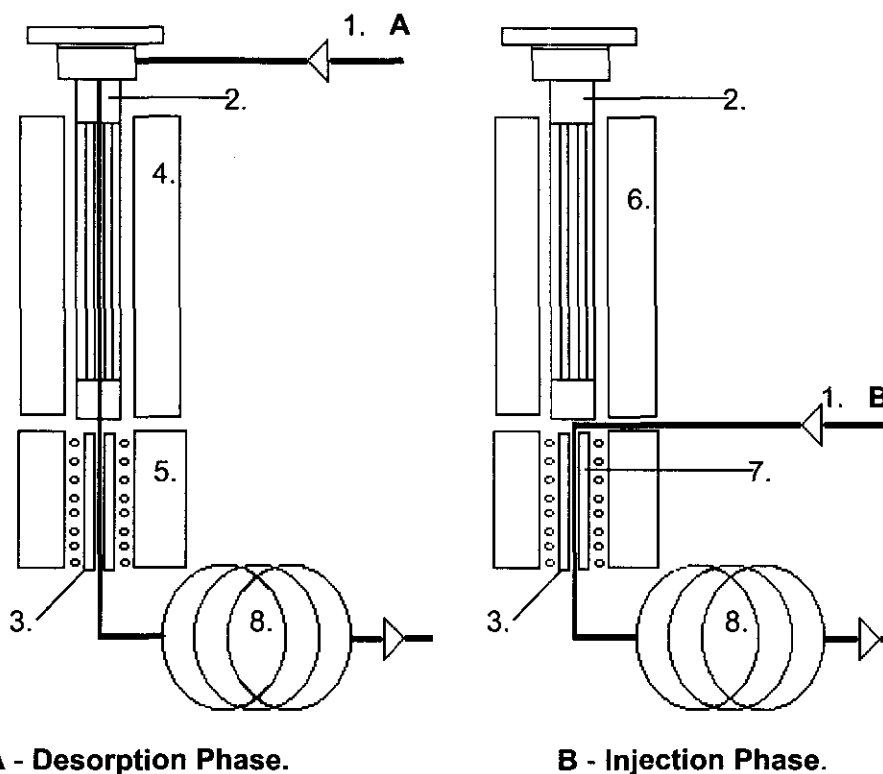
#### 5.1 THERMAL DESORPTION – CRYOGENIC TRAPPING UNIT (TCT)

Volatile compounds, which have been pre-concentrated on ad/absorbents, need to be quantitatively transferred as a narrow injection band onto the GC capillary column.

One method for achieving this is by using a thermal desorption cold trap injector. A ChromPack 4020 desorption unit was used in our study, Figure 5.1[116]. A glass tube, either empty or packed with sorbent, is placed in the desorption oven, where it is heated while the carrier gas transfers the volatiles from the tube onto a cold trap.

The cold trap consists of a fused silica capillary, 30cm long with an internal diameter of 0.53mm, which is coated with a thick film of stationary phase to increase its capacity. During desorption, the cold trap is cooled and maintained at sub-ambient temperatures ranging from 0°C to -100°C by using liquid nitrogen. Upon completion of desorption the cooling flow is stopped. A metal capillary tube, which surrounds the fused silica cold trap is heated ohmically. This ensures a ballistic temperature increase from, for example -100°C to 250°C within 1 minute. Within that time, the carrier gas transfers the contents of the cold trap and refocuses it onto the GC capillary column, which is at a lower temperature. Figure 5.1 shows the 2 main phases, namely desorption and injection, in the TCT - CP 4020 [116].





**A - Desorption Phase.**

**B - Injection Phase.**

1. **A** High purity Helium carrier gas flow during the **desorbtion** phase.
1. **B** High purity Helium carrier gas flow during the **injection** phase.
2. Glass tube containing ab-/ad-sorbent.
3. Fused Silica cold trap.
4. Heated desorbtion oven.
5. Liquid Nitrogen-cooled chamber.
6. Ambient desorbtion oven.
7. Ballistically heated fused silica cold trap.
8. Gas chromatograph.

Figure 5.1. The 2 main phases in the TCT 4020 thermal desorption unit.

## 5.2 GAS CHROMATOGRAPH (GC)

A GC consists of a carrier gas supply, an inlet, an oven containing a capillary column and a detector, as depicted in figure 5.5. The carrier gas (mobile phase) must be inert and of high purity. Typical gases used are nitrogen, helium or hydrogen. The choice of the gas used depends on the speed of analysis required and the detector used. In our experiments, helium was used as it is recommended for use with mass spectrometric detection [117]. The flow rate of the carrier gas should be chosen to

ensure the maximum number of chromatographic plates in the column, which in turn determines the degree of separation or resolution between the compounds [118,119].

The sample is introduced into the capillary column via the inlet. Samples are dissolved in an appropriate organic solvent and about 1  $\mu\text{L}$  injected using a micro litre syringe. The sample is injected instantaneously so that, in conjunction with the high temperature of the inlet, e.g. 250°C, the volatilised components in the sample are focussed onto the cooler column, eg.40°C, as a narrow injection band. The inlet can be set-up for either split or splitless injection. When the sample is too concentrated or injected as a large volume, split injection is used at a preset split-ratio so that only a small proportion is actually transferred onto the column. When sample components are present in trace amounts the entire sample can be transferred onto the column in splitless injection, thereby improving detection limits [118].

The thermal desorption unit is used an alternative "inlet" for the desorbed components of the trap (see above).

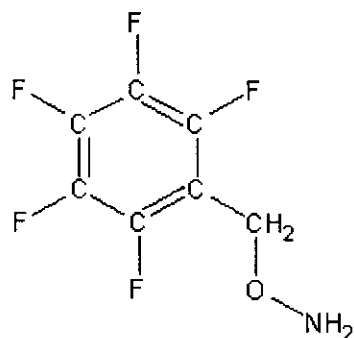
The capillary column used is 30m long and 0.25mm in internal diameter. It is coated on the inside with a thin film (0.25micron) of 95% polydimethylsiloxane and 5% methylphenylsiloxane stationary phase. We used a temperature program starting at 30°C held for 1 minute, ramped at 5°C per minute to 150°C then ramped again at 50°C to 280°C for 4 minutes. The last temperature ramp is used to remove silicone, released from the silicone traps during desorption, as well as other compounds still in the column. The eluted compounds then enter the detector.

Two kinds of detectors were used in our study. The Flame Ionisation Detector (FID) and a Mass Spectrometer (MS). They are discussed in detail below.

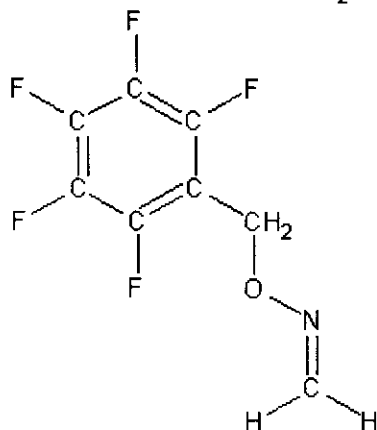
standards [122-124]. Figure 5.3 shows the estimation of the ECN contributions of PFBHA and the HCHO-Oxime. The ECN for the other aldehydes studied can be predicted in the same way. The calculation method used to determine the FID response for the HCHO-oxime and PFBHA are shown below.

Table 5.1. Contributions to the Effective Carbon Number (ECN) [120,122].

ATOM	TYPE	ECN CONTRIBUTION
C	Aliphatic	1
C	Aromatic	1
C	Olefinic	0.95
C	Acetylene	1.30
C	Carbonyl	0
C	Carboxyl	0
C	Nitrile	0.3
O	Ether	-1.0
O	Primary Alcohol	-0.5
O	Secondary Alcohol	-0.75
O	Tertiary Alcohol	-0.25
N	Amine	As for O in Alcohol
Cl	An olefinic C	+0.05
Cl	Aliphatic C with 2 Cl atoms	-0.12 per Cl



6 aromatic C - atoms	= 6 x 1
5 F - atoms	= 5 x 0.05
1 aliphatic C - atom	= 1 x 1
1 ether O - atom	= 1 x -1
1 primary amine	= 1 x -0.5
<u>sum total PFBHA</u>	<u>= 5.75</u>



6 aromatic C - atoms	= 6 x 1
5 F - atoms	= 5 x 0.05
1 aliphatic C - atom	= 1 x 1
1 ether O - atom	= 1 x -1
1 secondary amine	= 1 x -0.75
1 olefinic C - atom	= 1 x 0.95
<u>sum total OXIME</u>	<u>= 6.45</u>

Figure 5.3. Estimating Effective Carbon Numbers for PFBHA and the HCHO-Oxime.

Dodecane has 12 aliphatic carbon atoms, so similarly the ECN for dodecane(C12) is 12. Thus, assuming the FID response for C12 is 100%. Then the FID response, in terms of ECNs, for PFBHA and the HCHO-Oxime can be seen as a fraction of the FID response for C12. The FID response factor for C12 is given as

$$\frac{(\text{ECN C12})}{(\text{ECN C12})} \times \frac{(\text{C12 peak area})}{\text{amount C12 (ng)}}$$

The response for PFBHA can then be given as

$$\frac{(\text{ECN PFBHA})}{(\text{ECN C12})} \times \frac{(\text{C12 peak area})}{\text{amount C12 (ng)}}$$

The amount of PFBHA can then be determined by

$$\frac{(\text{PFBHA peak area}) / (\text{ECN PFBHA})}{(\text{ECN C12})} \times \frac{(\text{C12 peak area})}{\text{amount C12 (ng)}}$$

Similarly the HCHO-Oxime amount can be determined by

$$\frac{(\text{Oxime peak area}) / (\text{ECN Oxime})}{(\text{ECN C12})} \times \frac{(\text{C12 peak area})}{\text{amount C12 (ng)}}$$

The amount of aldehyde can then be calculated using elementary chemistry. The ratio between aldehyde and oxime formed is 1:1[50]. Since the ECNs for PFBHA and the HCHO-Oxime were estimated, the amounts calculated are not accurate.

However, they are sufficient for our purpose which is merely to have an indication of the amounts involved.

#### 5.4 THE MASS SPECTROMETER (MS)

The MS can be divided into three sections, all of which are under a vacuum of at least  $10^{-5}$  Torr. Compounds eluting from the GC are ionised in the ion source and then accelerated by a potential difference to pass through various focussing lenses towards the mass analyser and finally towards an electron multiplier [119,125,126]. Detection limits for MS detectors are typically 1 ng for Total Ion Monitoring and 1 pg for Selected Ion Monitoring [126].

Electron Impact (EI) ionisation is used by both the quadrupole and ion trap mass analysers that were used in our study. A hot tungsten or rhenium filament produces

electrons with an energy of 70eV, which is in excess of the energy required to ionise a molecule (~10eV). These high-energy electrons also provide enough energy to cause the ionised molecule ( $M^+$ ) to undergo significant fragmentation, unique to every compound. After the bombardment of electrons, the ions are accelerated by a potential of 5-15V towards the centre of the mass analyser [119,125,126].

The quadrupole is a mass analyser or rather a "mass filter", see figure 5.4 [119,125]. Four cylindrical metal rods are arranged in pairs in parallel beside each other. One pair is connected to the positive terminal of a dc potential, and the other pair to the negative dc potential. In addition, to each pair of rods, a variable Radio-Frequency (RF) ac potential, 180° out of phase, has been applied.

The ions have a constant velocity as they enter the quadrupole, in the z- direction, parallel to the metal rods (x and y-axes). As a result of the dc and RF voltages ( $V_{dc}$  and  $V_{rf}$ ) applied to the rods, the ions acquire complex oscillations in the x and y directions. Ions are deflected, by these oscillations, towards the rods, neutralised and carried away.

For a given set of conditions ( $V_{dc}$  and  $V_{rf}$ ), only ions of a single m/z ratio will have a stable oscillation and will be able to traverse the length of the quadrupole, without striking the rods. These ions will enter the electron multiplier detector. Mass scanning is achieved by varying each of the RF and dc frequencies while keeping their ratios constant [119,125,126].

Total Ion Chromatograms (TIC) are produced when the compounds eluting from the GC are scanned every 10 seconds, from the lowest mass to the highest mass within a selected mass range, usually m/z ratio 40 to 400. Compounds analysed by GC-EI-MS, normally have a single charge ( $z=1$ ), so the m/z ratio is the same as their actual mass (m) [125].

To improve sensitivity, Selected Ion Monitoring (SIM) can be used. In this case the quadrupole scans only for certain selected masses. This way more time is allocated

to the  $m/z$  ratio of interest whereas with Total Ion monitoring only a fraction of time is allocated to the detection of that  $m/z$  ratio.

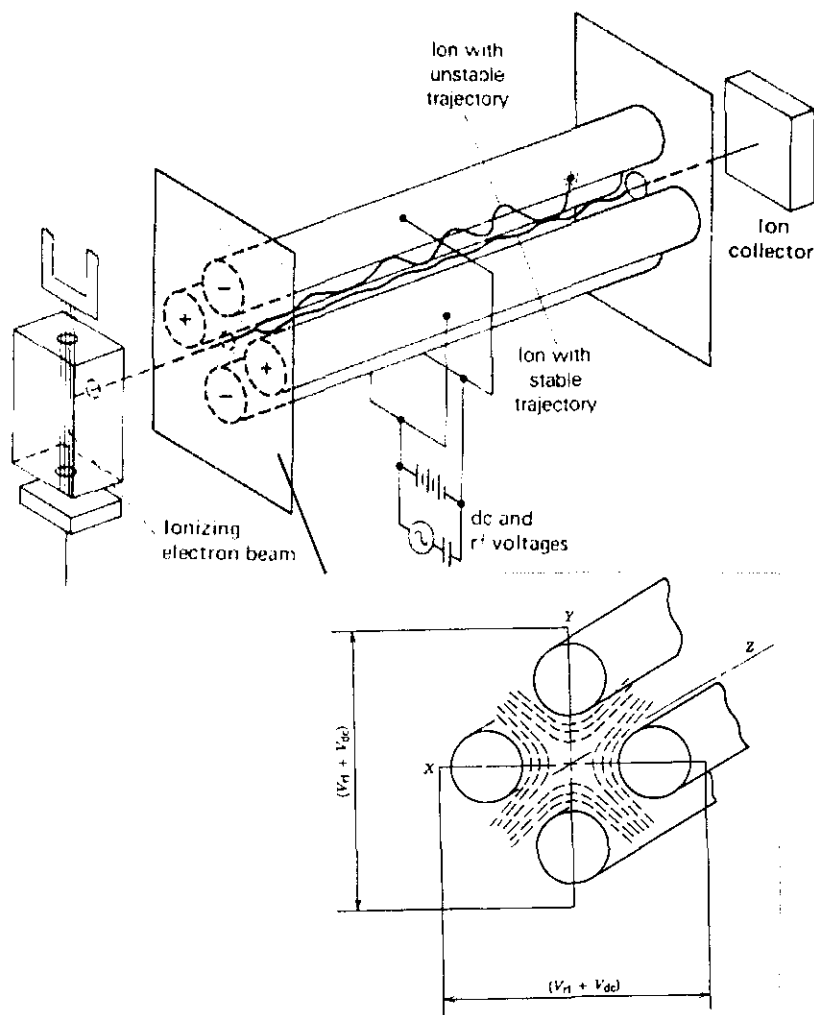


Figure 5.4. A Quadrupole Mass Spectrometer[125,126].

An ion trap (ITD) is the spherical configuration of the linear quadrupole, depicted in figure 5.5 [125]. In this case, the RF voltage is applied to a central doughnut-shaped ring electrode, which is enclosed on both ends with cap electrodes. Ions from the ion source enter the enclosure through a grid in the top end-cap. Unlike the linear quadrupole, ions are "trapped" temporarily within the ITD until they are sorted according to  $m/z$  ratios. The ions with appropriate  $m/z$  ratios are in a stable orbit

within the enclosure. As the electric field is scanned, the heavier ions are stabilized in their orbit while the lighter ones become unstable, collide with the wall of the ring electrode and leave the trap through the bottom end-cap. These emitted ions move towards the electron multiplier detector [119,125,126].

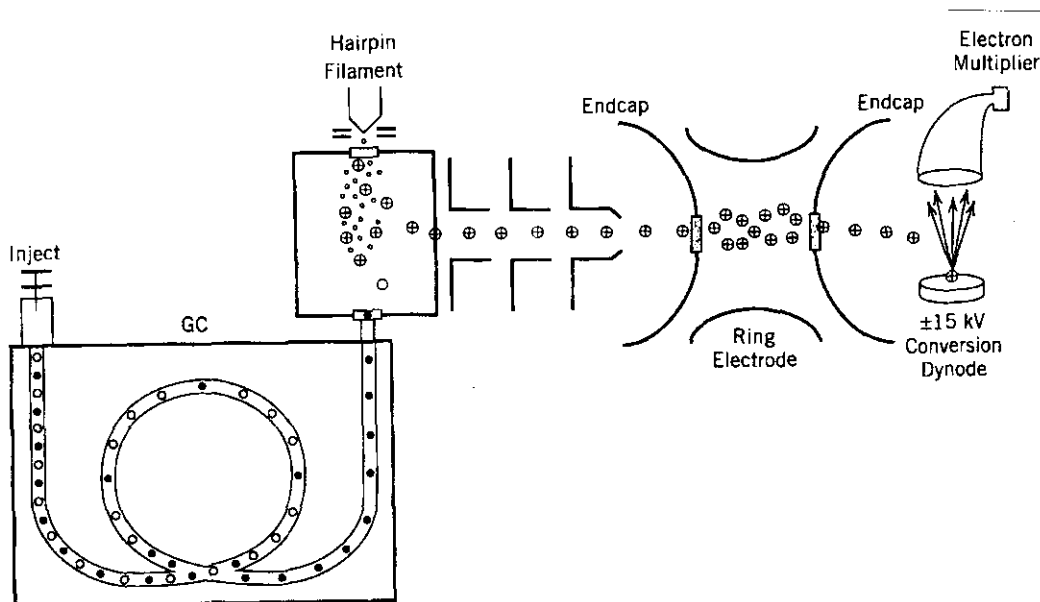


Figure 5.5. A Gas Chromatograph (GC) coupled to an Ion Trap Detector (ITD), having an external ion source [125].

The continuous-dynode electron multiplier is a glass trumpet-shaped device, which has been coated with lead on the inside. A potential difference of 1.8-2kV is applied across the length of the trumpet. The positive ions emitted from the mass analyser, enter the detector and strike the lead surface. Upon this impact, electrons are ejected, which in turn impact the surface and eject more electrons, this continues in a “zigzag” path until the tapered end of the trumpet is reached, which is connected to the amplifier. From here the data is acquired, converted and controlled by electronics, the output is sent to a data acquisition system on a computer [126].



## CHAPTER 6

### IN-SITU DERIVATISATION ON SILICONE RUBBER TRAPS

#### 6.1 IN-SITU DERIVATISATION

Low molecular mass aldehydes are both volatile and polar. In order to pre-concentrate them from the air, we must first convert them into thermally stable, less polar compounds. This is commonly achieved by using a derivatisation reaction, as described in chapter 2.

##### 6.1.1 SELECTING A DERIVATISING REAGENT

A derivatising reagent can be split into two parts, namely the bulk organic substituent and the reactive substituent [127]. The bulk organic substituent should enhance the detector sensitivity to the product and simultaneously decrease the volatility of the product; it is responsible for providing a chemically and thermally stable product. However, this group should be carefully considered since the bulk can also sterically hinder the reaction, affecting the reaction rate. The reactive substituent determines the selectivity of the reaction, by reacting only with certain functional groups in the presence of others [127].

Of the several reagents that have been used for the derivatisation of aldehydes, as seen in chapter 2, O- (2,3,4,5,6-PentaFlouroBenzyl) Hydroxyl Amine hydrochloride (PFBHA) was chosen for this study based on the following reasons. The reactive substituent, the amine, reacts only with carbonyl functional groups. The reaction efficiency is > 80% for HCHO and other low molecular mass aldehydes [50].

However, the reaction rate decreases for longer, more complex aldehydes [50]. This is due to the size of the bulk substituent, the pentafluorobenzyl group, which hinders the approach of the amine toward the aldehyde.

The pentafluorobenzyl group provides enhanced detectability, especially when using an electron capture detector. A base peak (100%) of  $m/z$  ratio 181 is obtained by EI-MS for the oxime products formed, which is ideal for Selected Ion Monitoring (SIM) [17,22,50,54,55].

The oxime-product is thermally stable and volatile [17,22,50] therefore ideal for GC analysis. Comparisons of reagents in the literature [22] also indicate that PFBHA, unlike other reagents, displays only one peak on the chromatogram corresponding to the reagent. In addition, since similar work using SPME has been performed with this reagent [22] it would allow for a comparison of the results obtained when using the silicone trap.

The suggested mechanism for the reaction between an aldehyde and O - (2,3,4,5,6-PentaFluoroBenzyl) HydroxylAmine hydrochloride (PFBHA), is shown in figure 6.1.

### 6.1.2. THE SILICONE RUBBER TRAP

Derivatisation is performed "*in-situ*" meaning in the collection medium, in our case, the silicone rubber. The procedure for *in-situ* derivatisation on the silicone rubber trap is depicted in figure 6.2.

As discussed in chapter 3, there are several reasons why the silicone rubber trap is ideal for pre-concentrating pollutants. It is particularly suitable for *in-situ* derivatisation because it is inert and will not participate or inhibit the reaction between the aldehyde and the PFBHA. The only fragments produced through silicone degradation have repeatable retention times and are easily identified using Mass Spectrometry. Figure 6.3, shows a typical blank chromatogram of a silicone trap desorption run on GC-FID,

using the conditions in table 6.1, temperature program B. Typical mass spectral silicone degradation fragments are  $m/z$  73, 207, 211 and 281. Sixteen-channel silicone rubber traps were used during this study; their preparation has previously been described by Ortnier and Rohwer [24-27].

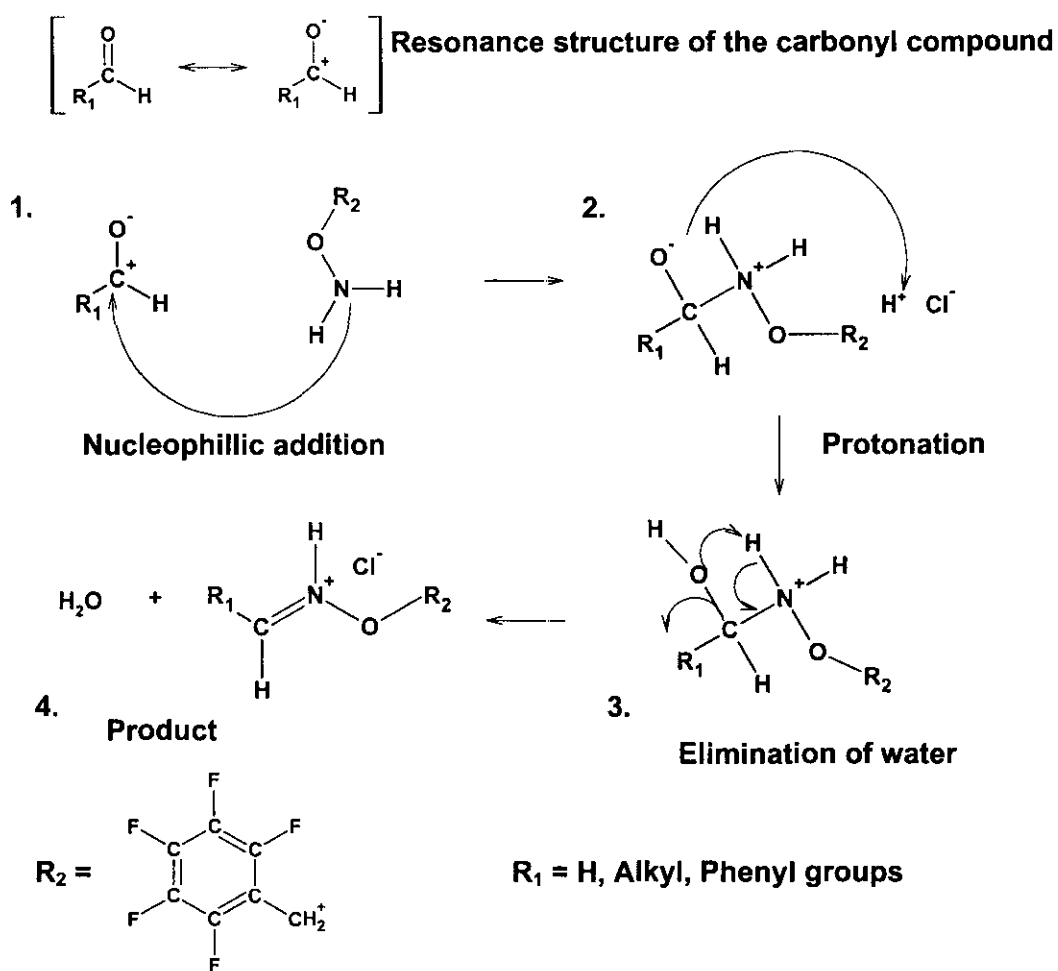


Figure 6.1. The suggested mechanism for the reaction of an aldehyde with PFBHA.

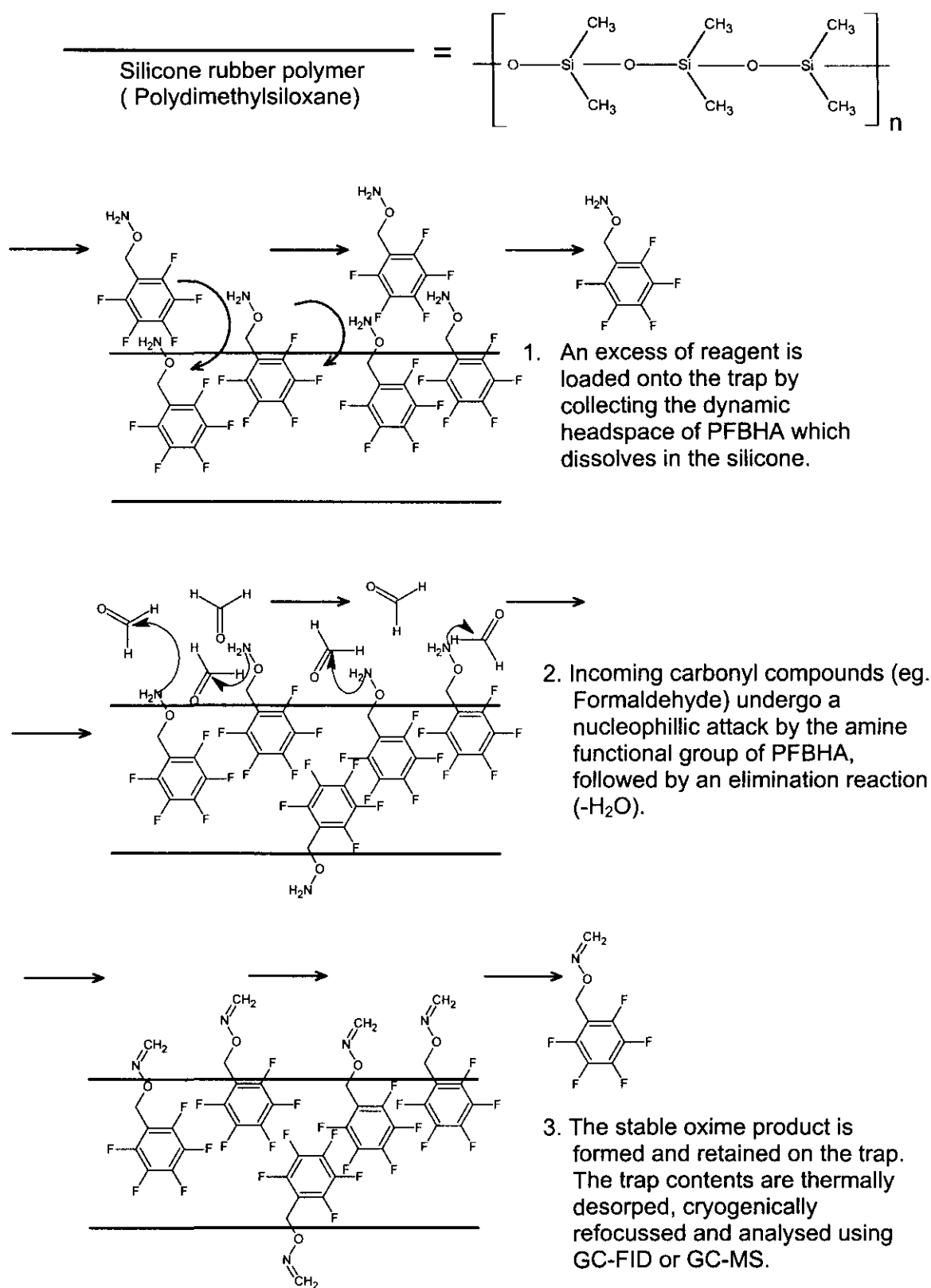


Figure 6.2. In-Situ derivatisation on the silicone rubber trap.

Table 6.1. Instrumentation Parameters.

<b>TCT 4020 UNIT:</b>	
ROD	250°C
PRECOOL	-100°C / 2min
DESORB	220°C / 15min
DESORB FLOW RATE	50 ml/min
INJECT	250°C / 1min
BACKFLUSH	280°C / 10min
BACKFLUSH FLOW RATE	60 ml/min
<b>HP5890 GC:</b>	
COLUMN	30m ZB-5, 0.25mm i.d., df 0.25µm
CARRIER GAS	Helium
VOLUME FLOW RATE	0.6ml/min
TEMPERATURE PROGRAM A	30°C / 1min // 5°C/min // 150°C // 50°C/min // 280°C / 4min
TEMPERATURE PROGRAM B	30°C / 1min // 5°C/min // 280°C / 4min
TEMPERATURE PROGRAM C	80°C / 2min // 5°C/min // 180°C // 40°C/min // 260°C / 2min
<b>HP 5890 FID:</b>	
FLAME GAS N <sub>2</sub> : H <sub>2</sub> : O <sub>2</sub>	20 : 60 : 300 ml/min
TEMPERATURE	300°C
RANGE	2 <sup>4</sup>
<b>HP 5988 QUADRUPOLE MS:</b>	
ION SOURCE TEMPERATURE	220°C
TRANSFER LINE TEMPERATURE	280°C
SCAN RANGE	40 - 400 amu
<b>VARIAN 3300 GC:</b>	
COLUMN	30m DB-5, 0.25mm i.d., df 0.25µm
CARRIER GAS	Helium
VOLUME FLOW RATE	0.4 ml/min
TEMPERATURE PROGRAM	30°C / 1min // 5°C/min // 150°C // 50°C/min // 280°C / 4min
<b>FINNIGAN MAT ION TRAP MS:</b>	
ION SOURCE TEMPERATURE	150°C
TRANSFER LINE TEMPERATURE	220°C
SCAN RANGE	40 - 400 amu

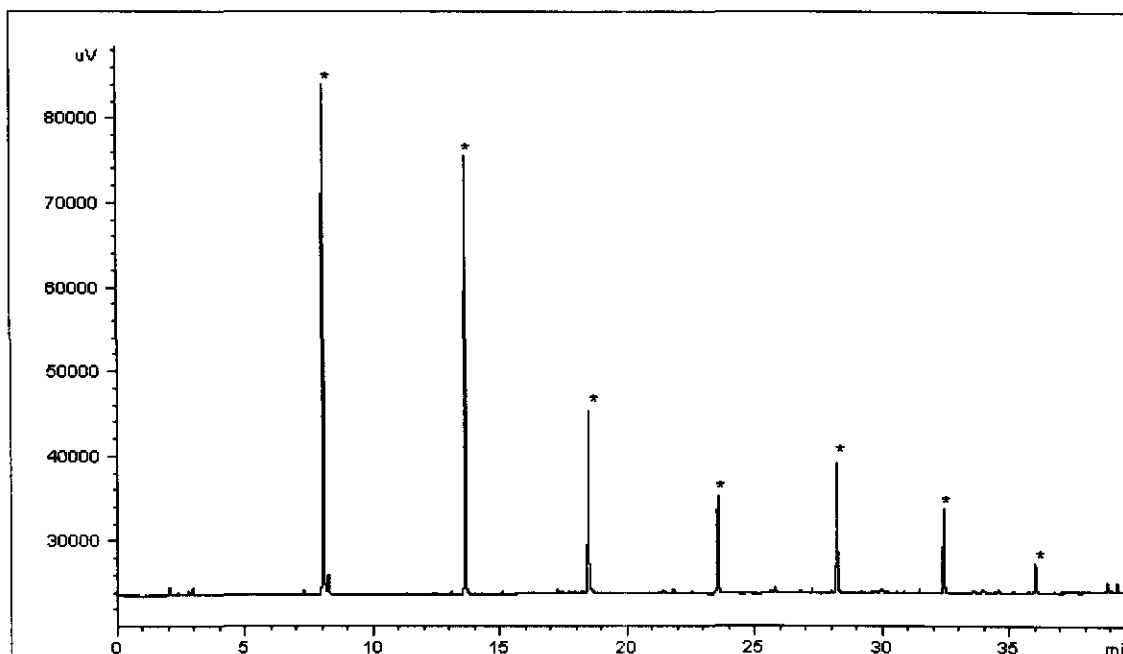


Figure 6.3. GC-FID chromatogram of a desorbed silicone rubber trap.

## 6.2 IDENTIFICATION OF THE REAGENT AND OXIME-PRODUCTS

A quick study was carried out in order to determine the mass spectra and elution order of the reagent and oxime products using a 100% PDMS SPME fibre. Reaction schemes for each aldehyde with PFBHA are shown in appendix 3, along with the product molecular formulas and masses.

The SPME fibre was exposed to the dynamic headspace of a 10g/L aqueous PFBHA solution, for 1min at a flow rate of 10ml/min, followed by exposure to the pure aldehyde for 10 seconds. This method was followed for each aldehyde. The fibre was desorbed in the inlet, splitless for 1min at 250°C, of the HP5890 GC followed by mass spectral analysis by a quadrupole mass analyser. Temperature program C in table 6.1 was used. Figure 6.4, shows the elution order of the aldehydes, except for the HCHO-oxime and PFBHA, which elute before acetaldehyde, as shown in figure 6.12 and figure 6.16.

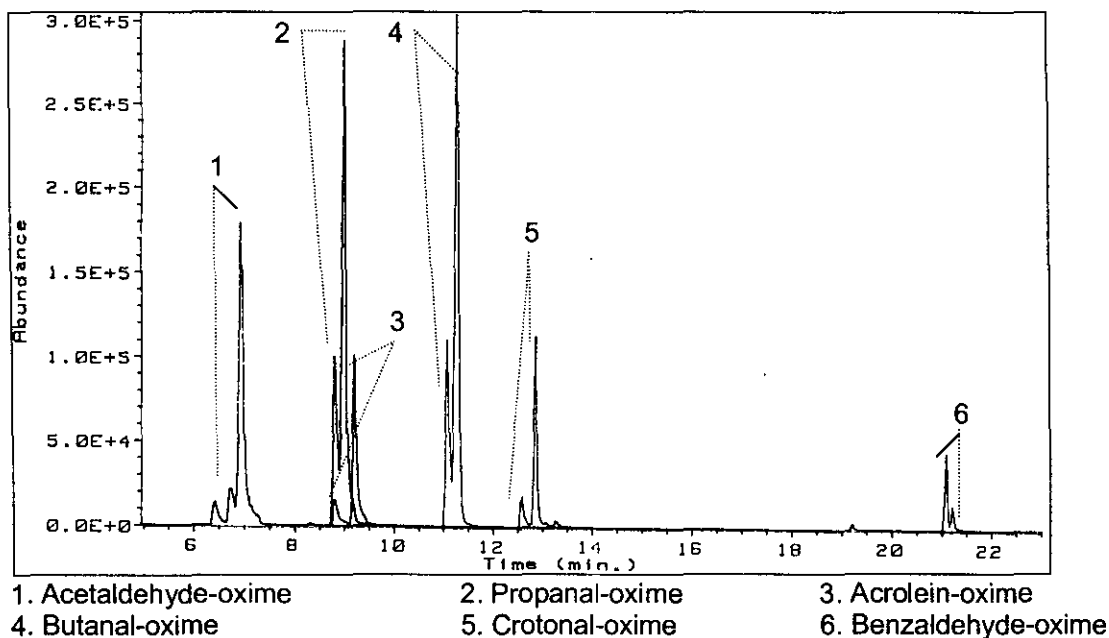


Figure 6.4. Overlaid TIC of SPME-PFBHA coated fibre exposure to pure aldehydes.

Non-symmetrical carbonyl groups will form E/Z isomers around the carbon-nitrogen double bond [50,128,129]. From the chromatogram, figure 6.4, we observed separated isomers for propanal, acrolein, butanal, crotonal and benzaldehyde. In our study, both peaks were integrated for quantitation.

Propanal and acrolein co-elute, but a separation can be achieved, if desired, by using a mass spectrometer, and selecting the  $m/z$  ratios unique to each compound, namely  $m/z$  236 for propanal and  $m/z$  250 for acrolein.

Mass spectra for the PFBHA, formaldehyde-oxime and acetaldehyde-oxime obtained, along with the corresponding NIST (National Institute for Standards and Technology) mass spectrum are shown in figure 6.5, 6.6 and 6.7 respectively. The mass spectra for other aldehydes studied can be found in the appendix 4. Table 6.2, lists the main mass spectral fragments for each aldehyde-oxime studied, obtained on the quadrupole MS. Where possible, these have been compared to literature values.

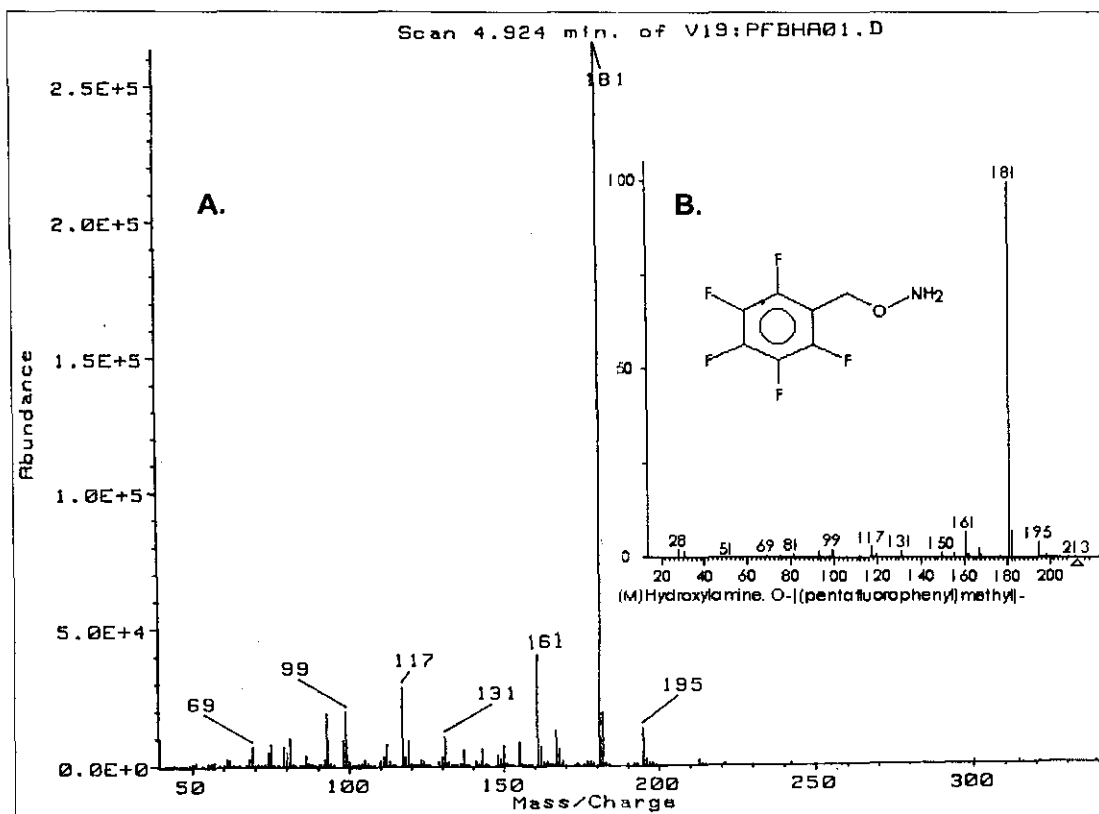


Figure 6.5. **A.** Obtained EI-Mass Spectrum for PFBHA.  
**B.** NIST library EI-Mass Spectrum for PFBHA'

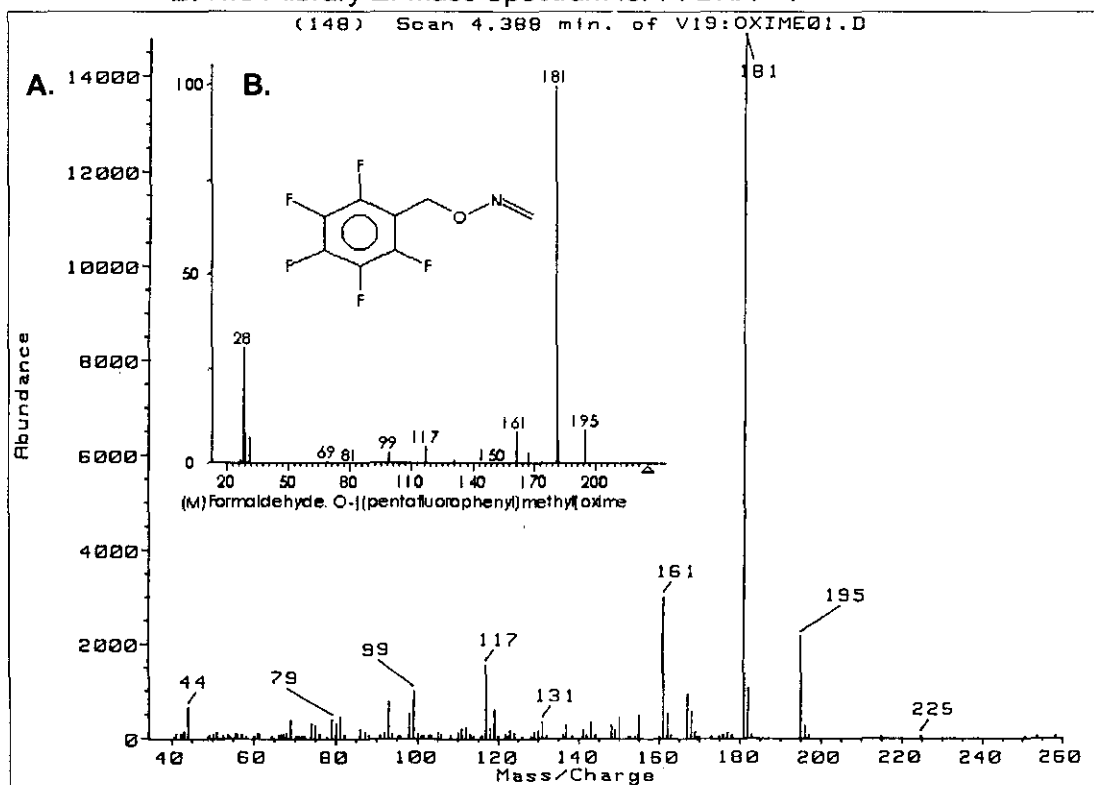


Figure 6.6. **A.** Obtained EI-Mass Spectrum for HCHO-Oxime.  
**B.** NIST library EI-Mass Spectrum for HCHO-Oxime.



Table 6.2. EI-Mass spectra for PFBHA-aldehyde derivatives.

Compound	Molecular mass		m/z Relative abundance									Description:
	compound	PFBHA - oxime										
Formaldehyde	30	213	[ M ] <sup>+</sup>	181	195	161	117	182	99	167	93	
				100	11	10	9	7	7	5	5	Pure oxime - liquid injection [50]
				100	12	10	9.9	6.7	9.6	5.4	6.3	Pure oxime - liquid injection [22]
				100	9.1	8.7	4.8	6.5	3.3	3.3	0.6	NIST
				<b>100</b>	<b>15.8</b>	<b>15.5</b>	<b>9.7</b>	<b>7.4</b>	<b>7.3</b>	<b>2.7</b>	<b>4.2</b>	<b>experimental EI-ITD</b>
				<b>100</b>	<b>12.1</b>	<b>9.7</b>	<b>6.7</b>	<b>7.7</b>	<b>4.9</b>	<b>4.5</b>	<b>3.7</b>	<b>experimental EI-QUADRUPOLE</b>
Acetaldehyde	44	239	[ M ] <sup>+</sup>	181	195	161	117	182	209	167	99	
				100	6	6	5	7	8	4	4	Pure oxime - liquid injection [50]
			3	100	4	3	2	9	11	3		PFBHA-oxime formed in beer [22]
				100				0.6	1.3			NIST
			<b>1.5</b>	<b>100</b>	<b>3.5</b>	<b>6.8</b>	<b>5.4</b>	<b>7.1</b>	<b>6.0</b>	<b>3.5</b>	<b>4.6</b>	<b>experimental EI-QUADRUPOLE</b>
Propanal	58	253	[ M ] <sup>+</sup>	181	195	161	117	182	223	236		
			1.2	100	3.7			7.1	5.5	8.6		Pure oxime - liquid injection [50]
			3	100	4	3	2	9	7	9		PFBHA-oxime formed in beer [17]
			0.8	100	3.4	3.6	1.6	7.6	6	9.4		NIST
			<b>0.6</b>	<b>100</b>	<b>3.3</b>	<b>4.9</b>	<b>4.3</b>	<b>8.4</b>	<b>2.1</b>	<b>10.1</b>		<b>experimental EI-QUADRUPOLE</b>
Acrolein	56	251	[ M ] <sup>+</sup>	181	195	161	117	182	250	99	42	
			<b>4.8</b>	<b>100</b>	<b>3.1</b>	<b>5.2</b>	<b>4.2</b>	<b>8.3</b>	<b>6.8</b>	<b>4.1</b>	<b>2.1</b>	<b>experimental EI-QUADRUPOLE</b>
Butanal	72	267	[ M ] <sup>+</sup>	181	195	167	250	182	239	99	41	
				100	7	3	6	10	14	3	4	PFBHA-oxime formed in beer [17]
			<b>0.4</b>	<b>100</b>	<b>5.8</b>	<b>2.3</b>	<b>3.7</b>	<b>7.9</b>	<b>6.0</b>	<b>3.1</b>	<b>8.0</b>	<b>experimental EI-QUADRUPOLE</b>
Crotonal	70	265	[ M ] <sup>+</sup>	181	195	161	117	182	250	251	43	
			<b>1.0</b>	<b>100</b>	<b>2.8</b>	<b>3.9</b>	<b>3.6</b>	<b>7.3</b>	<b>20.3</b>	<b>5.4</b>	<b>9.9</b>	<b>experimental EI-QUADRUPOLE</b>
Benzaldehyde	106	301	[ M ] <sup>+</sup>	181	77	69	103	182	271	51	65	
			<b>7.4</b>	<b>100</b>	<b>17.0</b>	<b>9.0</b>	<b>8.5</b>	<b>7.5</b>	<b>5.3</b>	<b>14.6</b>	<b>13.5</b>	<b>experimental EI-QUADRUPOLE</b>

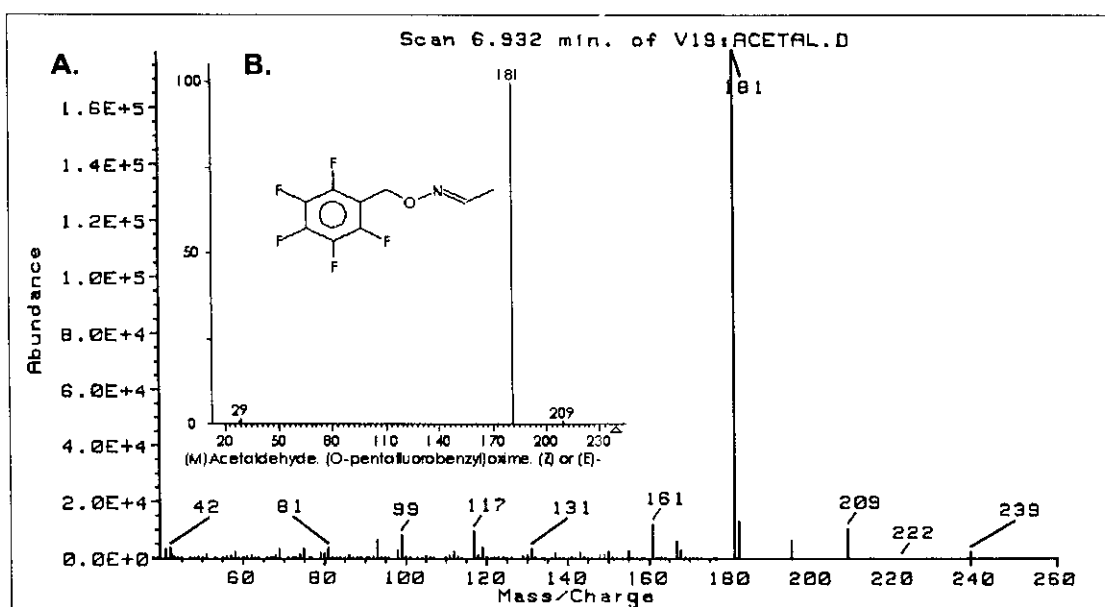


Figure 6.7. **A.** Obtained EI-Mass Spectrum for the acetaldehyde-oxime.  
**B.** NIST library EI-Mass Spectrum for the acetaldehyde-oxime.

All oximes produce a base peak of  $m/z$  181, which corresponds to the pentafluorotropylium ion, formed by the cleavage of the bond in the  $\beta$ -position to the pentafluoro-benzene ring [50,125]. Figure 6.8, demonstrates the formation of the pentafluorotropylium ion from the PFBHA-aldehyde derivative.

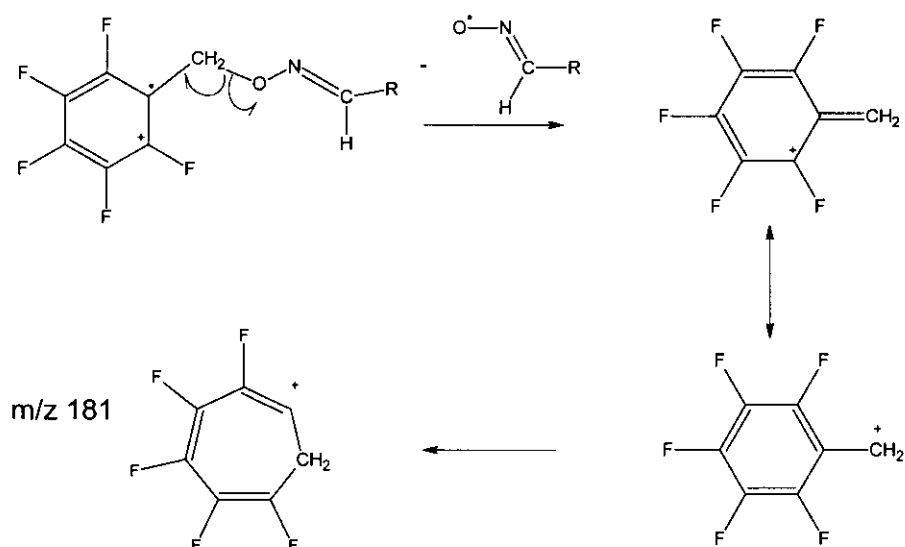


Figure 6.8. Formation of the pentafluorotropylium ion  $m/z$  181 [50,125].

However, most PFBHA derivatives, excluding aldehydes that have an  $\alpha, \beta$  double bond (acrolein, crotonal), afford very poor, often absent, molecular ions, which make the deduction of  $M^+$  difficult [130].

Longer chain aliphatic aldehydes, C4 and longer, form PFBHA-oximes that produce an  $m/z$  239 resulting from a McLafferty rearrangement [130], as demonstrated in figure 6.9 for the butanal-oxime. The  $m/z$  239 ion was observed for our butanal-oxime, see appendix 4 and table 6.2.

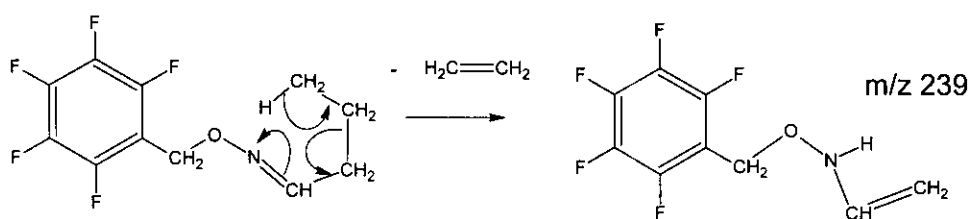


Figure 6.9. McLafferty rearrangement of the butanal-oxime to form  $m/z$  239 [130].

The ion  $m/z$  250 is predominant in most  $\alpha, \beta$  double bond aldehydes. Spiteller et.al. [130], have suggested a mechanism for the generation of  $m/z$  250, as depicted in figure 6.10.

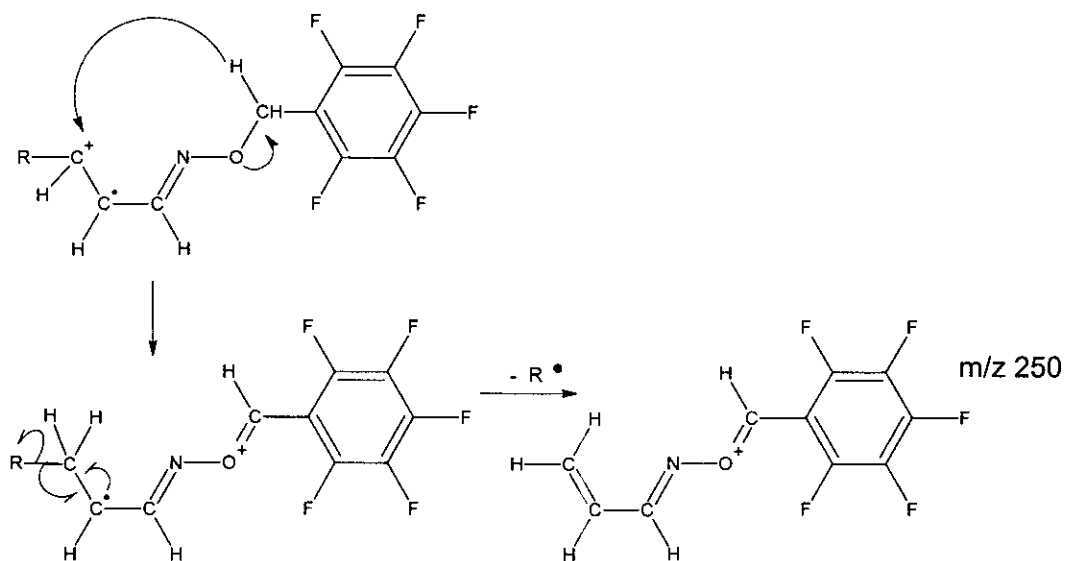


Figure 6.10. Mechanism for the formation of  $m/z$  250 from 2-alkenal-oximes, where  $R^{\cdot} = H$  (acrolein) and  $CH_3$  (crotonal) [130].

The ionised molecule undergoes a hydride migration from the benzylic hydrogen to the positive carbon atom, followed by carbon-carbon cleavage and the formation of a double bond. Both mass spectra for acrolein and crotonal display the  $m/z$  250 ion, see appendix 4 and table 6.2.

Other ions formed are  $m/z$  167, 155, 93 and 62 corresponding to the  $C_6F_5^+$ ,  $C_5F_5^+$ ,  $C_3F_3^+$  and  $C_2F_2^+$  ions, respectively. The abundances for these ions are below 5% for most aldehyde-oximes [50], as was also observed in our study.

Short chain aldehyde-oximes, such as acetaldehyde and propanal show the  $m/z$   $[M - 30]^+$ , formed by the loss of NO from  $M^+$ [50]. Our acetal and propanal-oximes, displayed the  $m/z$  209 and 223 respectively, corresponding to the suggested loss of NO  $[M - 30]^+$ .

Longer chain aldehydes will show a hydrocarbon pattern with successive losses of  $m/z$  14 in the lower mass range of the mass spectrum [50]. For the benzaldehyde-oxime,  $m/z$  77 and  $m/z$  105 were observed representing the benzene and benzaldehyde ions respectively (see appendix 4).

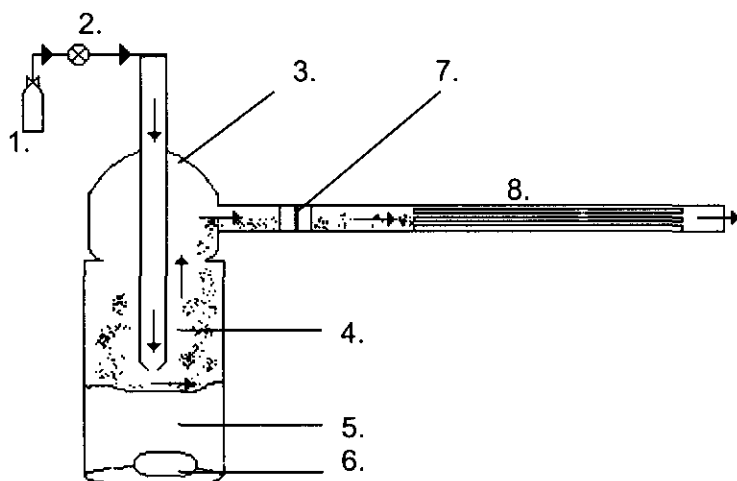
With this information available, we could also test the permeation and diffusion standards prepared at the time. Figure 4.5 And 4.6 show the reconstructed ion chromatograms of  $m/z$  181 for exposure of the SPME fibre for 5 and 10 min to the diffusion standards and permeation standards respectively.

## 6.3 THE DERIVATISING REAGENT

### 6.3.1 LOADING THE REAGENT ONTO THE SILICONE RUBBER TRAP

Methods commonly used to coat sorbents involve coating the sorbent with a solution containing the reagent followed by additional steps to remove the solvent [54,55]. We decided against this technique first, because it would be tedious and time consuming. Second, should all the solvent not be totally removed (particularly if the solvent is water) this would lead to deterioration of the column, the Mass Spectrometer ion source filament and extinguishing of the flame on the Flame Ionisation Detector. Instead, based on previous work by Martos and Pawliszyn [22] on SPME fibres, we decided to load the headspace of the PFBHA from an aqueous solution onto the trap, as this would preclude these disadvantages.

### 6.3.2 LOADING FROM AN AQUEOUS SOLUTION OF REAGENT



- |                              |                              |
|------------------------------|------------------------------|
| 1. High purity nitrogen gas. | 5. Aqueous reagent solution. |
| 2. Mass flow controller.     | 6. Glass coated stirrer.     |
| 3. Glass impinger.           | 7. Teflon tube connection.   |
| 4. Headspace of the reagent. | 8. Silicone rubber trap.     |

Figure 6.11. Set-up for loading headspace from aqueous reagent.

Figure 6.11, shows the set-up used. A 10g/L aqueous solution of PFBHA was prepared in 4ml of MilliQ water. Initially, the solution was placed in a fritted glass bubbler, without a magnetic stirrer. However, we found that this technique led to increased amounts of water condensing in the silicone trap, during collection. An impinger was used instead. The amount of solution was such that the nozzle was just above the surface of the solution. A glass-coated stir-bar was used to stir the solution at 250 rpm, while nitrogen gas was blown over the surface of the stirred solution, at a flow rate of 10ml/min. The dynamic headspace of PFBHA was collected for 30 seconds.

Thermal desorption and analysis of the trap, using a Varian GC - Finnigan Mat ITD, showed that the reagent was successfully loaded. Table 6.1, shows the experimental conditions used and figure 6.12, shows the chromatogram obtained for the collection of a 5 ppm HCHO atmosphere collected at a flow rate of 10ml/min for 10 seconds.

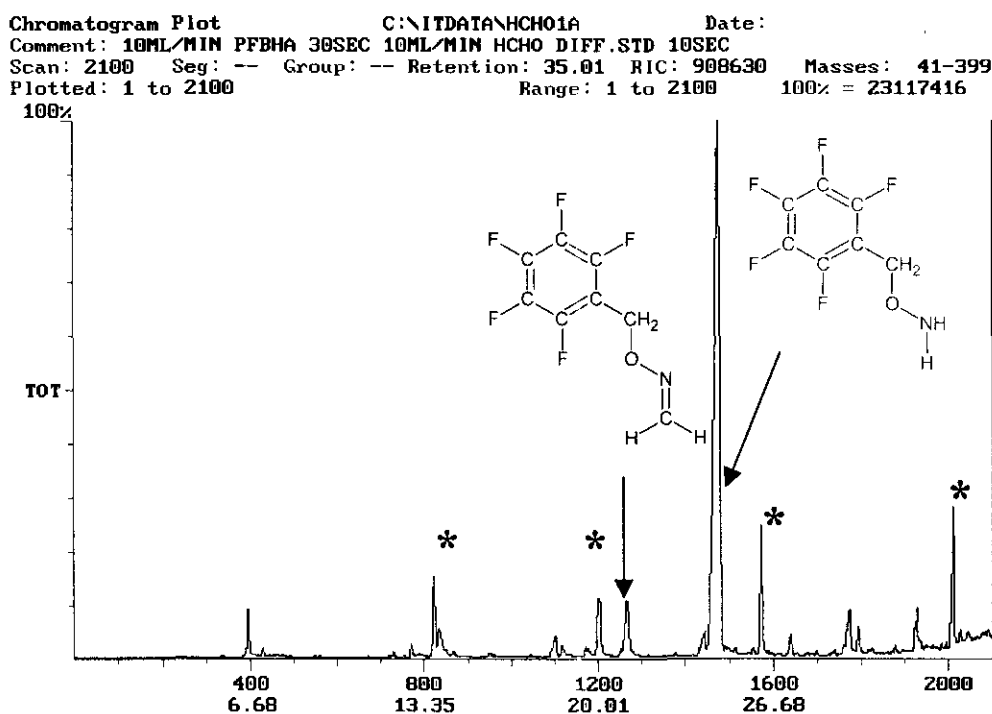


Figure 6.12. GC-ITD MS Total Ion Chromatogram of PFBHA (loaded from aqueous headspace) and 30sec sampling of a 5ppm HCHO atmosphere.

This set-up proved problematic, as discussed below.

Although silicone rubber is hydrophobic in nature, micro-litres of water collected on the trap. This amount of water, in combination with the excessive amount (micrograms) of reagent entering the ion trap contributed to the deterioration of vacuum conditions inside the ion trap (ITD). The instrument could not be used further until the vacuum was restored and most of the water removed, this procedure can take up to two whole days. Removal of water from an ion trap is made difficult by the fact that the ion trap is held at a lower temperature (150°C) than, for example, the quadrupole mass analyser (250°C). In addition, because ions are held in the ion trap before mass separation, M+1 peaks were produced as a result of self chemical ionisation protonation. Figure 6.13, shows the mass spectrum for the HCHO-oxime obtained from the EI - ITD.

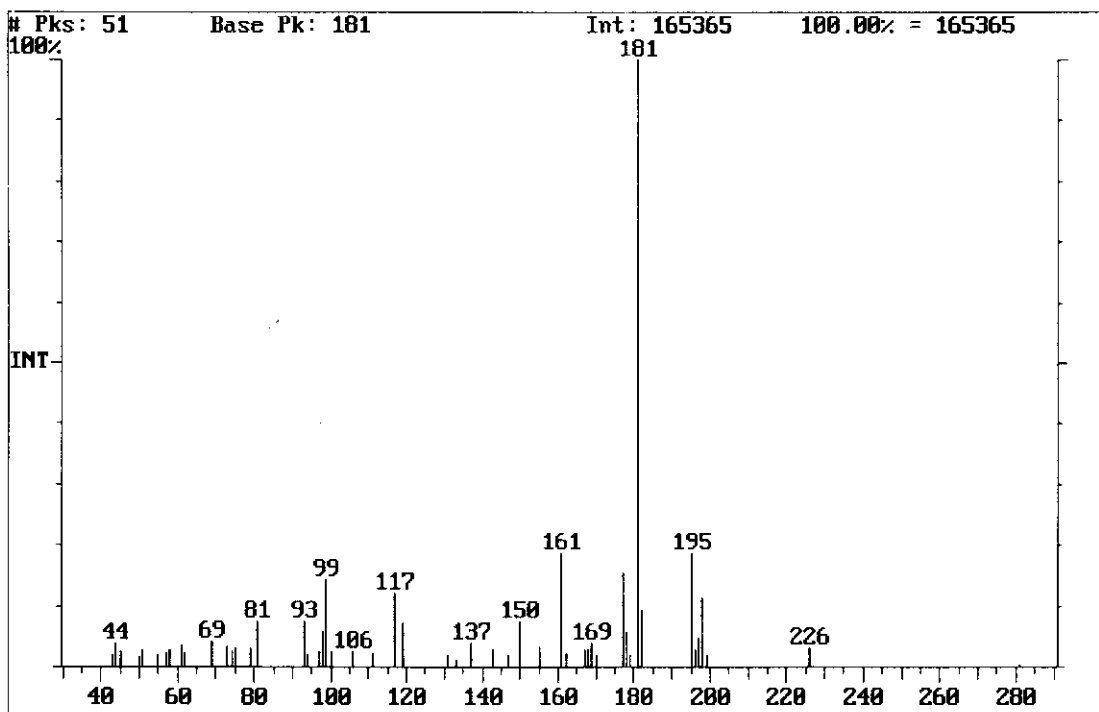


Figure 6.13. ITD EI-Mass spectrum of the formaldehyde-oxime.

Hence, we decided that the quadrupole mass analyser would be more suitable for any further mass spectrometry in this study.

In addition, prevention of excess water condensation in the silicone rubber trap could be achieved by keeping the temperature of the PFBHA aqueous solution a few degrees lower than the temperature of the trap. This was made possible by placing the impinger in a water-bath containing ice. The temperature was reduced from 18°C to 12°C. However, the repeatability of temperature for each PFBHA collection is difficult to maintain in this way.

### 6.3.3 REAGENT PURITY

We found formaldehyde-oxime contamination in the reagent blank. This is a serious problem experienced by several other users of PFBHA [51,128,129] and derivatisation reagents in general (chapter 2). Suggested reasons for this are first, HCHO is a by-product of ozonated water [51]. Second, HCHO is present in air which then dissolves in water [51]. Bidistilled, analytical reagent water, KMnO<sub>4</sub> oxidised and Milli-Q/ MilliPore water all contain the HCHO-Oxime [51,129], with the tandem Milli-Q system providing the lowest blank value [129]. Preliminary work showed that distilled water and Milli-Q water, in our labs, also displayed the oxime blank. The percentage of HCHO-Oxime relative to PFBHA collected is shown in figure 6.14.

The reagent blank is reported in this manner as the amount of oxime loaded appears to be proportional to the amount of PFBHA loaded, which is not a repeatable process (see section 6.3.5). However, since no amount of water purification could completely remove the HCHO-Oxime in the reagent blank, we decided to collect the headspace from the pure reagent, as this would surely remove the contamination present due to water.



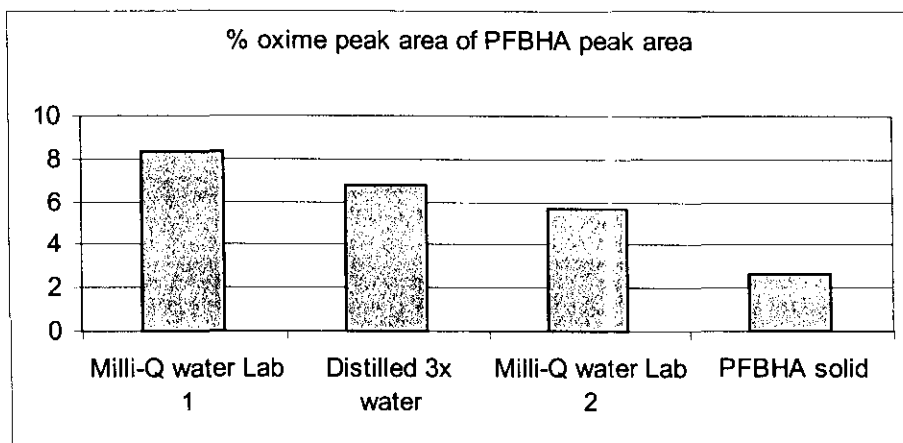
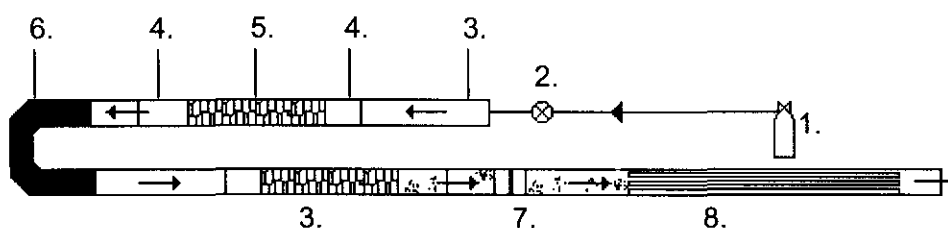


Figure 6.14. Comparison of HCHO-oxime in PFBHA (aq) and PFBHA (s).

### 6.3.4 LOADING FROM THE PURE REAGENT



- |                                    |                             |
|------------------------------------|-----------------------------|
| 1. High purity nitrogen gas.       | 5. Pure solid reagent.      |
| 2. Mass flow controller.           | 6. Activated charcoal trap. |
| 3. Glass tube packed with reagent. | 7. Teflon tube connection.  |
| 4. Glass wool plug.                | 8. Silicone rubber trap.    |

Figure 6.15. Set-up for loading headspace from the pure reagent.

A PFBHA pre-trap and activated charcoal trap were included in the set-up to ensure that no trace amounts of HCHO potentially present in the nitrogen gas could enter the PFBHA loading trap. Any HCHO arising from the nitrogen gas would be derivatised by the first PFBHA trap and then trapped by the activated charcoal before reaching the tube containing the PFBHA from which the headspace would be concentrated in the silicone rubber trap. Figure 6.15, shows the set-up used. All collections were made at a room temperature of 22°C, maintained by air-conditioning in the lab. From the results obtained, it is clear that the reagent is also contaminated. Hence, we had to determine the reagent blank. An acceptable reporting method is to take the

average HCHO amount in a series of blanks plus 3 times the standard deviation for the series of blank runs [129]. This results in a reagent blank value of 23ng HCHO in a 10min collection of PFBHA at a flow rate of 5ml/min (n=5).

Figure 6.16, shows a GC-FID chromatogram of a typical reagent blank collected using this set-up.

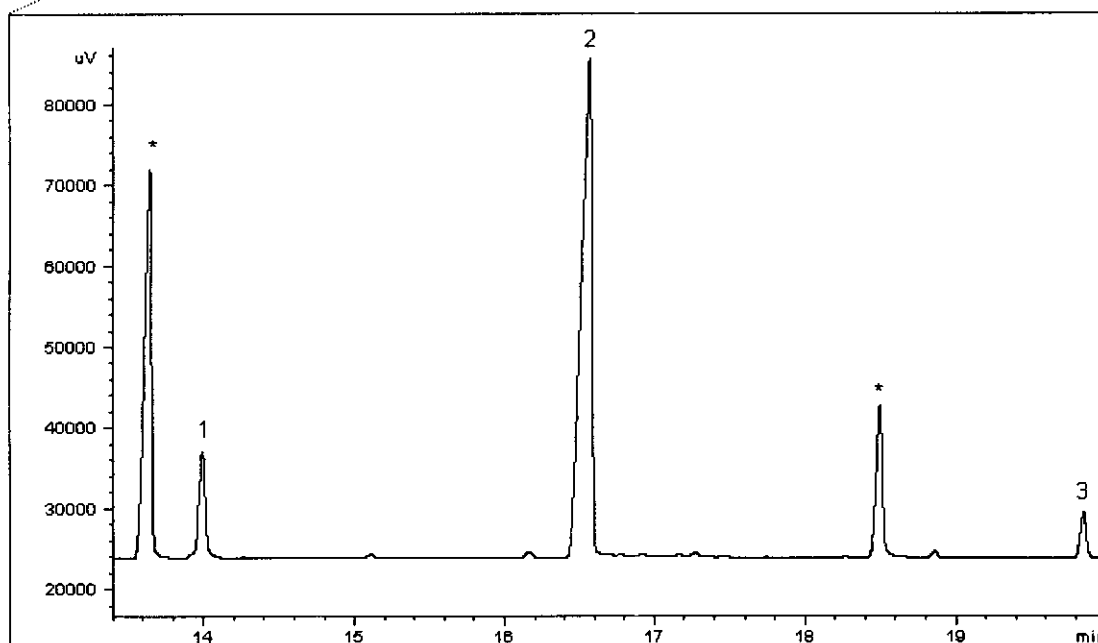
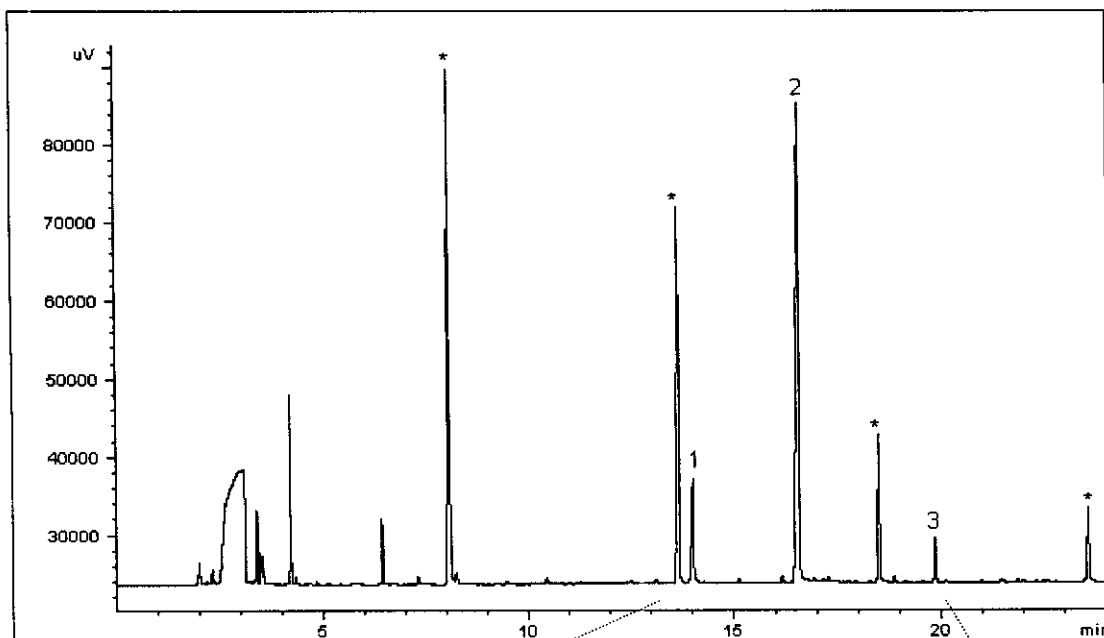
### 6.3.5 REAGENT LOADING REPEATABILITY

At the start of the study it was not necessary to know precisely how much reagent was on the trap as long as it was present in excess. However, with the introduction of the reagent blank it became important that the amount of HCHO-oxime remain constant, as this would determine the detection limit for HCHO.

To study the collection from an aqueous solution of PFBHA (section 6.3.2), the silicone rubber trap was used to collect the dynamic headspace of PFBHA for 1 min at a flow rate of 10ml/min. Nitrogen gas would then be blown over the solution for a time and then another silicone trap would be loaded. This method was followed several times. All traps were analysed using the TCT4020 HP GC-FID instruments, with the parameters used described in table 6.1, using temperature program A and FID range 2<sup>0</sup>. A repeat collection of PFBHA was performed the following day under the same conditions.

Figure 6.17, shows the curve for all the PFBHA (aq) collections over time.

From the repeated aqueous PFBHA collection a similar trend was noted. Namely, there is first a steep increase followed by a steady decrease in the amount of PFBHA collected. This could be due to the PFBHA first coating the inside of the glass vessel surfaces and then moving towards the trap, after which the vapour pressure of the PFBHA begins to decline.



- \* Silicone peaks
- 1. Formaldehyde – oxime
- 2. PFBHA
- 3. 20ng C12

Figure 6.16. GC-FID chromatogram of the PFBHA reagent, headspace collected from the pure solid for 10min at 5ml/min.

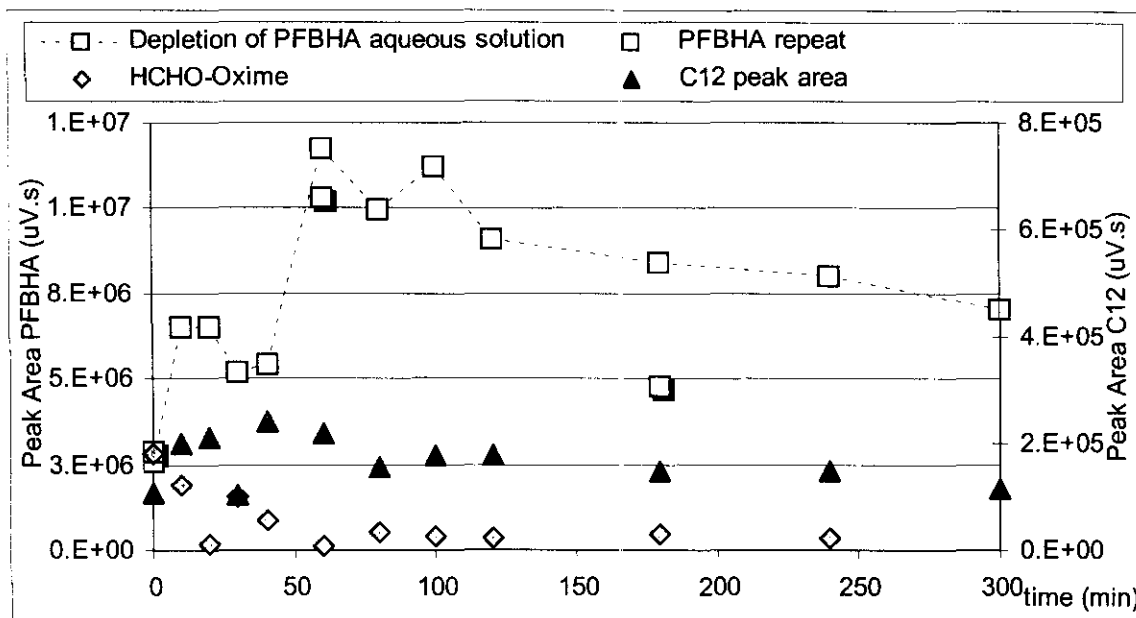


Figure 6.17. The depletion of PFBHA headspace from an aqueous solution.

A similar study was performed on the collection of PFBHA from the pure reagent (section 6.3.4). Silicone rubber traps were loaded with the headspace of PFBHA, as described in 6.3.4, for 10min at a collection flow rate of 10ml/min. They were loaded one after the other, except for the last trap which was loaded the next day.

Instrumental conditions are described in table 6.1, using the TCT4020 HP GC-FID instruments, temperature program A and FID range 2<sup>4</sup>. Results shown in figure 6.18.

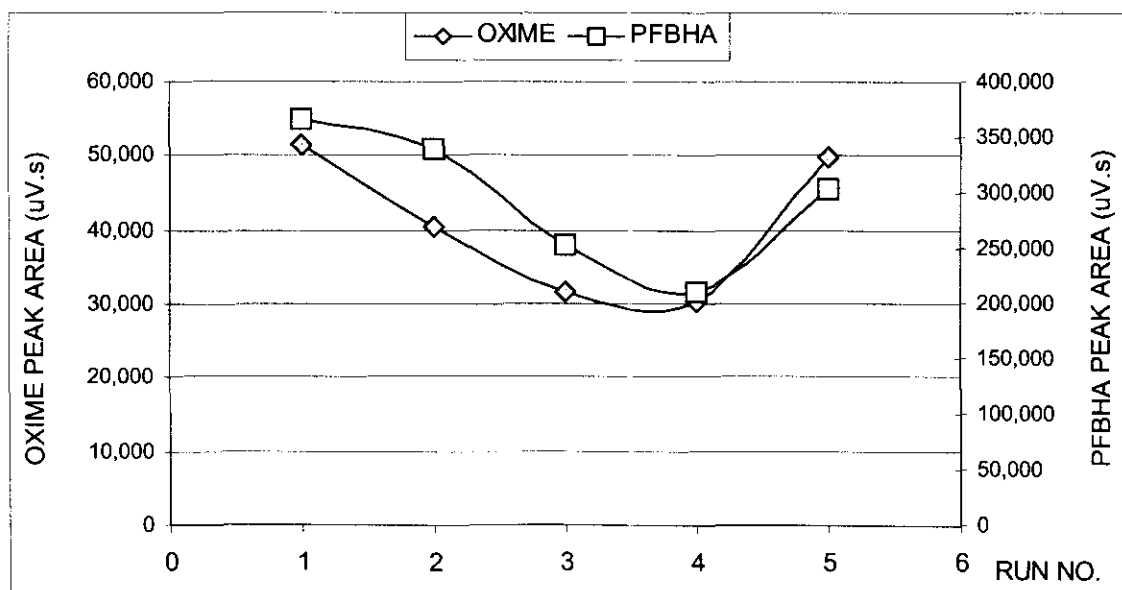


Figure 6.18. The depletion of PFBHA headspace from the pure reagent.

Figure 6.18, shows that the oxime amount changes proportionally with the amount of reagent loaded. Again, we noted that the amount of reagent collected decreases with every collection. However, the last data point is higher again, as this trap was loaded the following day. It would appear that the vapour pressure of the PFBHA decreases with every collection, and increases again over time when no collections are made.

This was also observed with the aqueous PFBHA headspace collections.

It was becoming increasingly obvious that loading the reagent repeatably would be a problem. Since we decided not to collect PFBHA from the aqueous solution, a closer look at collecting from the pure reagent was made. Perhaps, by decreasing the collection flow rate from 10ml/min to 5ml/min, we could increase PFBHA loading repeatability.

A series of PFBHA collections from the pure reagent were made, at both flow rates, for increasing amounts of time. All traps were analysed using the TCT4020 HP GC-FID instrument parameters in table 6.1.

Figure 6.19, shows the increase in PFBHA and HCHO-oxime peak area with increasing loading volume at 5ml/min and 10ml/min. From the graph, it would appear that loading at a flow rate of 10ml/min seems ideal. It appears that more PFBHA is loaded at 10ml/min than at 5ml/min. However, the variation of the oxime peak area relative to PFBHA peak area is reduced from 67 % RSD to 19% RSD when moving from a collection flow rate of 10ml/min to 5ml/min, respectively. Thus using a collection flow rate of 5ml/min for reagent loading would provide more certainty on the amount of HCHO-Oxime already present in the reagent, before sample collection. However, from the graph, it is also clear that the amount of reagent loaded is greatly reduced at this flow rate. We are therefore limited to short sample collection times, as the reaction rate is dependent on an excess presence of reagent [22]. The collection volume can of course be extended if only trace amounts of aldehydes are present and the reagent is not depleted.

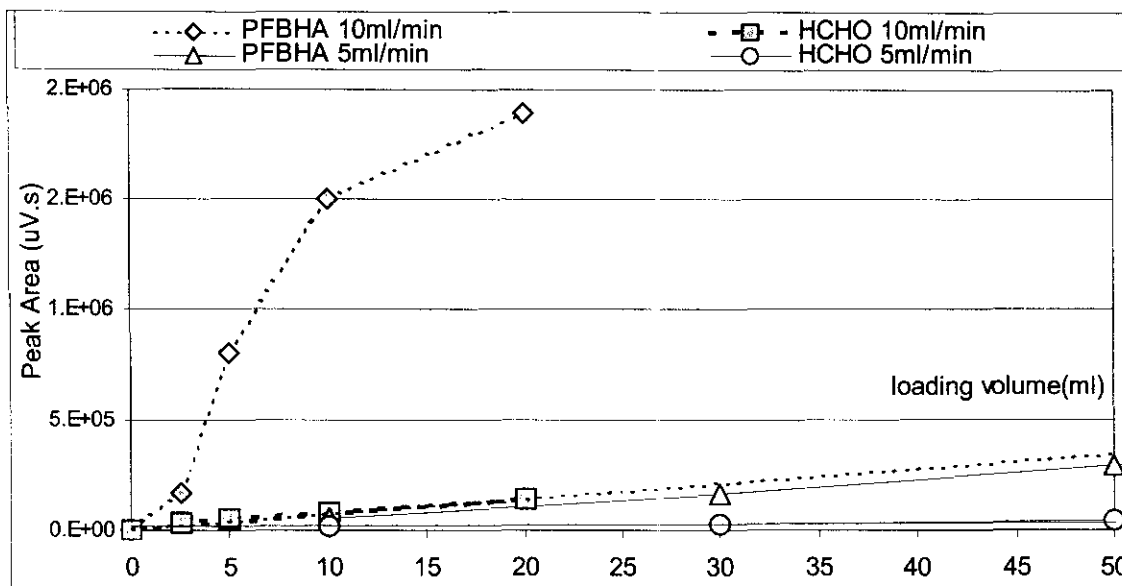


Figure 6.19. Peak area of PFBHA and HCHO-oxime with increasing loading volume at 5 and 10ml/min collection flow rates.

Martos and Pawliszyn [22], demonstrated, during their fibre selection process, by blowing nitrogen over the fibres, that the PFBHA is not as well retained on the 100% PDMS fibre as on their more polar variations. This was also observed on the silicone rubber trap, as shown in Figure 6.20, that the PFBHA depletes with increased collection time of nitrogen gas from the gas standard oven. Notice that the HCHO-oxime remains constant, indicating a better retention of this compound on the trap.

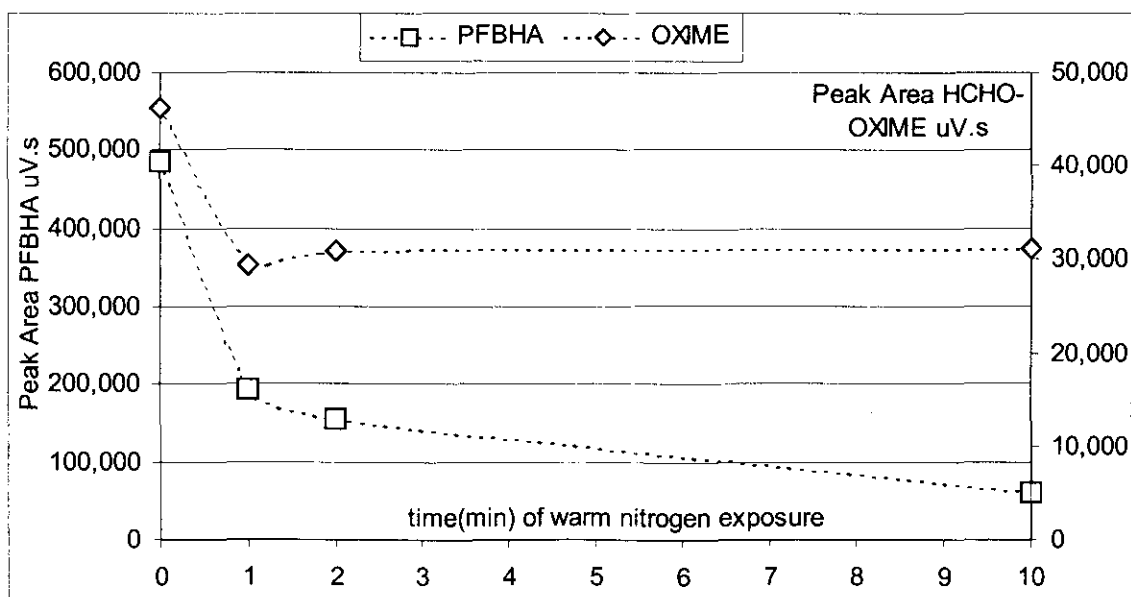


Figure 6.20. The depletion of PFBHA from the silicone trap with exposure to nitrogen at a flow rate of 10ml/min.

## 6.4 THERMAL DESORPTION – CRYOGENIC FOCUSING

A description of the instrument was given in chapter 5. An experiment was performed to determine the conditions under which the HCHO-oxime would be completely transferred to the GC column i.e. when the desorption process is complete.

The silicone rubber trap, described in chapter 3, can be compared to a chromatographic column having a polydimethylsiloxane stationary phase. Literature [22, 50, 129] and our own studies indicate that the HCHO-oxime elutes before the PFBHA. It could therefore be assumed that the PFBHA would “elute” off the silicone trap after the HCHO-oxime. Since no HCHO-oxime standard was available, determining the total transfer by using the PFBHA peak would have to suffice. (The alternative could also be to synthesise the HCHO-Oxime.)

However, after an initial exercise done by injecting PFBHA directly onto the column, it became clear that the PFBHA, being an amine, did not chromatograph well. Due to amine-interactions with the fused silica surface, tailing peaks were produced and not the ideal gaussian peak shapes required for normal integration. PFBHA would therefore be an unsuitable compound for quantitation.

Based on the above observations, we then decided to use dodecane (C12), which elutes after PFBHA. 1 $\mu$ L of a 20ng/ $\mu$ L C12 in CS<sub>2</sub>, was placed onto the top of the silicone trap using a 5  $\mu$ L syringe. As desorption flow is from the top to the bottom of the trap, once the C12 is completely desorbed it is obvious that any compound which elutes before C12 on the trap has also been completely desorbed. Traps were analysed using the TCT4020 HP GC-FID instruments, temperature program A, as shown in Table 6.1.

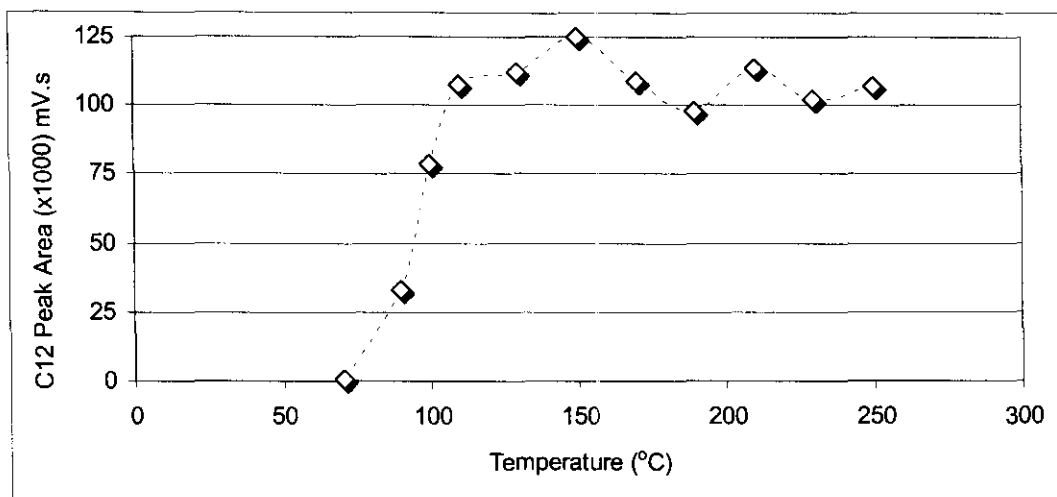


Figure 6.21. Optimisation of the thermal desorption of dodecane (C12) from a silicone trap

Figure 6.21, shows a graph of C12 peak area *versus* desorption temperature. From these results we can see that the C12 has reached a maximum peak area at 150 °C which is stable up to 250°C. A temperature of 220°C was chosen for the desorption process. Silicone degradation increases with higher temperatures, which result in increased silicone peak areas [26], causing additional problems such as peak overlap, column overload and contamination of the MS ion source. For this reason higher temperatures were not chosen. A blank run of the silicone trap after this desorption cycle indicates complete transfer of the oxime and reagent and no carry-over. We also decided to include a backflush cycle at 280°C for 10 min to remove any other compounds not desorbed at 220°C from the trap. In doing so we could ensure a clean, conditioned trap which is ready for use again.

Dodecane (C12) was added, as an internal standard, to all traps just before desorption in the TCT unit. The C12 was used not only to quantitate the amount of oxime formed, as described in section 5.3, but also as a means to check for any losses in the TCT unit during the desorption process.



## 6.5 REACTION EFFICIENCY

The ability of PFBHA to react with formaldehyde inside the silicone rubber was investigated. A linear increase of derivatised HCHO against collection volume would indicate that pre-concentration is occurring. The silicone rubber trap was loaded with pure PFBHA headspace for 10min at 5ml/min, followed by exposure to a HCHO-atmosphere for increasing time intervals, then analysed using the standard conditions described in table 6.1, temperature program A, TCT4020 HP GC-FID.

Two atmospheres were sampled: an 80ng/min HCHO gas standard provided a 5.98ppm HCHO atmosphere, and a 100ng/min HCHO gas standard sampled from the dilution system, described in chapter 4, yielded 1.33ng/min of HCHO which provided a 0.1ppm HCHO atmosphere.

Various exposure times were chosen in order to construct two curves of HCHO (ng) *versus* collection time. One curve is the plot of HCHO reacted against collection time, the other curve is the plot of HCHO flowing through the trap against collection time. The amount of HCHO reacted is calculated from the HCHO-oxime peak area and the peak area of the C12 internal standard, desorbed from the trap, using the method described in section 5.3.

The amount of HCHO flowing through the trap is determined based on the gravimetric measurement of the mass loss rate (ng/min) of the HCHO permeation gas standard and the calculated dilution factor (see chapter 4).

A comparison of the gradients of the two curves would indicate whether the reaction is 100% efficient or if it is below the expected mass loss rate of the HCHO gas standard. The assumption is made that no HCHO gas is lost in the set-up due to leaks, polymerisation or adsorption on surfaces in the set-up.

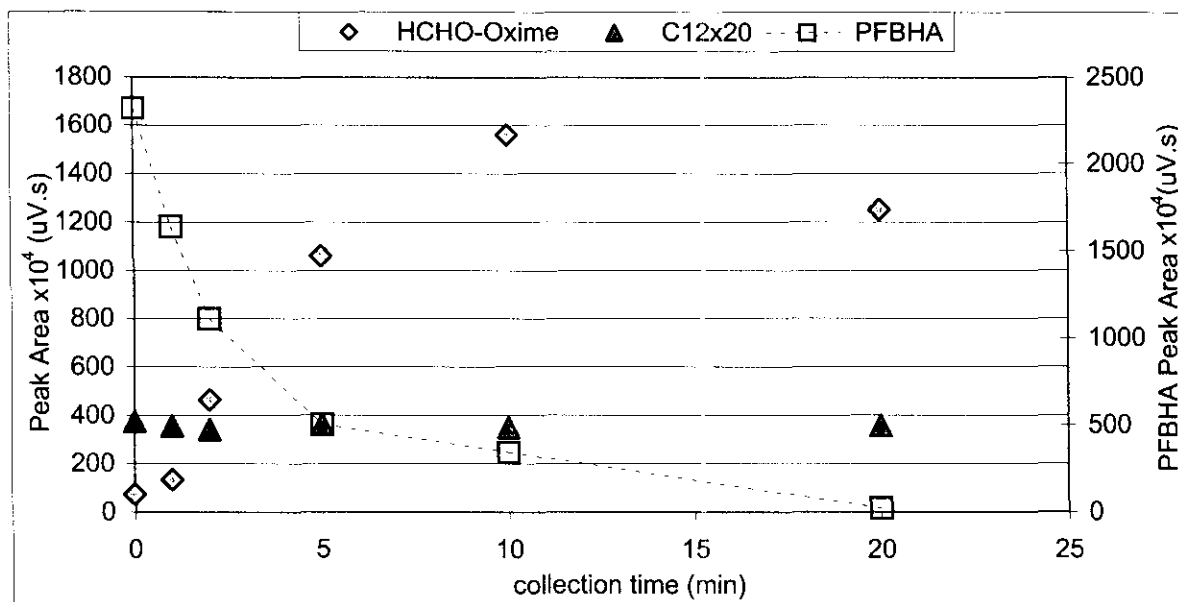


Figure 6.22. Collection of a 5.98ppm HCHO atmosphere at 10ml/min over time.

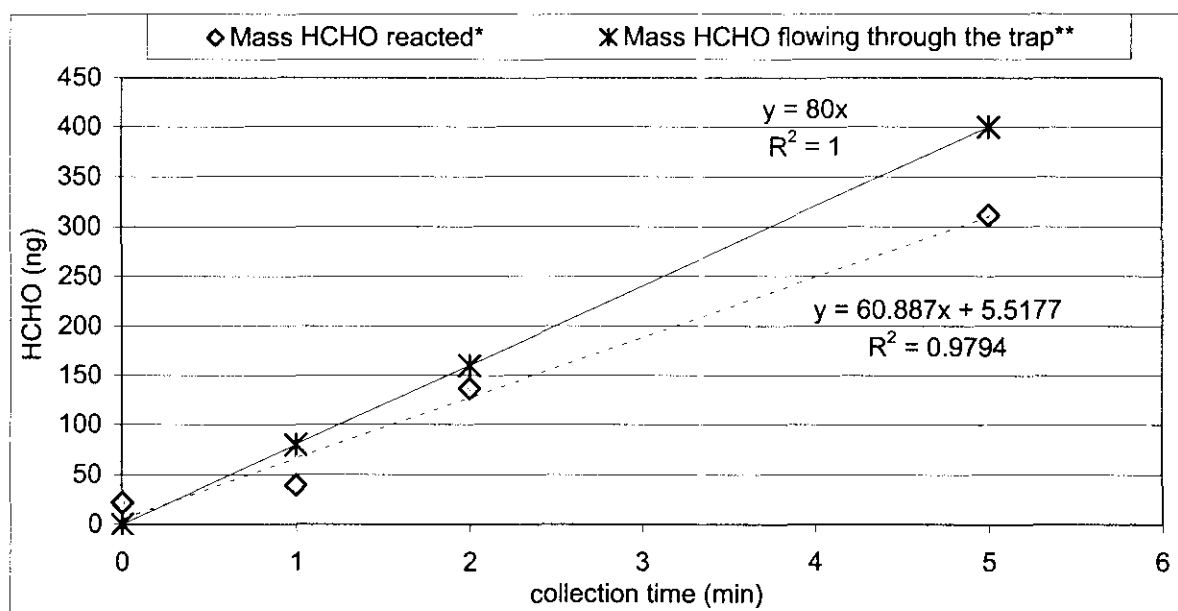


Figure 6.23. Determination of reaction efficiency of 5.98ppm HCHO with PFBHA.

\*Mass of HCHO reacted is calculated with the HCHO-Oxime peak area (shown in Figure 6.22), the C12 internal standard peak area and relative response factor, using the method shown in section 5.3.

\*\*Mass of HCHO flowing through the trap is determined from the gravimetrically measured mass loss rate (ng/min) of the HCHO gas standard sampled.

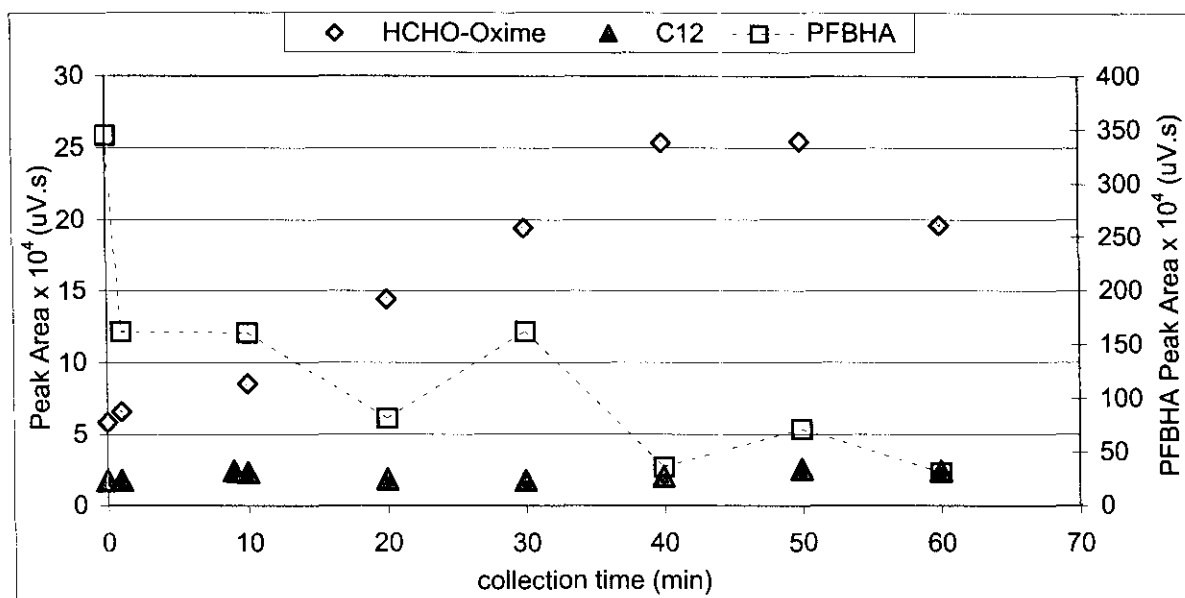


Figure 6.24. Collection of a 0.1ppm HCHO atmosphere at 10ml/min over time.

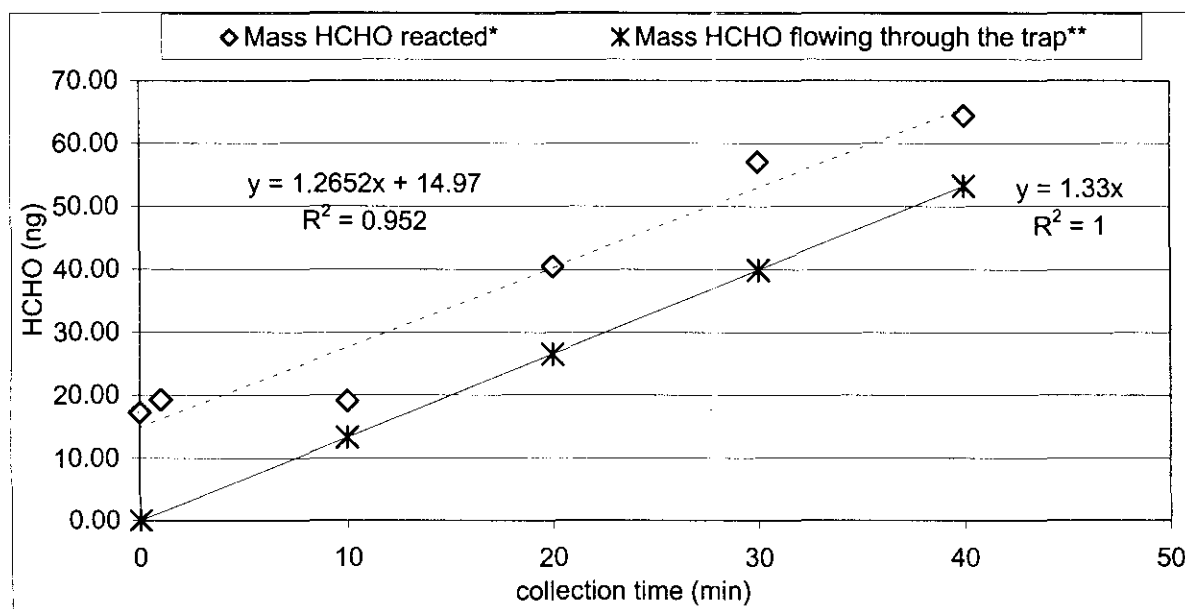


Figure 6.25. Determination of reaction efficiency of 0.1ppm HCHO with PFBHA.

\*Mass of HCHO reacted is calculated with the HCHO-Oxime peak area (shown in Figure 6.24), the C12 internal standard peak area and relative response factor, using the method shown in section 5.3

\*\*Mass of HCHO flowing through the trap is determined from the gravimetrically measured mass loss rate (ng/min) of the HCHO gas standard (and the calculated dilution factor) sampled.

Figure 6.22 shows the graph of peak area *versus* collection time, obtained for the sampling of a 5.98ppm HCHO atmosphere. Figure 6.23, shows the comparison of the gradients of HCHO (ng) reacted and HCHO (ng) flowing through the trap, for the first 60ml collected from the 5.98ppm HCHO atmosphere.

Similarly, figure 6.24 shows the graph of peak area *versus* collection time, for a 0.10ppm HCHO atmosphere. Figure 6.25 shows the comparison of gradients of HCHO (ng) reacted, and HCHO (ng) flowing through the trap, for the first 400ml collected from the 0.1ppm HCHO atmosphere.

Trapping from the 5.98ppm HCHO atmosphere (figure 6.22 and 6.23) shows a linear increase ( $R^2 = 0.9794$ ) of the HCHO-Oxime peak area (figure 6.22) or the amount of HCHO reacted (figure 6.23), from 0 to 5 min collection time (50ml collection volume). Thereafter, the curve is no longer linear, and even starts to decrease, as the amount of PFBHA is depleted and therefore not available to react with the HCHO gas entering the trap. Thus trapping of concentrations above 5.98ppm, for longer than 100ml at 10ml/min, will not be quantitative. In addition, a comparison of the gradients (figure 6.23) indicates that the trapping is 75% of what we expected. Our HCHO gas standard provided HCHO gas flow through the trap at a rate of 80ng/min, but the HCHO was only being trapped (reacted) at a rate of 60ng/min.

Likewise, sampling of the 0.1ppm HCHO atmosphere (figure 6.24 and 6.25), indicates a linear increase ( $R^2 = 0.952$ ) from 0 to 40 min (400 ml collection volume), then starts to decrease as PFBHA depletes. However, for this lower concentration, a comparison of the gradients in figure 6.25, indicates 95 % trapping efficiency during the first 400 ml collected. That is our HCHO gas standard provides HCHO gas flow through the trap at a rate of 1.33ng/min and this HCHO is being trapped at a rate of 1.26ng/min on our PFBHA-coated silicone rubber trap.

From these curves we are also convinced that our method to calculate the amount of aldehyde present, using Effective Carbon Numbers (ECN), the C12 internal standard and relative response factors, described in section 5.3, performs well.

This procedure was also applied to the other aldehydes in our study. Permeation standards of type 2 were used for acetaldehyde, propanal, acrolein and crotonal. Butanal and Benzaldehyde were type 1 permeation standards. Their respective permeation rates can be obtained from table 4.1. Figure 6.26, shows the chromatogram obtained for the sampling of the aldehyde permeation gas standards (type 2). These aldehydes were identified by their elution temperatures, obtained by the study above (section 6.2). Propanal, butanal and benzaldehyde were not detected.

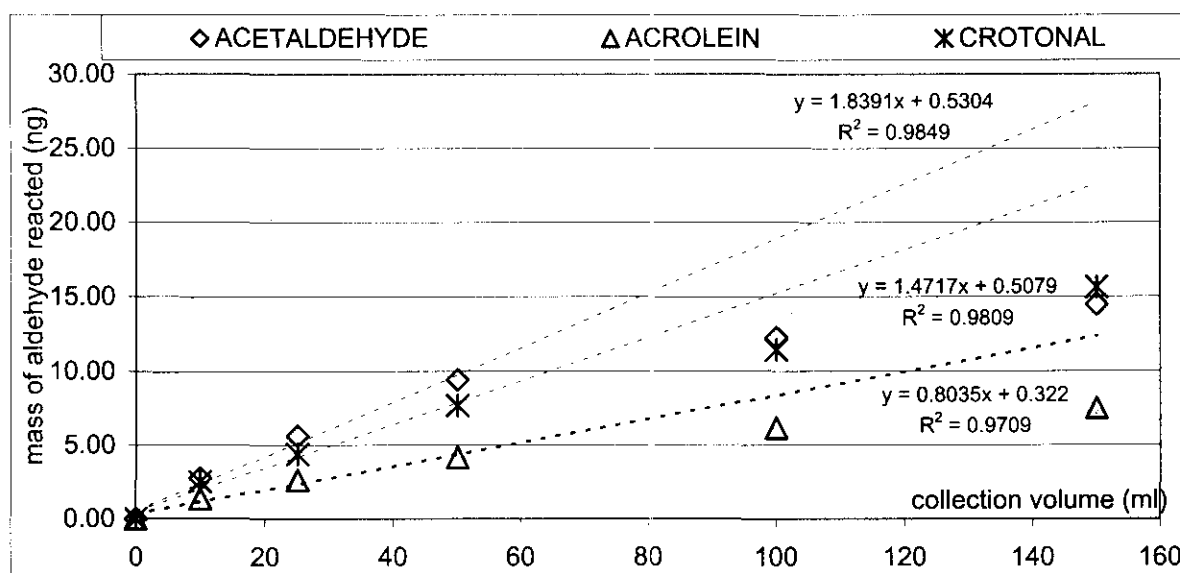
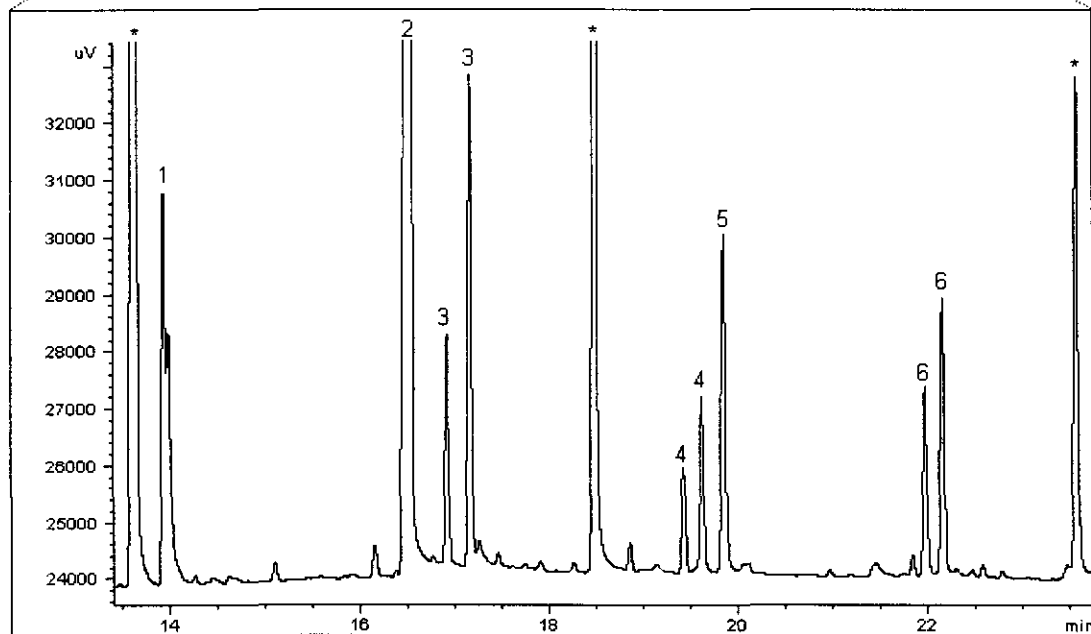
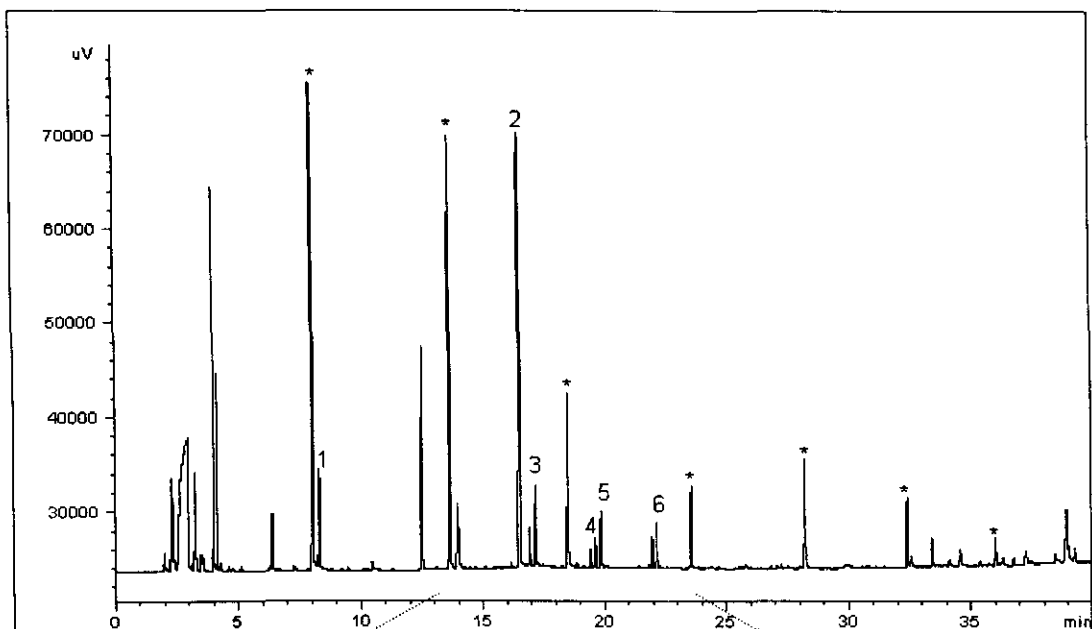


Figure 6.27. Determination of reaction efficiency of 3ppm acetal, 1.5ppm acrolein and 2.5ppm crotonal with PFBHA.

Mass of aldehyde reacted is calculated with aldehyde-oxime peak area, C12 internal standard and relative response factors using the method shown in section 5.3. The predicted ECN for acetaldehyde is 7.45, for acrolein 8.35 and crotonal 9.35.



- |   |                         |
|---|-------------------------|
| * Silicone peaks                            | 3. Acetaldehyde – oxime |
| 1. Formaldehyde – oxime<br>(from the PFBHA) | 4. Acrolein – oxime     |
| 2. PFBHA                                    | 5. 20ng C12             |
|   | 6. Crotonal - oxime     |

Figure 6.26 GC-FID chromatogram obtained for the collection of 3, 1.5 and 2.5 ppm acetal, acrolein and crotonal respectively, for 10 min at a flow rate of 10ml/min

Figure 6.27, shows the plot of reacted aldehyde over collection time for acetaldehyde, acrolein and crotonal at concentrations of 3, 1.5 and 2.5 ppm respectively, the dotted lines are the trend lines for the linear portions of each curve. In the first 5 minutes (50ml collection volume) there is a linear increase for each aldehyde, but upon comparison with the aldehyde amounts flowing through the trap (determined from the gas standards), they all indicate roughly a 4% reaction efficiency. It may be that these aldehydes do not react as rapidly with the PFBHA as HCHO does. However, we suspect that the gas standard glass impinger was not leak tight, and a more suitable leak-tight set-up should be made before further studies using these aldehydes are performed.

Based upon these results, table 6.3, lists the average percentage peak area of the first isomer peak to the second isomer peak, for acetal, acrolein and crotonal oxime. The ratio of these peaks appear to be constant, so in addition, this will allow for easier identification of the compounds when using an FID.

Table 6.3. The variation in the ratio of the isomer peaks of acetal, acrolein and crotonal-oximes.

	average % peak area 1 of peak area 2	%RSD	n
acetaldehyde-oxime	50.60	13.40	7
acrolein-oxime	59.38	8.31	6
crotonal-oxime	79.39	16.03	6

We also wanted to determine, based on these experiments, what would be the minimum detectable concentration of these aldehydes. For this calculation, using the results from the 1 min (10ml) collection of the permeation standards, we obtained the signal-to-noise (s/n) ratio of the second isomer peak of the aldehyde-oximes. We then

solved for the minimum concentration that can be detected at a s/n ratio of 3. Table 6.4 shows the minimum detectable concentrations for acetaldehyde, acrolein and crotonal. From these results, we are content to see that the detection limits we obtained for these aldehydes are below their Permissible Exposure Limits (PEL) [6]. In addition, we know that these results are based on a sample collection time of only 1 min, therefore a longer sample collection time would result in even lower detectable concentrations.

Table 6.4. Determination of minimum detectable concentrations for acetaldehyde, acrolein and crotonal.

	acetal	acrolein	crotonal
Permissible Exposure Limit (ppm) [6]	100	0.1	2
gas standard concentration (ppm)	3.0	1.5	2.5
s/n isomer peak 2	257.7	79.1	118
minimum detectable concentration (ppm) at s/n 3	0.035	0.057	0.064

## 6.6 REAGENT DEPLETION *versus* BREAKTHROUGH VOLUME

In chapter 3, we discussed the retention capability of a sorbent trap in terms of its breakthrough volume. In this study two silicone traps, coated with PFBHA, were arranged in series. The first trap remained at the outlet of the 0.1 ppm HCHO atmosphere, while the second trap was analysed for breakthrough. The second trap was replaced each time with a new PFBHA coated trap. All traps were analysed as in section 6.5. FID range was 2<sup>0</sup>. Figure 6.28, shows the curve obtained for a



breakthrough study of HCHO and its derivative. All data points are obtained from the analysis of the second trap, except for the last data points (after 3000ml) for the HCHO-oxime and the PFBHA which, are from the first trap.

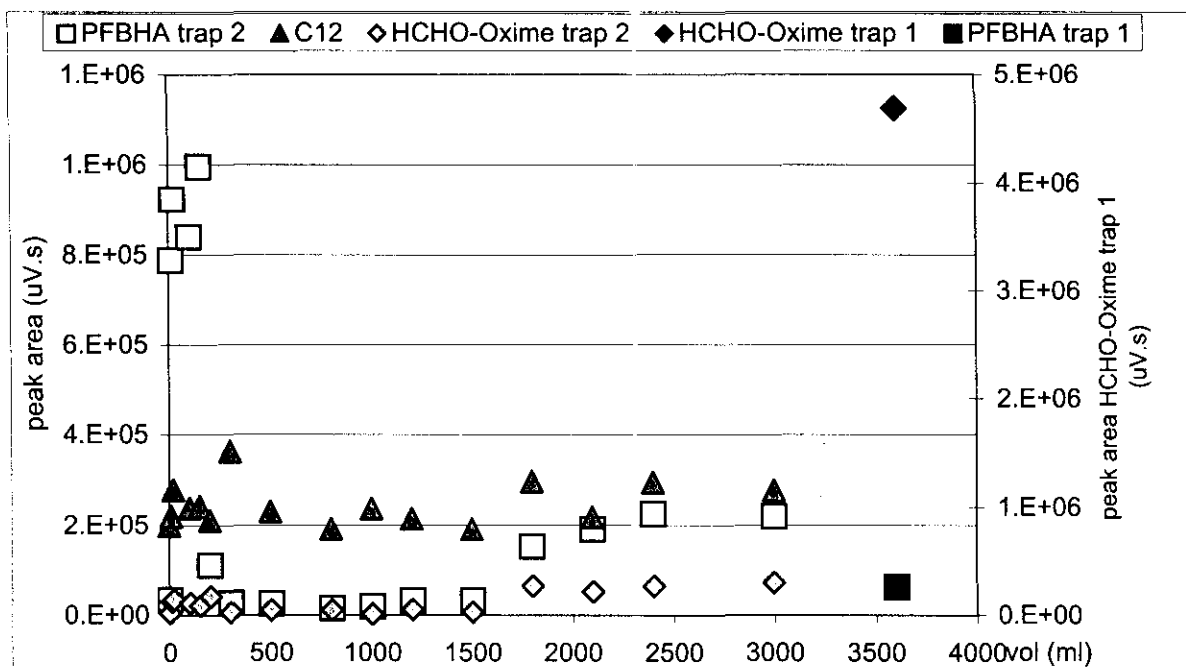


Figure 6.28. Determining the breakthrough volume of the HCHO-oxime onto the second trap\*.

\*Two PFBHA-coated traps were arranged in series at the exit of the 0.1ppm HCHO atmosphere. The second trap is analysed after the various collection volumes indicated. Collection flow rate 10ml/min. Dodecane (C12) is the internal standard. Data points after 3500ml were obtained from the first trap.

After 3 litres of sampling, we expected some breakthrough onto the second trap, as surely the PFBHA would be depleted on the first trap at this time, as discussed above in section 6.5. The slight increase of HCHO-oxime from 1800 ml onwards we attribute to the proportional increase in PFBHA loaded on the second trap.

Since there was no clear increase of HCHO-oxime on the second trap, the HCHO was still being retained somehow. Upon desorbing the first trap, it was clear that there was no breakthrough of HCHO-oxime, even after 3 litres of sampling. The PFBHA was still present on the first trap, but no longer in excess as seen in figure 6.28.

From this curve, it is clear that the HCHO-oxime is well retained on the trap.

Nevertheless, of greater importance is the depletion of the PFBHA. We suspect that once the reagent is totally consumed on the first trap, breakthrough of HCHO will occur. It is possible that some HCHO, not efficiently trapped by the depleting PFBHA on the first trap, could have broken through but that it never exceeded the background HCHO amount in the reagent on the second trap.

Since the HCHO-oxime is well retained on the silicone trap, we can also deduce that the other aldehyde-oximes, which elute after the HCHO-oxime, will have an even better retention on the silicone rubber trap.

## 6.7 CONCLUSION

From these studies, we can conclude that *in-situ* derivatisation on silicone rubber traps is possible. A simpler method is used for coating the sorbent with derivatising reagent, which effectively reduces sample preparation time. Aldehydes are pre-concentrated and retained on the silicone by reacting with the PFBHA in the silicone to form the stable oxime products. These products have been successfully desorbed from the silicone rubber trap and analysed by Flame Ionisation Detection and Mass Spectrometry.

However, our biggest problem remains the high formaldehyde-oxime contamination in the PFBHA reagent. In addition, the reagent cannot be loaded onto the silicone rubber trap with high repeatability. Consequently, our next step in this project, is to investigate possible methods such as recrystallisation [50] to eliminate these problems as it severely restricts our detection limit for HCHO. HCHO atmospheres as low as 0.1ppm has been detected. This detectable amount does meet certain exposure limits

set by OSHA, ACGIH and the WHO, shown in table 1.1, but not the NIOSH PEL of 0.016ppm.

We have shown that permissible concentration exposure limits for acetaldehyde, acrolein and crotonal can be reached with our method (table 6.4). Lower detection limits are possible for these aldehydes as they are not present in the reagent blank. For this reason we could have loaded more PFBHA onto our silicone rubber traps for the determination of the reaction efficiency of these aldehydes with PFBHA, and for determination of their minimum detectable concentrations. However, further work is required on the gas standard set-up, as a leak was suspected.

## CHAPTER 7

### TESTING THE SILICONE RUBBER TRAP ON REAL SAMPLES

#### 7.1. INTRODUCTION

In the previous chapters we have shown, using gas standards, that aldehydes can be derivatised and pre-concentrated on the silicone rubber trap. They are successfully thermally desorbed and analysed by GC - FID or MS. However, it is also important to study the ability of the silicone rubber trap to derivatise and pre-concentrate aldehydes from real life gaseous samples.

In this chapter, the use of the silicone rubber trap is tested on several real samples. These samples were collected from both indoors and outdoors as well as inside cars. These are areas where we usually expect formaldehyde to be present. In addition the headspace of three different beers were sampled for acetaldehyde analysis.

In view of the difficulties experienced with the purity and loading of the derivatising reagent, as well as the method of quantitation used, the results obtained are at best semi-quantitative. These tests serve only to demonstrate the application of *in-situ* derivatisation on silicone rubber traps for real sample analysis.

#### 7.2 EXPERIMENTAL

The traps, used to analyse for HCHO content, were coated with PFBHA headspace from the pure reagent (section 6.3.4) for 10min at a flow rate of 5ml/min. All air

samples were collected for 50min, using a GilAir-3 air sampling system from Gilian, set at a collection flow rate of 10ml/min.

The traps, used for the beer analysis, were coated with PFBHA headspace from the pure reagent for 50min at a flow rate of 10ml/min, except the Black Label beer which was loaded for 10min. Acetaldehyde in beer was analysed by collecting the dynamic headspace of approximately 40ml of beer from an impinger type device, similar to that used for the collection of aqueous PFBHA (section 6.3.2). The nozzle of the impinger is above the surface of the beer, which was stirred by a glass coated magnetic stirrer at 500 rpm. The impinger was immersed in a water-ice bath to limit the amount of water condensation in the trap. Nitrogen gas was used to load the headspace of the beer at a flow rate of 10ml/min for 10 minutes. The combination of stirring and nitrogen gas blowing over the beer surface, allowed for minimal foaming of the beer. Hence, no anti-foaming agent was required.

All samples were collected using 2 silicone rubber traps arranged in series connected with a teflon tube. The traps were analysed using the TCT4020 HP GC-FID instruments, with the conditions as described in table 6.1. The temperature programs used are listed in table 7.1 and 7.2.

Ideally gas chromatography with mass spectrometric detection should be used when testing real samples, as overlapping peaks can easily be discerned. Unfortunately, we could not use our quadrupole mass spectrometer at the time, as it was not providing adequate sensitivity.

## 7.3 RESULTS AND DISCUSSION

Table 7.1 lists the air samples collected and formaldehyde amounts obtained from both traps, calculated as described in section 5.3. The formaldehyde-oxime blank value (peak area) was subtracted from the real sample HCHO-oxime peak areas, before the HCHO amount was calculated. The peak area blank value was calculated by taking the average of a series of PFBHA blanks plus 3 times the standard deviation thereof resulting in a peak area of 67,781 uV.s (i.e. 23.69ng HCHO). The HCHO gaseous concentration in part-per-million (ppm), was calculated by taking the sum of HCHO (ng) in each trap and dividing it by the collection volume. This value was then divided by the conversion factor of 1.23 [6] to convert the HCHO unit of ng/ml to ppm, shown in table 7.1. The percentage trapping efficiency was also determined.

Table 7.2 lists the beer samples collected and acetaldehyde ( $\text{CH}_3\text{CHO}$ ) amounts obtained from both traps, calculated as described in section 5.3. The  $\text{CH}_3\text{CHO}$  gaseous concentration in part-per-million (ppm), was calculated by taking the sum of  $\text{CH}_3\text{CHO}$  (ng) in each trap and dividing it by the collection volume. This value was then divided by the conversion factor of 1.8 [6] to convert the  $\text{CH}_3\text{CHO}$  unit of ng/ml to ppm, shown in table 7.2. The percentage trapping efficiency was also determined.

### 7.3.1 AIR SAMPLES

All air samples collected, listed in table 7.1 are depicted in figures 7.1 to 7.7 for trap 1. Immediately apparent in all of these chromatograms is the repeatable retention times and peak heights of the silicone degradation peaks, indicated with an asterisk (\*). In

addition, the PFBHA, HCHO-oxime and C12 peaks display consistent retention times throughout.

Figure 7.4 shows a chromatogram of parking lot air sampled using the silicone trap, without any PFBHA loaded on it. Figure 7.3 shows a dramatic decrease in the complexity of the chromatogram obtained, when sampling air from the parking lot using a PFBHA-coated silicone trap. Several peaks have disappeared; we believe this is a result of various carbonyl compounds in the air reacting with the PFBHA. We assume most of the other peaks are hydrocarbons emitted from the car exhausts. As expected, formaldehyde is present in the air, particularly as a result of incomplete combustion of hydrocarbons in fuel.

A problem occurring with the parking lot samples was the extinguishing of the flame on the FID, as seen after 5 min on the chromatogram in figure 7.4. In addition the sensitivity of the instrument was halved after these samples were run. We suspect that fine dust particles may have entered the column, blocking it in the process. The sensitivity was restored by cutting off 30cm of the capillary column.

Figure 7.5, showing the air sampled from a bar, indicates the presence of formaldehyde resulting from tobacco smoke. In addition, alcohol (ethanol) eluting at 2min, and acetaldehyde are also present as expected. Notice, however, that the ratio of the acetaldehyde-oxime peaks are not what we expected, peak 1 should usually be half the size of peak 2. Analysis with an MS would have eliminated this uncertainty. A comparison of the chromatograms for sampling the indoor air of a new car (figure 7.6 ) and an old car (figure 7.7) indicate the presence of HCHO in both, with the new car having a much higher amount (table 7.1). Nevertheless, HCHO is present in the older car too, along with other volatiles notably absent from the newer car. This HCHO probably originates from the exhausts of other cars during traffic.

The results obtained in table 7.1 indicate breakthrough onto trap 2, despite PFBHA still being present on trap 1. Consequently, the calculated trapping efficiencies are much lower than expected. This contradicts our breakthrough (section 6.6) and reaction efficiency (section 6.5) studies. From these studies we observed no breakthrough of the HCHO-Oxime after 3 litres of air sampling at a flow rate of 10ml/min. We only sampled 500ml of air. In addition, reaction efficiencies for HCHO and PFBHA were observed to be between 75 and 95%.

Martos and Pawliszyn [22] have suggested that the reaction rate between PFBHA and HCHO is directly proportional to the concentration of HCHO, only while the PFBHA is minimally consumed. Once the reagent is no longer in excess, the reaction rate will decrease.

With this information, we can deduce why breakthrough occurred onto the second trap. The average peak area (plus 3 times the standard deviation) of PFBHA loaded onto the trap for 10min at 5ml/min is 482,562uV.s (n=5). For the data from the newly carpeted laboratory, the peak area of PFBHA remaining on trap 1 is 199,580uV.s. This indicates that 58%, more than half, of the PFBHA has been consumed. The reaction rate between PFBHA and HCHO has therefore decreased and we no longer have the >80% trapping efficiency. Similar trends were observed for the other air samples, except for the indoor air of the new car (trap 1). Here we suspect that the amount of PFBHA loaded onto the trap was more than we expected.

Our tests in the laboratory were based on the reaction between PFBHA and HCHO alone. With the real samples, however, other aldehydes and carbonyl groups are present in the air and will also react with the PFBHA, contributing to its rapid depletion and consequent decreased reaction rate with HCHO. It is therefore necessary to use a back-up trap when collecting the real gaseous samples.



### 7.3.2 HEADSPACE BEER SAMPLES

Figures 7.8 to 7.11 show the chromatograms obtained by sampling the dynamic headspace of various beers, from trap 1. Once again, the silicone, PFBHA, HCHO-oxime and acetaldehyde-oxime peaks show consistent retention times.

Unfortunately, extinguishing of the flame on the FID was also experienced with these samples, as shown in figure 7.8 at 5 min. A temperature difference of at least 10°C between the beer and the trap, had to be maintained during sampling to avoid condensation of water in the trap and consequent extinguishing of the flame.

Also noted, was a co-elution of a compound from the beer with our internal standard, dodecane (C12). An average peak area of 15,000  $\mu\text{V}\cdot\text{s}$  for C12 was used for the calculations (section 5.3). Another peak, at 13.5 min also co-eluted with one of our silicone peaks. If these peaks were of interest to us, the use of a mass spectrometer would be ideal, as the silicone peak can easily be subtracted from the co-eluting peak based on its unique  $m/z$  ratios.

It has been suggested that beers not brewed locally have a higher acetaldehyde content, as a result of the ageing process. These beers take longer to reach the public, as they must be transported in, from outside the country first. Windhoek Light, is an example of a lager beer not brewed locally. From table 7.2, it is clear that the amount of acetaldehyde in the Windhoek Light, is nearly twice as much as for the Castle Lager, which is a local brew.

Figure 7.11 shows the comparison of the collection of the dynamic headspace of Castle Lager beer, with and without PFBHA *in-situ* derivatisation. Unlike the parking lot sample, no peaks seem to have disappeared in the derivatisation trap. Several carbonyl compounds are present in beer [17]. However, longer sampling times would be required to derivatise these carbonyls from the headspace of beer.

Similar to the air samples, we again noted a contradiction with the results listed in table 7.2, and our studies performed in section 6.5. In this case, our concerns for the lack of a leak-tight gas standard sampling set-up, is confirmed by the trapping efficiencies we obtained from the beer samples. These ranged from 14% to 60 %, which is above the 4% reaction efficiency for CH<sub>3</sub>CHO pure gas standard with PFBHA determined in section 6.5. The amount of PFBHA on trap 2 for the Castle and Windhoek Light lagers, are higher than the amount of PFBHA on trap 1. This is because trap 2 in both cases was coated with PFBHA first. Trap 1 was loaded with PFBHA immediately afterwards. Based on our previous studies on reagent loading, we presume that the reagent vapour pressure was drastically depleted at that time.

As with the air samples, we believe breakthrough occurred because the PFBHA on trap 1 was consumed by more than 10% of the original amount. This lead to a decreased reaction rate between acetaldehyde and PFBHA

In addition, the isomer peak ratios for the acetaldehyde-oximes obtained from the headspace of beer, are not what we expected. From the reaction of PFBHA with our acetaldehyde gas standard in section 6.5, we determined the average ratio of isomer peak 1 to isomer peak 2 to be 50%. The isomer ratios for the acetaldehyde-oxime from Castle Lager, Black Label Beer and Windhoek Light were 35%, 33% and 66% respectively. We imagine that the isomer ratios may be concentration dependant and that it may also be affected by the presence of moisture in the surroundings.

## 7.4 CONCLUSION

From the results obtained for analysing real gaseous samples using *in-situ* derivatisation on the silicone rubber trap, we can safely say that it is a very promising technique. Loading the reagent and sampling with the portable pump is quick and easy and the actual collections did not have to be supervised.

In addition, the traps were immediately reusable after every analysis and no loss in performance was observed for the traps.

However, the trapping efficiencies for HCHO and CH<sub>3</sub>CHO, were contradictory to our expectations based on our studies in the previous chapter. PFBHA is not minimally consumed and the reaction rates with HCHO and CH<sub>3</sub>CHO has decreased. Ideal sampling conditions must still be determined.

Table 7.1. Quantitation of collected real samples for formaldehyde (HCHO) analysis.

air samples	trap 1					trap 2					HCHO ** (ppm)	temperature program	%trapping efficiency
	t <sub>R</sub> (min)	HCHO-oxime peak area (uV.s)	t <sub>R</sub> (min)	PFBHA peak area (uV.s)	HCHO * ng	t <sub>R</sub> (min)	HCHO-oxime peak area (uV.s)	t <sub>R</sub> (min)	PFBHA peak area (uV.s)	HCHO * ng			
newly-carpeted laboratory	13.812	108,259	16.283	199,580	13.39	13.822	103,590	16.346	463,402	11.84	>0.0410	A	11.53
poorly ventilated office	13.91	86,075	16.371	130,121	6.05	13.843	20,313	16.278	12,654	below detection limit	>0.0098	A	~
parking lot	no reagent loaded					13.92	138,493	16.405	246,975	23.39	>0.0380	A	~
bar with tobacco smoke	13.817	129,436	16.280	113,792	20.39	13.82	115,738	16.314	263,611	15.86	>0.0589	B	22.22
indoor air of a new car	13.843	130,070	16.363	463,016	20.60	13.836	131,729	16.332	281,955	21.15	>0.0679	B	~
indoor air of an 11 year old car	13.851	96,150	16.335	190,944	9.38	13.844	74,816	16.369	303,590	2.33	>0.0190	A	75.20

116

\* Mass of HCHO(ng) calculated by first subtracting HCHO-blank peak area ( 67781 uV.s) from the HCHO-oxime peak area. Second, this value is divided by the FID-RRF for the HCHO-Oxime relative to C12 (403.125). Third, the value obtained ( HCHO-Oxime (ng)) is divided by the molar mass of the HCHO-Oxime (225g/mol) to give the nmol of HCHO. Finally this value is multiplied by the molar mass of HCHO (30g/mol) to give HCHO (ng).

\*\* HCHO (ppm) calculated by taking the sum of HCHO(ng) of trap 1 and trap 2 and dividing by the volume sampled (500ml). This value is then divided by the HCHO conversion factor (1.23). HCHO conversion factor 1ppm=1.23ng/ml [6].

% Trapping efficiency = [ 1 - (HCHO-trap2/ HCHO-trap1) ] x 100

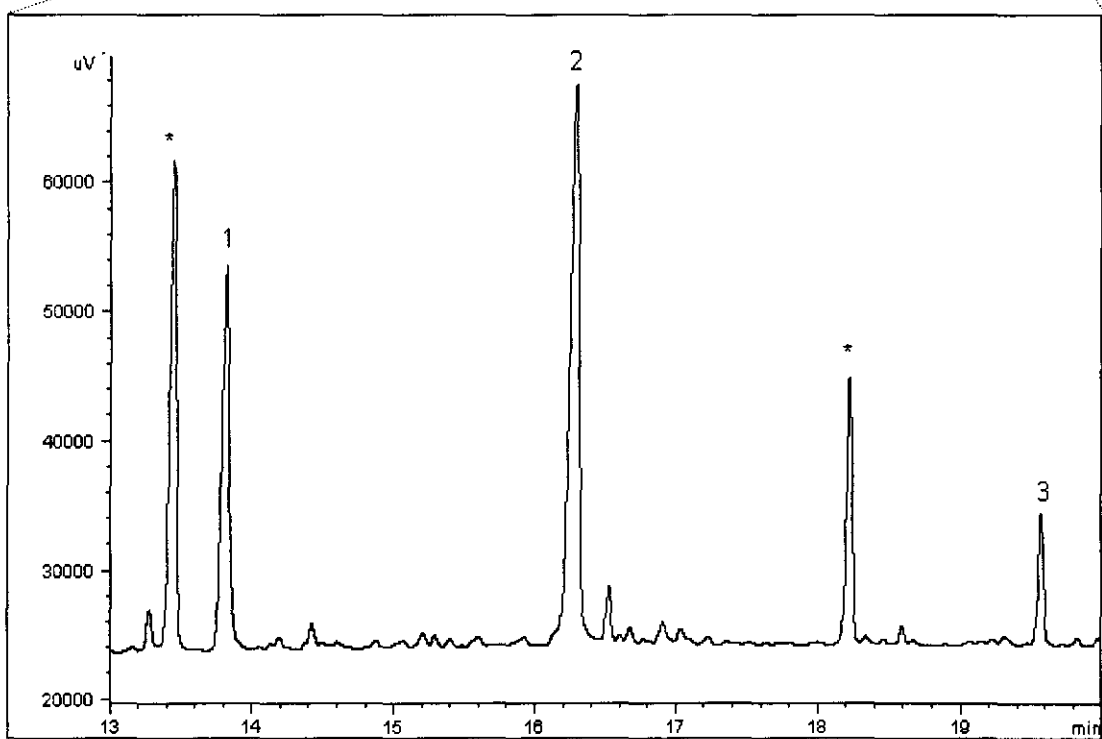
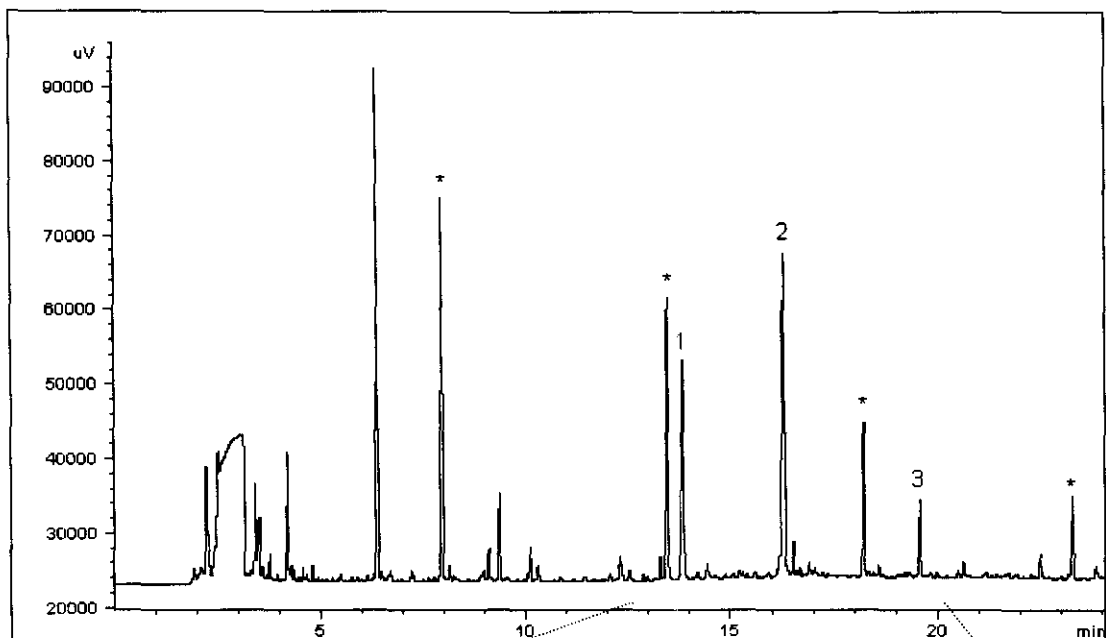
Table 7.2. Quantitation of collected real samples for acetaldehyde (CH<sub>3</sub>CHO) analysis .

headspace beer samples	trap 1					trap 2					CH <sub>3</sub> CHO <sup>##</sup> (ppm)	temperature program	%trapping efficiency
	t <sub>R</sub> (min)	acetal-oxime peak area (uV.s)	t <sub>R</sub> (min)	PFBHA peak area (uV.s)	CH <sub>3</sub> CHO <sup>#</sup> ng	t <sub>R</sub> (min)	acetal-oxime peak area (uV.s)	t <sub>R</sub> (min)	PFBHA peak area (uV.s)	CH <sub>3</sub> CHO <sup>#</sup> ng			
castle lager	16.767	105,718	16.422	913,378	<b>160.26</b>	16.756	82,671	16.334	333,340	<b>107.96</b>	>1.4901	B	32.63
	17.044	299,607				17.021	190,382						
black label	16.956	43,909	16.501	38,076	<b>69.34</b>	16.935	19,062	16.521	98,901	<b>28.39</b>	>0.5429	B	59.06
	17.224	131,469				17.188	52,738						
windhoek light	16.794	242,898	16.429	1,160,526	<b>241.33</b>	16.758	180,366	16.285	90,094	<b>205.61</b>	>2.4830	B	14.80
	17.054	367,473				17.034	339,661						

117

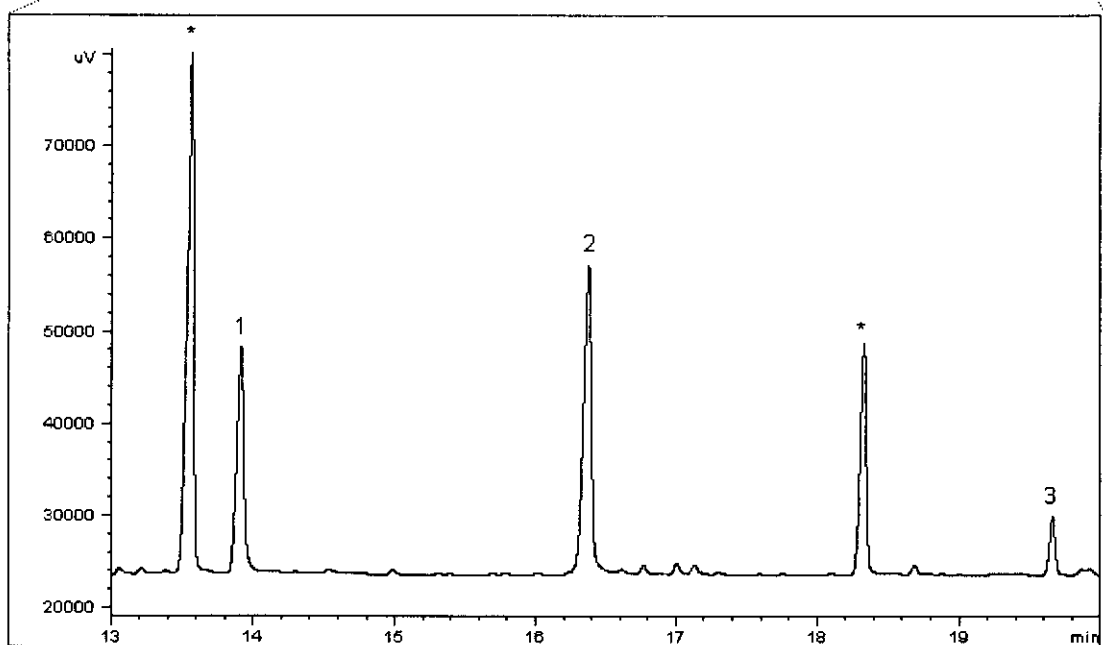
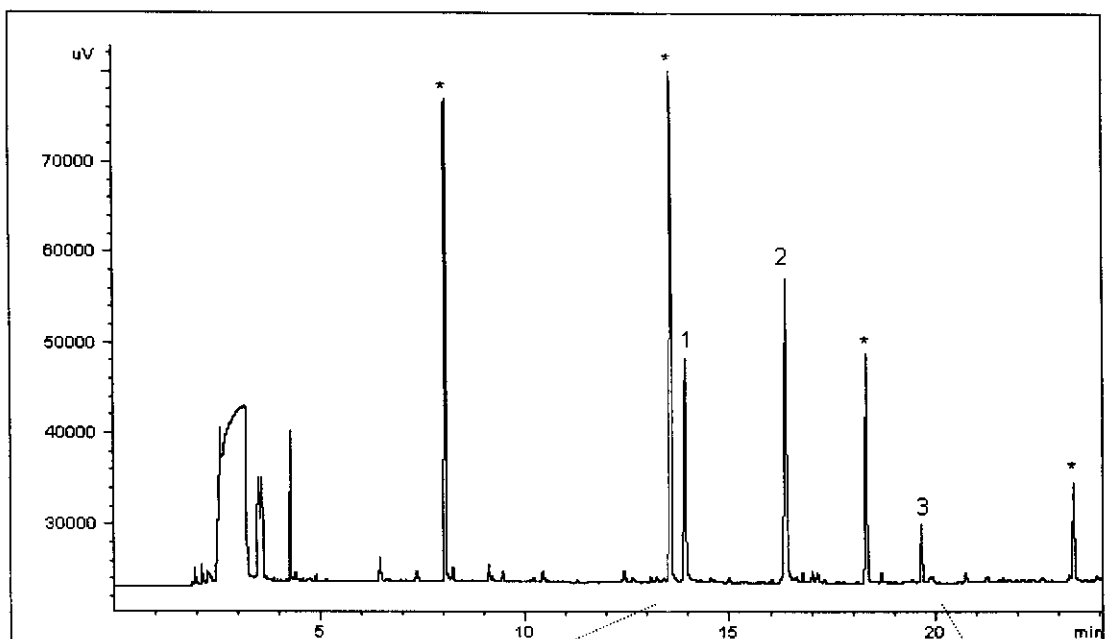
# Mass of CH<sub>3</sub>CHO(ng) calculated by first adding the 2 peak areas obtained for the CH<sub>3</sub>CHO-oxime. Second this value is divided by the FID-RRF for the CH<sub>3</sub>CHO-oxime relative to C12 (465.625). Third, this value obtained (CH<sub>3</sub>CHO-oxime (ng)) is divided by the molar mass of the CH<sub>3</sub>CHO-oxime (239g/mol) and then multiplied by the molar mass of CH<sub>3</sub>CHO (44g/mol) to give the mass of CH<sub>3</sub>CHO(ng).

## CH<sub>3</sub>CHO (ppm) calculated by taking the sum of CH<sub>3</sub>CHO(ng) of trap 1 and trap 2 and dividing by the volume sampled (100ml). This value is then divided by the conversion factor (1.8). CH<sub>3</sub>CHO conversion factor 1ppm=1.8ng/ml.



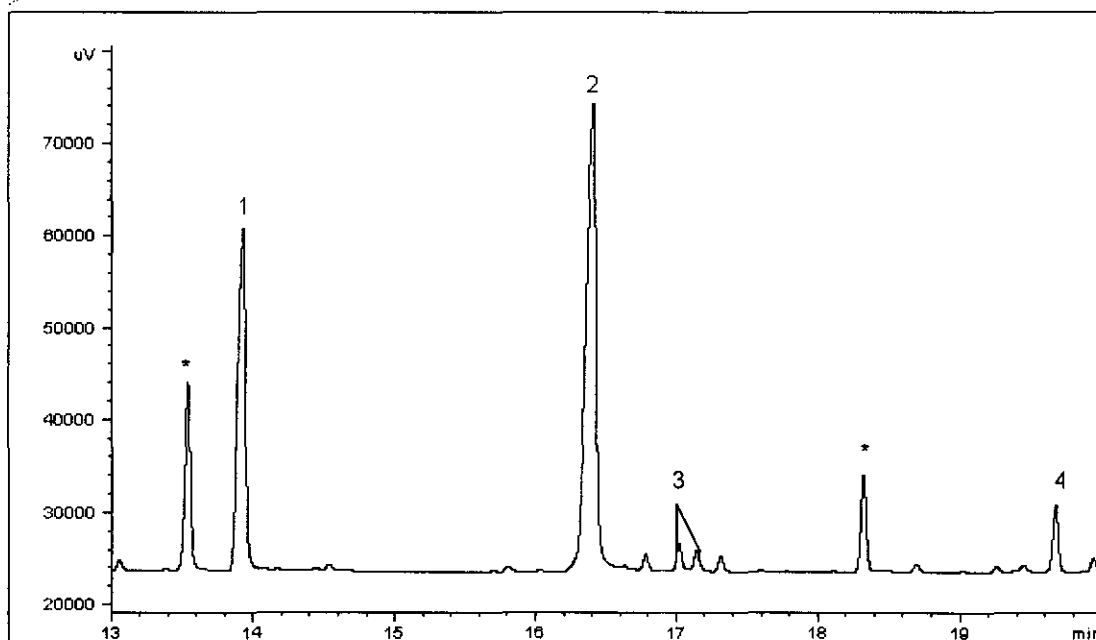
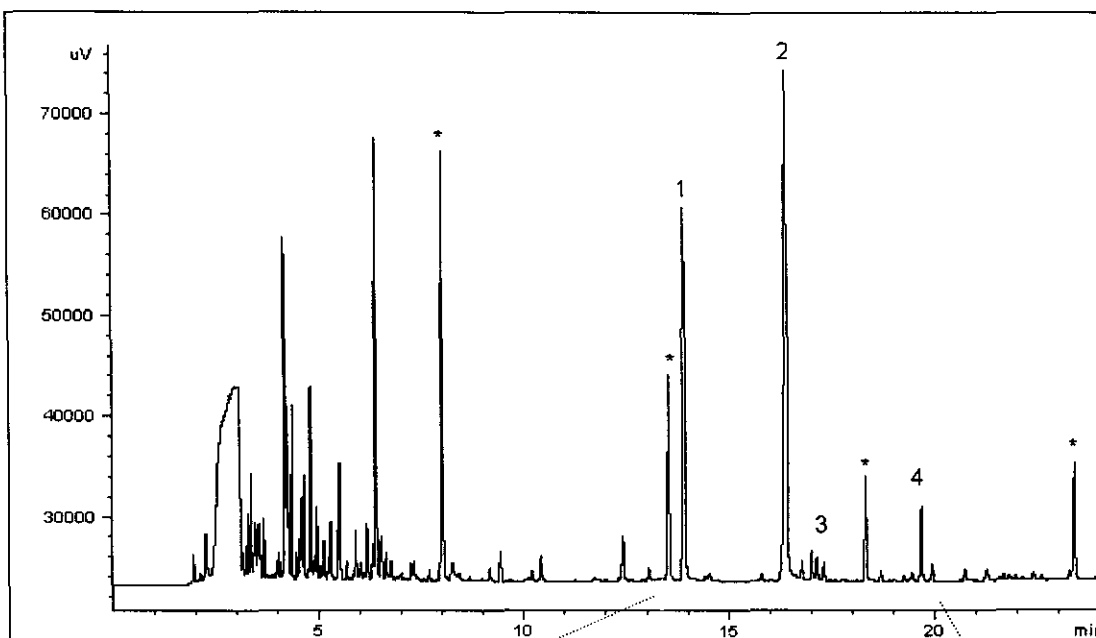
- \* Silicone degradation peaks
- 1. HCHO-Oxime
- 2. PFBHA
- 3. 20ng C12

Figure 7.1. GC-FID chromatogram of an air sample from a newly-carpeted laboratory.



- \* Silicone degradation peaks
- 1. HCHO-Oxime
- 2. PFBHA
- 3. 20ng C12

Figure 7.2. GC-FID chromatogram of an air sample from a poorly ventilated office.



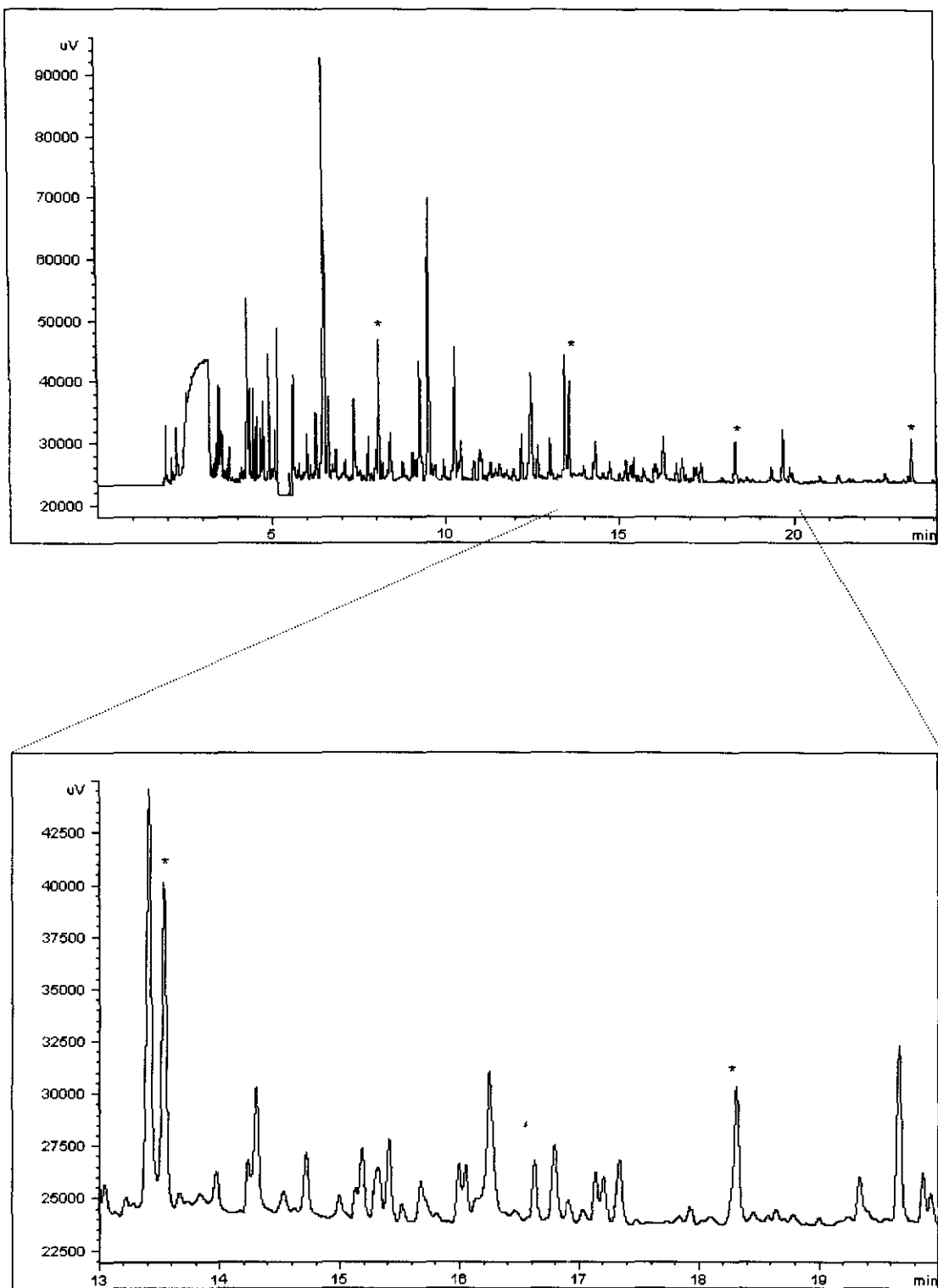
\* Silicone degradation peaks  
2. PFBHA

1. HCHO-Oxime  
3. Acetaldehyde-oxime

4. 20ng C12

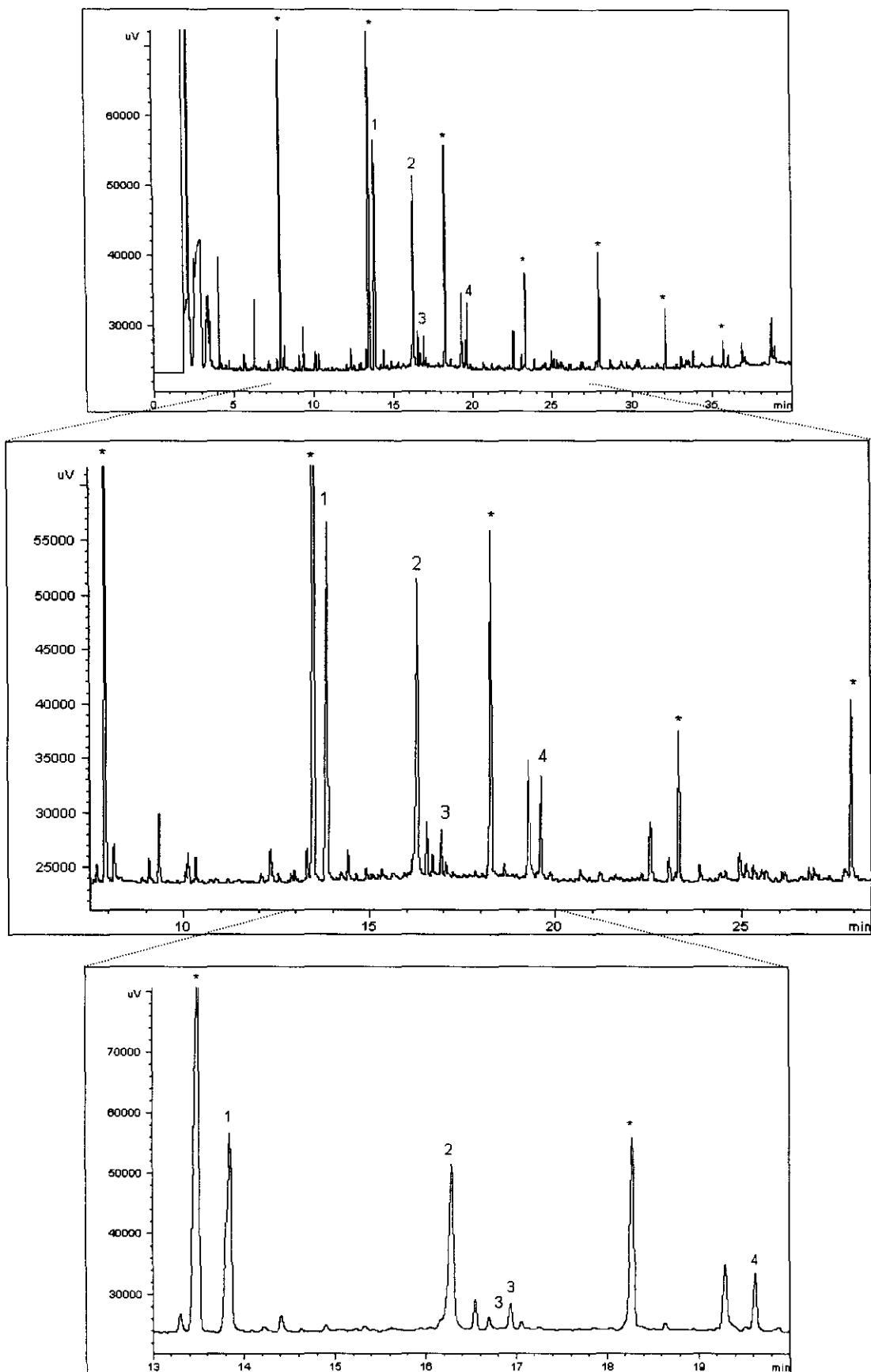
Figure 7.3. GC-FID chromatogram of an air sample from a parking lot.





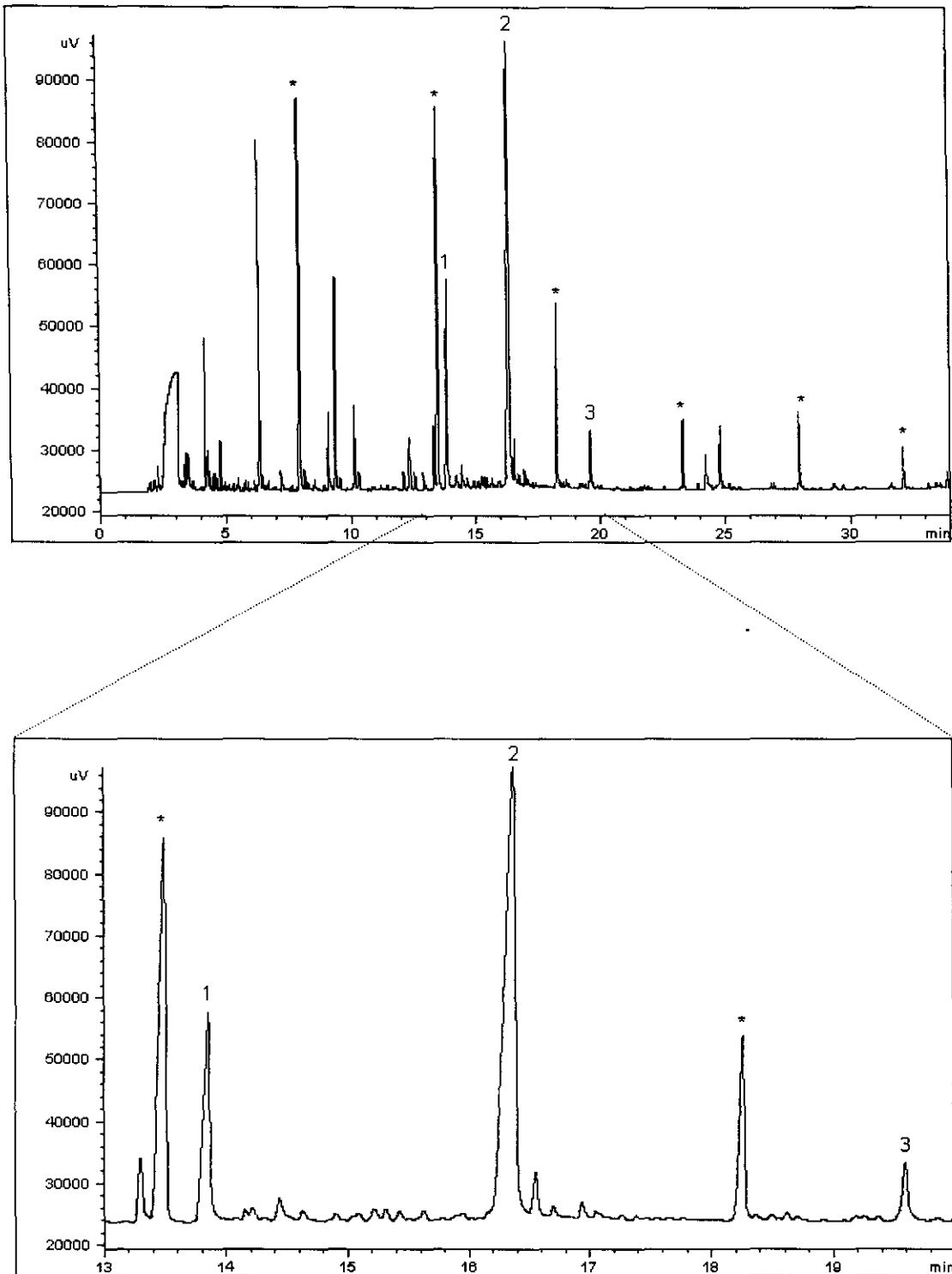
\* Silicone degradation peaks

Figure 7.4. GC-FID chromatogram of parking lot air sample without PFBHA in-situ derivatisation.



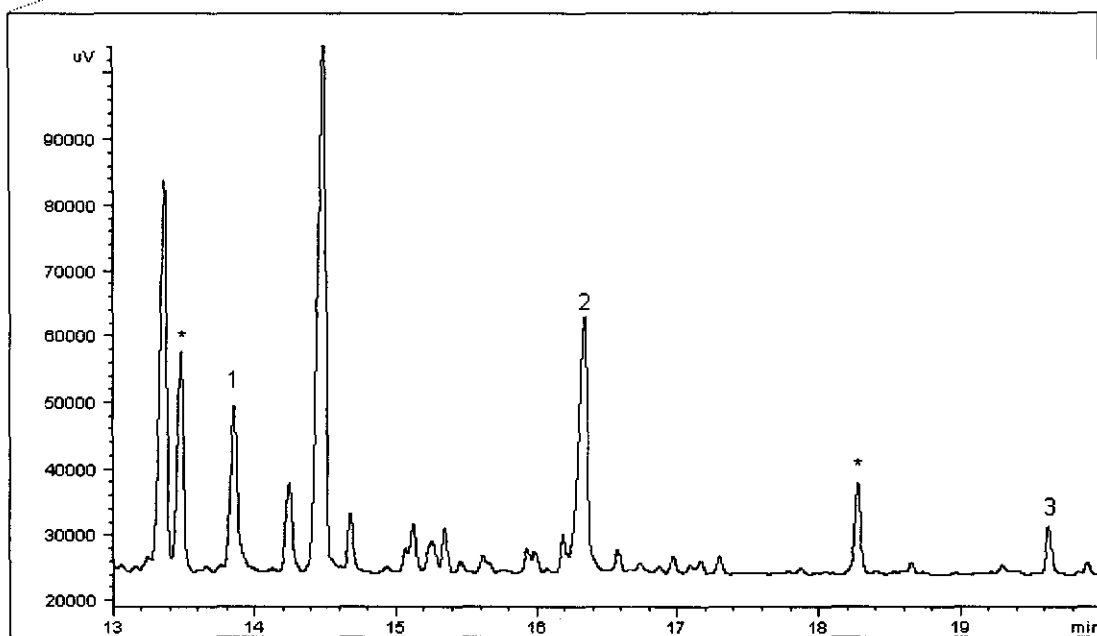
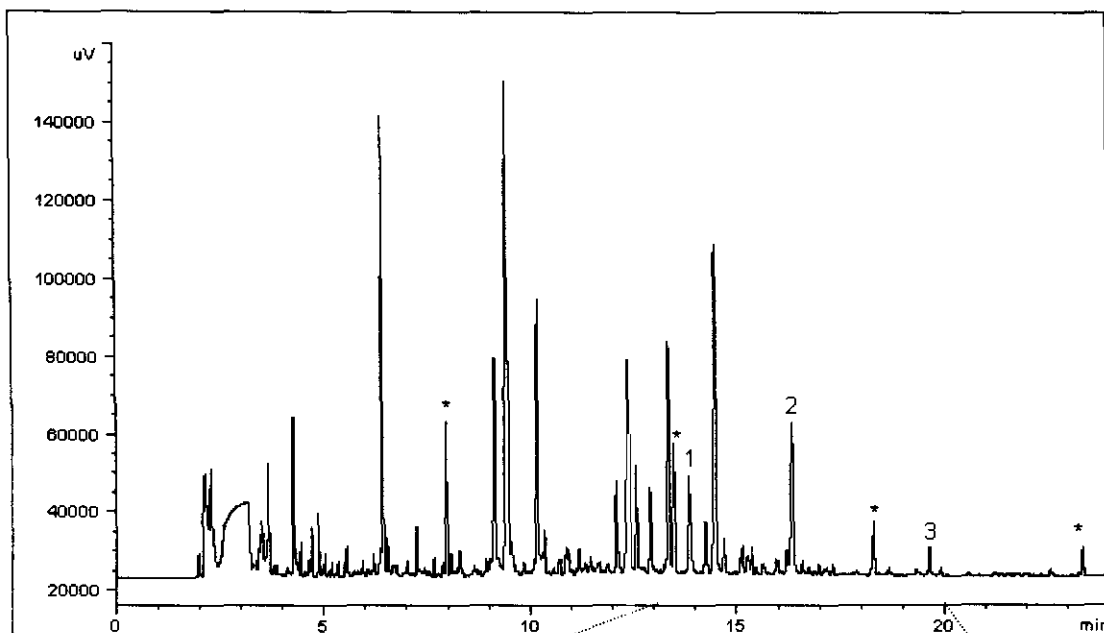
\* Silicone degradation peaks      1. HCHO-Oxime      2. PFBHA  
3. Acetaldehyde-Oxime      4. 20ng C12

Figure 7.5. GC-FID chromatogram of an air sample from a bar filled with tobacco smoke



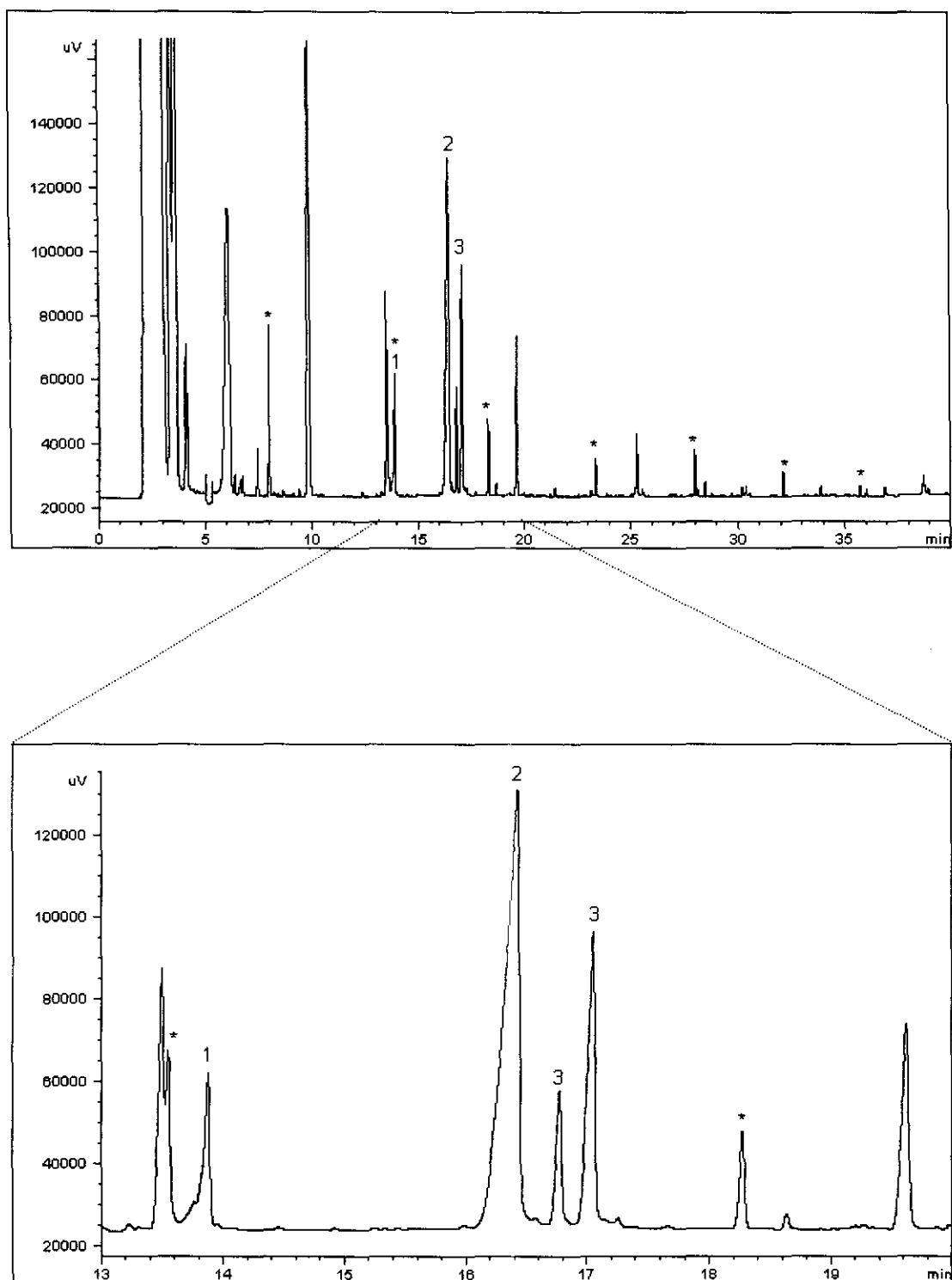
- \* Silicone degradation peaks
- 1. HCHO-Oxime
- 2. PFBHA
- 3. 20ng C12

Figure 7.6. GC-FID chromatogram of the indoor air of a new car.



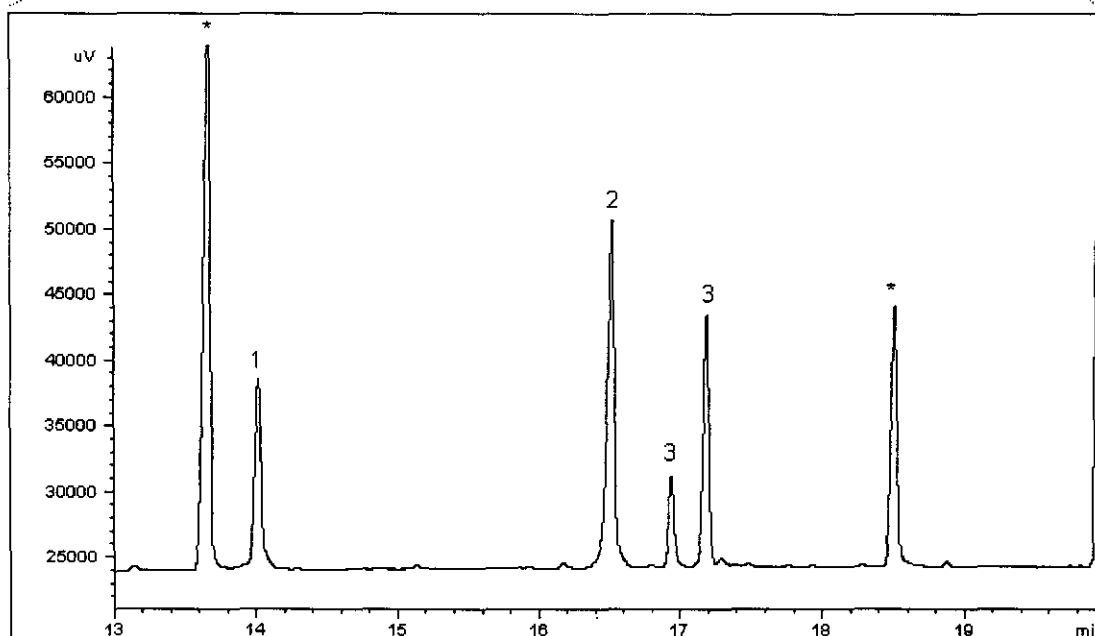
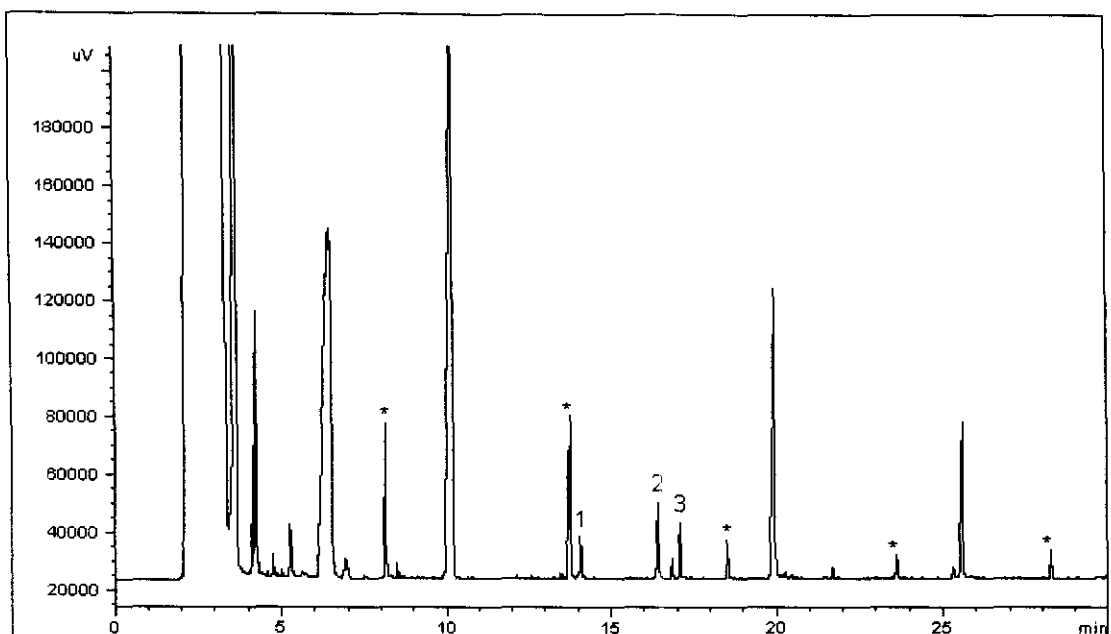
- \* Silicone degradation peaks
- 1. HCHO-Oxime
- 2. PFBHA
- 3. 20ng C12

Figure 7.7. GC-FID chromatogram of the indoor air of an 11 year old car.



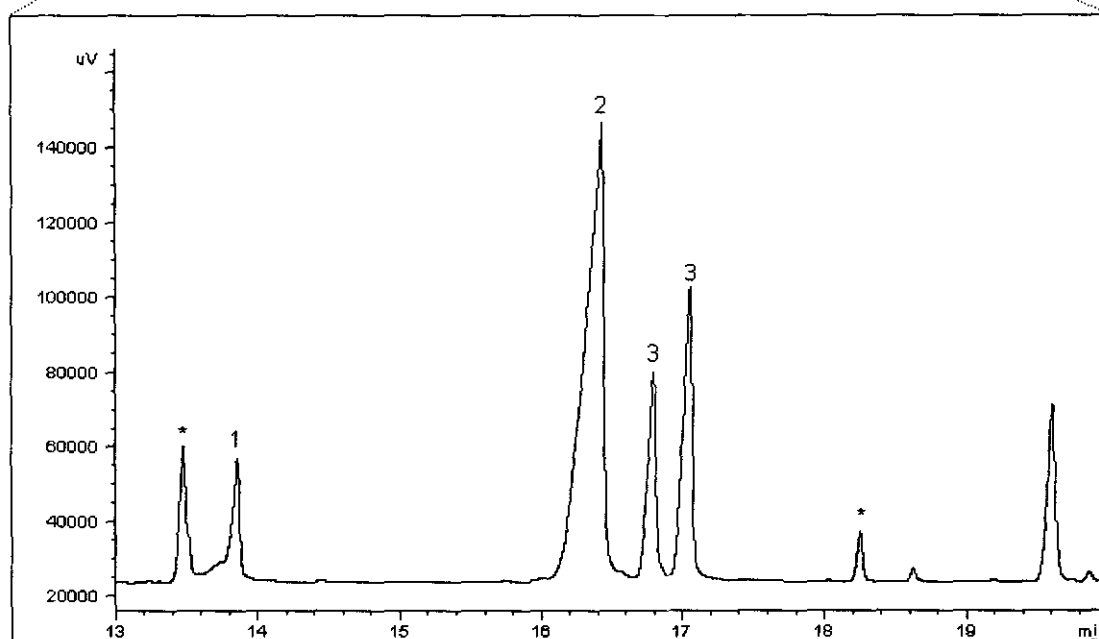
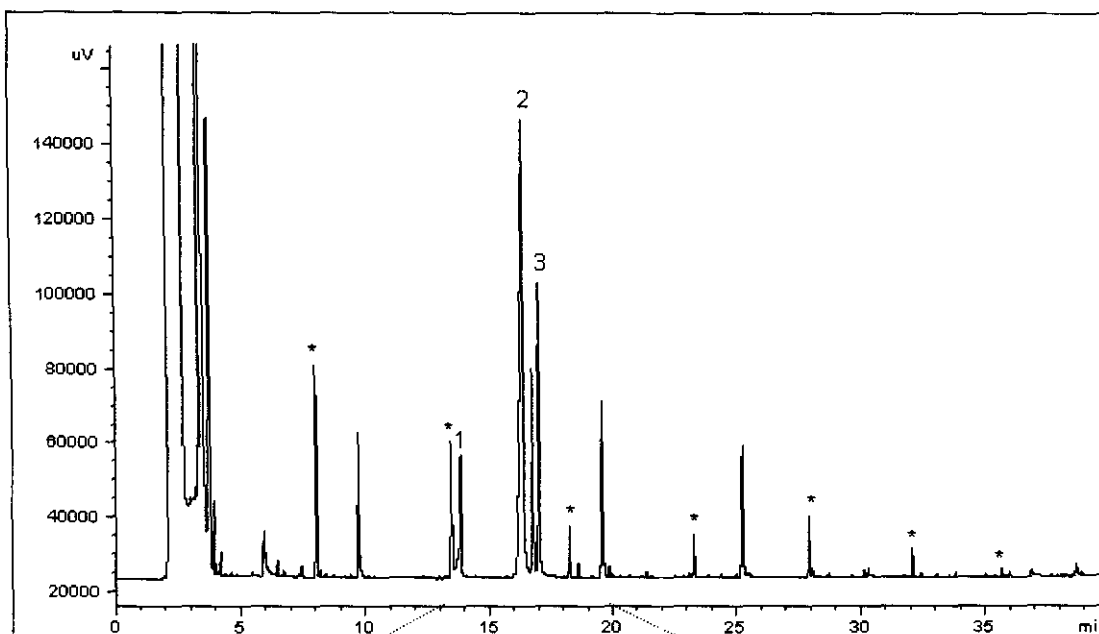
- \* Silicone degradation peaks
- 1. HCHO-Oxime
- 2. PFBHA
- 3. Acetaldehyde-Oxime

Figure 7.8. GC-FID chromatogram of Castle Lager headspace sample.



- \* Silicone degradation peaks
- 1. HCHO-Oxime
- 2. PFBHA
- 3. Acetaldehyde-oxime

Figure 7.9. GC-FID chromatogram of Black Label Beer headspace sample from trap 2.



- \* Silicone degradation peaks
- 1. HCHO-Oxime
- 2. PFBHA
- 3. Acetaldehyde-oxime

Figure 7.10. GC-FID chromatogram of Windhoek Light beer headspace sample.

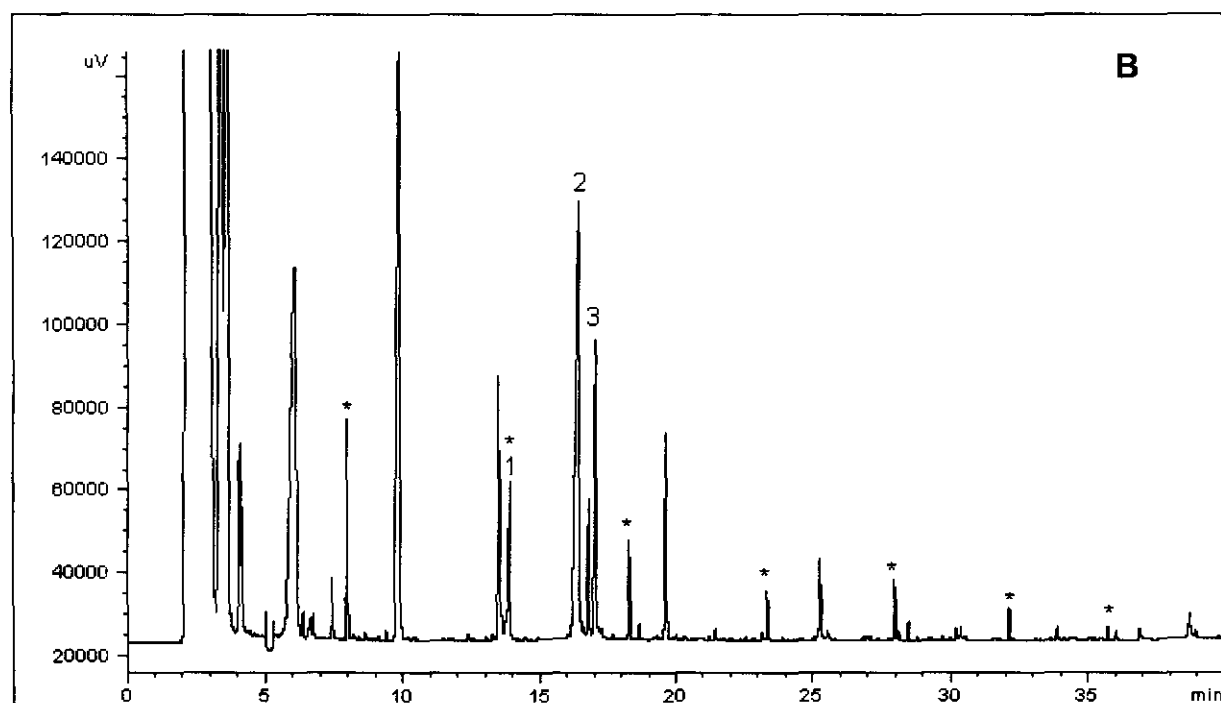
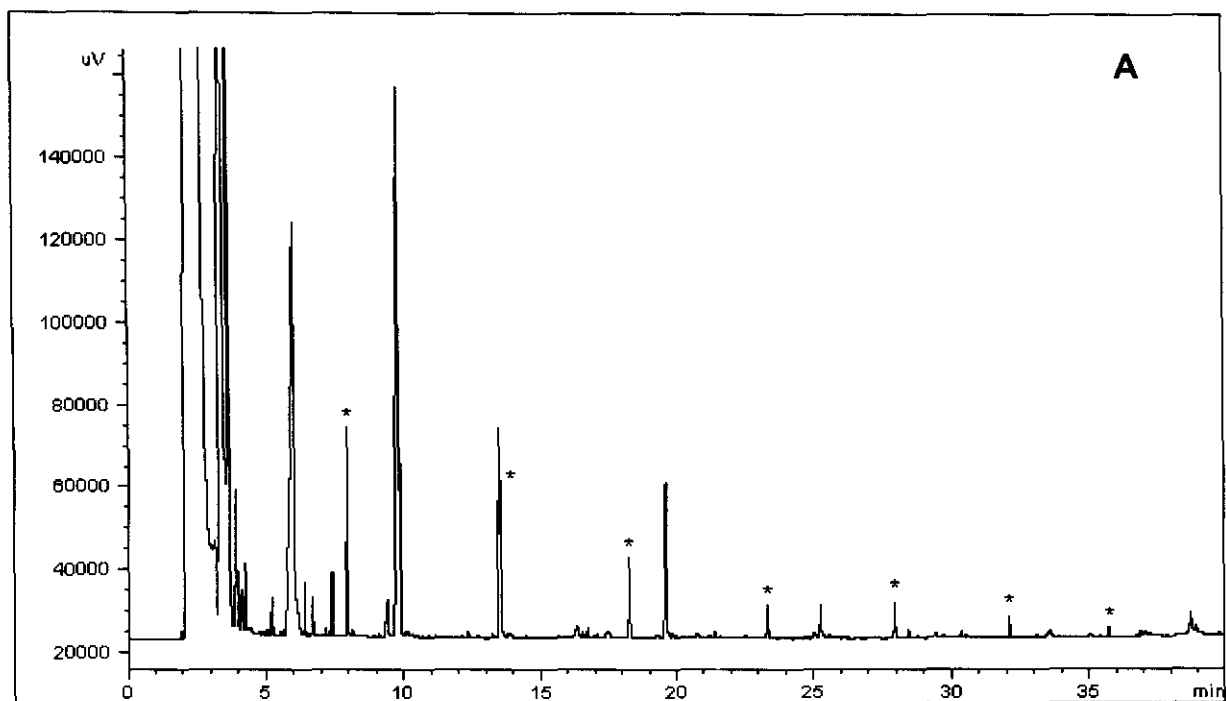


Figure 7.11. **A** GC-FID chromatogram of Castle Lager headspace sample without PFBHA *in-situ* derivatisation.  
**B** GC-FID chromatogram of Castle Lager headspace sample with PFBHA *in-situ* derivatisation (figure 7.8).



## CHAPTER 8

### CONCLUSION

*In-situ* derivatisation on silicone rubber traps in order to pre-concentrate volatile aldehydes was investigated for the first time. Unlike so many other pre-concentration techniques for determining aldehydes, the silicone rubber trap is inert, rugged, simple and inexpensive. Recovery is by thermal desorption which (1) removes the need for expensive, toxic solvents and (2) renders the silicone trap immediately reusable. Thermal degradation of the silicone rubber resulted in chromatographic peaks, which showed repeatable retention times and peak heights, throughout the study. No deterioration in the performance of the traps was observed.

Diffusion tubes and several types of permeation tubes were successfully prepared and calibrated to provide reliable aldehyde gas standards in the ppm range. A dilution system was successfully constructed in order to obtain concentrations of HCHO in the ppb range. Unfortunately, the sampling set-up for the other aldehydes did not prove leak-tight.

PFBHA was selected as the most suitable derivatising reagent for the study. Sample preparation time was reduced by loading the headspace vapour of the PFBHA directly into the silicone rubber. This was achieved by packing a glass tube with the pure PFBHA reagent. The silicone trap was attached to the one end of the PFBHA tube. From the other end, high purity nitrogen gas was blown through the PFBHA tube towards the silicone trap at a flow rate of 5ml/min. This method however did not load amounts of PFBHA with high repeatability.

The presence of formaldehyde-oxime in the reagent blank, severely restricted our detection level for HCHO. In a 10 minute collection of PFBHA headspace at a flow rate of 5ml/min, 23 ng of HCHO was present. Future work would involve finding a way of trying to clean up the reagent, thereby lowering HCHO detection limits.

We then set out to demonstrate the efficient pre-concentration of the aldehyde gas standards using PFBHA *in-situ* derivatisation on our silicone traps. Two HCHO atmospheres were sampled over time. Comparison of the amount of HCHO trapped and the amount of HCHO released by the gas standard indicated a reaction efficiency of 95% for 0.1ppm HCHO and 75% for 5.98ppm HCHO. HCHO could be detected at the 0.1ppm level. This did not meet the NIOSH Permissible Exposure Limits (PEL) of 0.016ppm. However, the PELs set by the WHO, ACGIH and OSHA could be detected.

A similar test for the other aldehyde gas standards yielded a 4% reaction efficiency, which led us to believe there was a leak in our sampling set-up. Since these aldehydes were not present in the reagent blank, we could determine the minimum detectable concentrations ( $s/n = 3$ ) for acetaldehyde, acrolein and crotonal to be 0.035 ppm, 0.057ppm and 0.064ppm respectively. These concentrations are well below PELs set by the various health organisations. In addition, these detectable levels are for a sampling time of only one minute, as such even lower concentrations will be detectable over longer collection times. These result clearly illustrate that a lower detection limit for HCHO (having close to 100% reaction efficiency) is possible, once the HCHO-oxime impurity is removed from the reagent blank.

Back-up trap sampling of the 0.1 ppm HCHO atmosphere at a flow rate of 10ml/min, indicated no breakthrough of the HCHO-Oxime from the silicone trap after a collection volume of 3 litres.

The contents of the silicone rubber was successfully recovered by thermal desorption with cryogenic focussing. The optimum desorption conditions were determined by desorbing the C12 internal standard (which elutes off the silicone trap after PFBHA and the HCHO-Oxime) from the top of the trap. The optimum desorption temperature was found to be 220°C. No carry-over was detected. In addition, the HCHO-Oxime, PFBHA and C12 peaks displayed consistent retention times.

The aldehyde-oximes were successfully identified using Mass Spectrometry. Based on elution temperatures and retention times the oximes could be identified using the FID. The desorbed analytes were semi-quantitated using the C12 internal standard, which could be related to the FID relative response and the Effective Carbon Numbers (ECN) of the aldehyde-oximes, for which no standards were available. This calculation method gave a very good indication of the trapped aldehyde amounts.

We also demonstrated *in-situ* derivatisation on our silicone rubber traps with real gaseous samples. The results were very promising. Pre-concentration of HCHO from air samples and acetaldehyde from the headspace of beer was achieved. Loading the PFBHA and sampling with the portable pump was quick and easy. No supervision during sampling was required. However, breakthrough and lower reaction efficiencies were observed, differing from our expectations based on our previous studies using the gas standards. The presence of other carbonyls in air also reacting with PFBHA, depleted the reagent thereby decreasing the reaction rate and consequent trapping efficiency. Further work would have to be performed in order to obtain the ideal sampling conditions.

Our study has revealed that the silicone rubber trap is a promising pre-concentration device for *in-situ* derivatisation. The silicone proved inert and reusable. Loading of derivatising reagent requires less time and effort, and the sample collection set-up is cheap, convenient and portable for fieldwork.

## REFERENCES

1. Chemical, Toxicity, Safety and Environmental Analysis Information for Formaldehyde. Internet: <http://www.instantref.com/formald.htm>. Access: 27 Aug 1999.
2. Occupational Safety and Health Administration U.S. Department of Labor, *OSHA Regulations - Formaldehyde. 1910.1048*. Internet: <http://www.osha-slc.gov>. Access: 2 Nov 2000.
3. Method 2016,1998. Formaldehyde by HPLC-UV. *NIOSH Manual of Analytical Methods*, 4<sup>th</sup> Edition.
4. CRUMP, D.R., 1995. Volatile organic Compounds in Indoor air in "Volatile Organic Compounds in the Atmosphere", editors Hester, R.E., Harrison, R.M. Issues in Environmental Science and Technology, vol 4, The Royal Society of Chemistry, U.K.
5. Occupational Safety and Health Administration U.S.Department of Labor, "OSHA Fact Sheets - 01/01/1995 - Occupational Exposure to formaldehyde.". Internet: <http://www.osha-slc.gov>. Access: 2 Nov 2000.
6. BRABEC, M.J., 1981. Aldehydes and acetals in *Patty's Industrial Hygiene and Toxicology*, editors Clayton, G.D, Clayton, F.E. 3rd revised edition, John Wiley&Sons. Vol 2A, 2692-2669.
7. WALKER, M., 2000. Something in the air. *New Scientist*, vol. 2221, 5.
8. NISHIKAWA, H., Sakai, T.,1995. REVIEW: Derivatization and chromatographic determination of aldehydes in gaseous and air samples. *J. Chromatogr. A*, 710(1), 25-Aug, 159-165.
9. VON KEYSERLINGK, C., 1999. Sasol bereik ooreenkoms oor alkohol in petrol. *Beeld, Sake Beeld - Johannesburg Finaal*. Thurs, 22 July.
10. OTSON, R., Fellin, P., Tran, Q., Stoyanoff, R., 1993. Examination of sampling methods for assessment of personal exposures to airborne aldehydes. *Analyst*,118, Oct, 1253-1259.
11. OTSON, R., Fellin, P.,1988. Review: A review of techniques for measurement of airborne aldehydes. *Science of the Total Environment*, 77, 95-131.
12. DE GOEDE, S., 1997. Monitoring van die emissies van vonkontstekingsenjins onder verskillende rykondisies en met verskillende brandstofformulerings. *MSc thesis, University of Stellenbosch, Stellenbosch*.
13. BAKER, H., 1997. Chemical warfare at work. Internet: <http://www.newscientist.com/ns/970621/features.html>. Access: 14 Jun 2001
14. NORBACK, D., Wieslander, G., Edling, C., 1995. Occupational exposure to volatile organic compounds (VOCs), and other air pollutants from the indoor application of water-based paints. *Ann. Occup. Hyg.*, 39, 6, 783-794.

15. REUSS, G., Disteldorf, W., Grundler, O., Hilt, A., 1998. Formaldehyde in *Ullmann's Encyclopedia of Industrial Chemistry*, VCH, executive editor Gerhartz W., vol A11, 619-651.
16. LUONG, J., Sieben, L., Fairhurst, M., 1996. Determination of low levels of formaldehyde and acetaldehyde by gas chromatography/flame ionization detection with a nickel catalyst. *J. High Resolut. Chromatogr.* 19, Oct, 591-594.
17. OJALA, M., Kotiaho, T., Siirila, J., Sihvonen, M., 1994. Analysis of aldehydes and ketones from beer as O-(2,3,4,5,6-pentafluorobenzyl)hydroxylamine derivatives. *Talanta*, 41, 1297-1309.
18. BALTUSSEN, H.A., 2000. New Concepts in Sorption Based Sample Preparation for Chromatography. *D.Phil. Thesis, Technical University Eindhoven, Eindhoven.*
19. BEREZKIN, V.G., Drugov, Y.S., 1991. Gas chromatography in air pollution analysis. *Journal of Chromatography Library*, Elsevier, Germany, vol. 49, 35-119.
20. DALENE, M., Persson, P., Skarping, G., 1992. Determination of formaldehyde in air by chemisorption on glass filters impregnated with 2,4-dinitrophenylhydrazine using gas chromatography with thermionic specific detection. *J.Chromatogr. A*, 626, 284-288.
21. KENNEDY, E.R., Teass, A.W., Gagnon, Y.T., 1985. Industrial Hygiene Sampling and analytical methods for formaldehyde - past and present in *Formaldehyde - Analytical chemistry and toxicology*, editor Turoski, V. *Advances in chemistry and toxicology series*, 210, 1-11.
22. MARTOS, P.A., Pawliszyn, J., 1998. Sampling and determination of formaldehyde using solid phase microextraction with on-fibre derivatization. *Anal.chem.*, 70, 2311-2320.
23. THOMAS, P., McGill, C.L., Towill, C.D., 1997. Determination of formaldehyde by conversion to hexahydroxazolo[3,4-a]pyridine in a denuder tube with recovery by thermal desorption and analysis by GC-MS. *Analyst*, 122, 1471-1476.
24. ORTNER, E.K., Rohwer, E.R., 1996. Trace analysis of semi-volatile organic air pollutants using thick film silicone rubber traps with capillary gas chromatography. *J. High Resolut. Chromatogr.*, 19, June, 339-344.
25. ORTNER, E.K., Rohwer, E.R., 1999. Trapping efficiency of aqueous pollutants using multichannel thick film silicone rubber traps with capillary gas chromatography. *J. Chromatogr.A*, 863, 57-68.
26. ORTNER, E.K., 1994. Alternative concentration techniques for the trace analysis of semi-volatile organic air pollutants by capillary gas chromatography. *MSc thesis, University of Pretoria, Pretoria.*
27. ORTNER, E.K., 1999. Analysis of aqueous samples with the multichannel silicone rubber trap and capillary gas chromatography. *D.Phil. Thesis, University of Pretoria, Pretoria.*

28. DILLON, H.K., Gao, P., 1994. Laboratory evaluation of a novel reactive passive sampler for the quantitative determination of formaldehyde in air. *Am. Ind. Hyg. Assoc. J.*, 55, Nov, 1061-1068.
29. HOPPS, H.B., 2000. Purpald®: A reagent that turns aldehydes purple! *Aldrichchimica Acta*, 33, 28-30.
30. AGUIN, M.L., Vindevogel, J., Sandra, P., 1993. Utilisation of the bisulfite addition reaction for the separation of neutral aldehydes by capillary electrophoresis. *Chromatographia*, 37, Oct, 451-454.
31. OLLETT, D.G., Morgan, E.D., 1987. Identification and determination of parts-per-million formaldehyde and lower carbonyl homologs by gas chromatography. *Microchemical Journal*, 35, 296-304.
32. ANDRAWES, F.F., 1984. Detection of traces of formaldehyde in pure air by gas chromatography and helium ionisation detection. *J. Chromatogr. Sci*, 22, Nov, 506-508.
33. FELIX, U., Dettmer, K., Engewald, W., Mohnke, M., 2000. Application of a unique selective PLOT capillary column for the analysis of oxygenated compounds in ambient air. *Riva Del Garda Chromatography Conference Poster*.
34. WU, N., Shen, Y., Lee, M.L., 1999. Fast solvating GC of environmentally important compounds using polymer-encapsulated silica particles. *J. High Resolut. Chromatogr.*, 22, 541-546.
35. HOSHIKA, Y., Muto, G., 1991. Capillary Gas Chromatography of lower aliphatic C2-C5 aldehydes in the free form as a group of pungent odorants in Air. *J. High Resolut. Chromatogr.*, 14, May, 330-334.
36. McGUIRE, J.M., Nahm, S.H., 1991. Determination, by GC-MS using deuterated internal standards of Formaldehyde and Methanol evolved during curing of coatings. *J.High Resolut.Chromatogr.*, 14, Apr, 241-244.
37. SCHLITT, H., 1997. Impinger sampling coupled to HPLC by a modified autoinjector interface. *J.Chromatogr. A.*, 762, 187-192.
38. RUTTEN, G.A., Burtner, C.W.J., Rijks, J.A., Visser, H., 1988. The determination of aldehydes in exhaust gases of LPG fuelled engines. *Chromatographia.*, 26, 274-280.
39. BEASLEY, R.K., Hoffmann, C.E., Rueppel, M.L., Worley, J.W., 1980. Sampling of formaldehyde in air with coated solid sorbent and determination by High Performance Liquid Chromatography. *Anal.chem.*, 52, 1110-1114.
40. GUENIER, J.P., Simon, P., Delcourt, J., Didierjean, M.F., Lefevre, C., Muller, J., 1984. Air Sampling of aldehydes - application to chromatographic determination of formaldehyde and acetaldehyde. *Chromatographia.*, 18, Mar, 137-144.
41. SAKURAGAWA, A., Yoneno, T., Inoue, K., Okutani, T., 1999. Trace analysis of carbonyl compounds by liquid chromatography-mass spectrometry after

- collection as 2,4-dinitrophenylhydrazine derivatives. *J. Chromatogr. A.*, 844, 403-408.
42. SESANA, G., Nano, G., Baj, A., Balestreri, S., 1991. New sampling tool for airborne volatile aldehydes. *Fresenius J. Anal. Chem.*, 339(7), Mar, 485-487.
  43. MARSEL, J., Velikonja Bolta, S., Zupancic Kralji, L., 1998. Gas chromatographic determination of formaldehyde in air using SPME sampling. *Chromatographia.*, 48, 95-99.
  44. GROSJEAN, E., Green, P.G., Grosjean, D., 1999. Liquid chromatography analysis of carbonyl (2,4-Dinitrophenyl)hydrazones with detection by diode array Ultraviolet spectroscopy and by atmospheric pressure negative chemical ionization mass spectrometry. *Anal.chem.*, 71, 1851-1861.
  45. DYE, C., Oehme, M., 1992. Comments concerning the HPLC separation of Acrolein from other C3 carbonyl compounds as 2,4-Dinitrophenylhydrazones : A proposal for improvement. *J. High Resolut. Chromatogr.*, 15, Jan, 5-8.
  46. SCHMIED, W., Przewosnik, M., Bachmann, K., 1989. Determination of traces of aldehydes and ketones in the troposphere via solid phase derivatisation with DNSH. *Fresenius J. Anal. Chem.*, 335, 464-468.
  47. STASHENKO, E.E., Ferreira, M.C., Sequeda, L.G., Martinez, J.R.; Wong, J.W., 1997. Comparison of extraction methods and detection systems in the gas chromatographic analysis of volatile carbonyl compounds. *J. Chromatogr. A.*, 779, 360-369.
  48. STASHENKO, E.E., Puertas, M.A., Salgar, W., Delgado, W., Martinez, J.R., 2000. Solid-Phase Microextraction with on-fibre derivatization applied to the analysis of volatile carbonyl compounds. *Riva Del Garda Chromatography Conference Poster CD-ROM*.
  49. LEMPUHL, D.W., Birks, J.W., 1996. New gas chromatographic-electron-capture detection method for the determination of atmospheric aldehydes and ketones based on cartridge sampling and derivatization with 2,4,6-trichlorophenylhydrazine. *J.Chromatogr. A.*, 740, 71-81.
  50. CANCELLA, D.A., Chou, C., Barthel, R., Que Hee, S.S., 1992. Characterization of the O-(2,3,4,5,6-pentafluorobenzyl)-hydroxylamine hydrochloride (PFBOA) derivatives of some aliphatic mono- and dialdehydes and quantitative water analysis of these aldehydes. *J.AOAC International*, 75, 842-854.
  51. NAWROCKI, J., Kalkowska, I., Dabrowska, A., 1996. Optimisation of solid phase extraction method for analysis of low ppb amounts of aldehydes-ozonation by-products. *J.Chromatogr. A.*, 749, 157-163.
  52. VIDAL, J.P., Estreguil, S., Cantagrel, R., 1993. Quantitative analysis of Cognac carbonyl compounds at the ppb level by GC-MS of their O - ( pentafluorobenzyl amine) derivatives. *Chromatographia*, 36, 183-186.
  53. STRASSNIG, S., Wenzl, T., Lankmayr, E.P., 2000. Microwave-assisted derivatization of volatile carbonyl compounds with O-( 2,3,4,5,6-pentafluorobenzyl)hydroxylamine. *J. Chromatogr. A.*, 891, 267-273.



54. LAHANIATI, M., Calogirou, A., Duane, M., Larsen, B., Kotzias, D., 1998. Identification of biogenic carbonyls in air with O-(2,3,4,5,6-pentafluorobenzyl)hydroxylamine hydrochloride (PFBHA) coated C18-silica gel cartridges. *Fresenius. Environ. Bull.*, 7, 302-307.
55. WUE, L.J., Que Hee, S.S., 1995. A solid sorbent personal air sampling method for aldehydes. *Am. Ind. Hyg. Assoc. J.*, 56, Apr, 362-367.
56. TSAI, S.W., Que Hee, S.S., 1999. A new passive sampler for aldehydes. *Am. Ind. Hyg. Assoc. J.*, 60, 463-473.
57. MARTOS, P.A., Pawliszyn, J., 1999. Time - weighted average sampling with solid-phase microextraction device: Implications for enhanced personal exposure monitoring to airborne pollutants. *Anal. chem.*, 71, 1513-1520.
58. KENNEDY, E.R., O'Connor, P.F., Gagnon, Y.T., 1984. Determination of Acrolein in air as an oxazolidine derivative by gas chromatography. *Anal. chem.*, 56, 2120-2123.
59. Method 2541, 1994. Formaldehyde by GC. *NIOSH Manual of Analytical Methods*, 4<sup>th</sup> edition.
60. Method 2539, 1994. Aldehydes, screening. *NIOSH Manual of Analytical Methods*, 4<sup>th</sup> edition.
61. MIYAKE, T., Shibamoto, T., 1995. Quantitative analysis by GC of volatile carbonyl compounds in cigarette smoke. *J. Chromatogr. A.*, 693, 376-381.
62. YASUHARA, A., Shibamoto, T., 1994. Gas chromatographic determination of trace amounts of aldehydes in automobile exhaust by a cysteamine derivatization methods. *J. Chromatogr. A.*, 672, 261-266.
63. KARTSOVA, L.A., Makarova, Y.L., Stolyarov, B.V., 1997. Selective gas chromatographic determination of formaldehyde in air. *J. Anal. Chem.*, 52(4), 337-340.
64. PELTONEN, K., Pfaffli, P., Itkonen, A., 1984. Determination of aldehydes in air as dimethone derivatives by gas chromatography with electron capture detection. *J. Chromatogr. A.*, 315, 412-416.
65. RECHE, F., Garrigos, M.C., Sanchez, A., Jimenez, A., 2000. Simultaneous supercritical fluid derivatization and extraction of formaldehyde by the Hantzsch reaction. *J. Chromatogr. A.*, 896, 51-59.
66. ZUREK, G., Karst, U., 1999. Liquid Chromatography - Mass Spectrometry method for the determination of aldehydes derivatized by the Hantzsch reaction. *J. Chromatogr. A.*, 864, 191-197.
67. POOLE, C.F., Poole, S.K., 1991. *Chromatography Today*. Elsevier, Amsterdam, 824-831.
68. DROZD, J., Novak, J., 1979. Headspace gas analysis by gas chromatography. *J. Chromatogr. A.*, 165, 141-165.



69. VITENBERG, A.G., Ioffe, B.V., 1989. Basic equations in continuous gas extraction and their application to headspace analysis. *J. Chromatogr. A.*, 471, 55-60.
70. CURVERS, J., Noy, Th., Cramers, C., Rijks, J., 1984. Possibilities and limitations of dynamic headspace sampling as a pre-concentration technique for trace analysis of organics by capillary gas chromatography. *J. Chromatogr. A.*, 289, 171-182.
71. HARPER, M., 2000. Review: Sorbent trapping of volatile organic compounds from air. *J. Chromatogr. A.*, 885, 129-151.
72. POOLE, C.F., Schuette, S.A., 1983. Isolation and concentration techniques for Capillary column GC analysis. *J. High Resolut. Chromatogr.*, 6, Oct, 526-549.
73. NAMIESNIK, J., 1988. Preconcentration of gaseous organic pollutants in the atmosphere. *Talanta*, 35, 567-587.
74. GRIMALT, J.O., Flesca, N.G., Castellnou, A., 1997. Refrigerated multibed adsorption in sampling and analysis of atmospheric light hydrocarbons at ppb(v/v) and sub ppb(v/v) concentrations. *J. Chromatogr. A.*, 778, 269-277.
75. MASTROGIACOMO, A.R., Pierini, E., Sampaulo, L., 1995. A comparison of the critical parameters of some adsorbents employed in trapping and thermal desorption of organic pollutants. *Chromatographia*, 41, Nov, 599-604.
76. SUPELCO Chromatography products for analysis and purification, 1999. *Supelco Chromatography Products*, 266.
77. HUCK, C.W., Bonn, G.K., 2000. Review: Recent developments in polymer - based sorbents for solid phase extraction. *J. Chromatogr. A.*, 885, 51-72.
78. DUNEMANN, L., Begerow, J., Bucholski, A., 1994. Sample preparation for trace analysis in *Ullmann's Encyclopedia of Industrial Chemistry*, volume editor Gunzler, H., VCH. Vol. B5, 84-89.
79. RAYMOND, A., Guiochon, G., 1975. The use of graphitized carbon black as a trapping material for organic compounds in light gases before GC-analysis. *J. Chromatogr. Sci.*, 13, 173-177.
80. LOVKVIST, P., Jonsson, J.A., 1987. Capacity of sampling and preconcentration columns with a low number of theoretical plates. *Anal. Chem.*, 59, March 15, 818-821.
81. BALTUSSEN, E., David, F., Sandra, P., Janssen, H.G., Cramers, C.A., 1997. A new method for sorptive enrichment of gaseous samples: Application in air analysis and natural gas characterization. *J. High Resolut. Chromatogr.*, 20, July, 385-393.
82. POOLE, C.F., Poole, S.K., 1991. *Chromatography Today*. Elsevier, Amsterdam, 735-840.
83. MOL, H.G.J., Janssen, H.G., Cramers, C.A., 1993. Use of open tubular trapping columns for on-line extraction-capillary gas chromatography of aqueous samples. *J. High Resolut. Chromatogr.*, 16, 413-418.

84. MORETTO, H.H., Schulze, M., Wagner, G., 1993. Silicones in *Ullmann's Encyclopedia of Industrial Chemistry*, editors Elvers, B., et al, VCH. Vol. A24, 64-69.
85. WELSCH, T., Teichmann, U., 1991. The Thermal immobilization of hydroxy-terminated Silicone phases in high-temperature-Silylated glass capillaries. A study of reaction mechanisms. *J. High Resolut. Chromatogr.*, 14, Mar, 153-159.
86. BALTUSSEN, E., David, F., Sandra, P., Janssen, H.G., Cramers, C.A., 1998. Capillary GC determination of amines in aqueous samples using sorptive preconcentration on polydimethylsiloxane and polyacrylate phases. *J. High Resolut. Chromatogr.*, 21, 645-648.
87. PAWLISZYN, J., 1997. *Solid Phase Microextraction - Theory and Practice*, Wiley-VCH, Canada.
88. LORD, H., Pawliszyn, J., 2000. Review: Evolution of Solid Phase Microextraction technology. *J. Chromatogr. A.*, 885, 153-193.
89. GROB, K., Habich, A., 1985. Headspace gas analysis: the role and design of concentration traps specifically suitable for capillary GC. *J. Chromatogr. A.*, 321, 45-58.
90. BURGER, B.V., Munroe, Z., 1986. Headspace gas analysis: Quantitative trapping and thermal desorption of volatiles using fused silica open tubular capillary traps. *J. Chromatogr. A.*, 370, 449-464.
91. BURGER, B.V., le Roux, M., Munroe, Z.M., Wilken, M.E., 1991. Production and use of capillary traps for headspace gas chromatography of airborne volatile organic compounds. *J. Chromatogr. A.*, 552, 137-151.
92. BURGER, B.V., le Roux, M., 1992. Headspace gas analysis: Comparison of the efficiency of thick film, ultra thick film, and activated charcoal Open tubular capillary traps for the concentration of volatile, airborne, organic compounds. *J. High Resolut. Chromatogr.*, 15, June, 373-376.
93. BLOMBERG, S., Roeraade, J., 1987. Preparative capillary gas chromatography II. Fraction collection on traps coated with a very thick film of immobilized stationary phase. *J. Chromatogr. A.*, 394, 443-453.
94. BLOMBERG, S., Roeraade, J., 1988. A technique for coating capillary columns with a very thick film cross-linked stationary phase. *J. High Resolut. Chromatogr.*, 11, June, 457-461.
95. BURGER, B.V., le Roux, M., Burger, W.J.G., 1990. Headspace analysis: A novel method for the production of capillary traps with ultra-thick stationary phase layers. *J. High Resolut. Chromatogr.*, 13, Nov, 777-779.
96. BALTUSSEN, E., David, F., Sandra, P., Janssen, H.G., Cramers, C.A., 1998. Sorption Tubes packed with polydimethylsiloxane: A new and promising technique for the preconcentration of volatiles and semi-volatiles from air and gaseous samples. *J. High Resolut. Chromatogr.*, 21, June, 332-340.

97. BALTUSSEN, E., David, F., Sandra, P., Janssen, H.G., Cramers, C.A., 1998. Retention model for sorptive extraction-thermal desorption of aqueous samples: application to the automated analysis of pesticides and polyaromatic hydrocarbons in water samples. *J. Chromatogr. A.*, 805, 237-247.
98. BALTUSSEN, E., den Boer, A., Sandra, P., Janssen, H.G., Cramers, C.A., 1999. Monitoring of nicotine in air using sorptive enrichment on polydimethylsiloxane and TD-CGC-NPD. *Chromatographia*, 49, 520-524.
99. Supelco Bulletin 923 - Solid Phase Microextraction: Theory and Optimization of Conditions, 1998. Sigma-Aldrich Co.1-8.
100. TIENPONT, B., David, F., Bicchi, C., Sandra, P., 2000. Headspace Sorptive extraction. *Riva Del Garda Chromatography Conference Proceedings CD-ROM*, 1-11.
101. HO, M.H., 1985. Generation of standard gaseous formaldehyde in test atmospheres in *Formaldehyde - Analytical chemistry and toxicology*, editor Turoski, V. Advances in chemistry and toxicology series, 210, 193-214.
102. GEISLING, K.L., Miksch, R.R., 1982. Generation of dry formaldehyde at trace levels by the vapour-phase depolymerisation of trioxane. *Anal.chem.*, 54, 140-142.
103. GODIN, J., Bouley, G., Boudene, Cl., 1978. Controlled formaldehyde atmospheres. *Analytical letters*, A11, 319-326.
104. DUMAS, T., 1982. Determination of formaldehyde in air by gas chromatography. *J.Chromatogr. A.*, 247, 289-295.
105. POOLE, C.F., Poole, S.K., 1991. *Chromatography Today*. Elsevier, Amsterdam, 844-848.
106. BEREZKIN, V.G., Drugov, Y.S., 1991. Gas chromatography in air pollution analysis. *Journal of Chromatography Library* -Elsevier, Germany. Vol. 49, 150-163.
107. NAMIESNIK, J., 1984. Generation of standard gaseous mixtures. *J. Chromatogr. A.*, 300, 79-108.
108. NISHIKAWA, H., Hayakawa, T., Sakai, T., 1986. Determination of micro amounts of acrolein in air by gas chromatography. *J. Chromatogr. A.*, 370, 327-332.
109. SCARANGELLI, F.P., O'Keefe, A.E., Rosenberg, E., Bell, J.P., 1970. Preparation of known concentrations of gases and vapours with permeation devices calibrated gravimetrically. *Anal. Chem.*, 42, 8 July, 871-876.
110. LUCERO, D.P., 1971. Performance characteristics of permeation tubes. *Anal. Chem.*, 43, 13 Nov, 1744-1749.
111. O' KEEFE, A.E., Ortman, G.C., 1966. Primary standards for trace gas analysis. *Anal. Chem.*, 38, May, 760-763.

112. DAVOLI, E., Rossi, O., Fanelli, R., 1993. Stable isotope permeation tubes for GC-MS analysis of VOC's in air. *J. High Resolut. Chromatogr.*, 16, 626-628.
113. STELLMACK, M.L., Street-Jnr, K.W., 1983. Permeation devices for high pressure gases. *Analytical letters*, 16(A2), 77-100.
114. McKELVEY, J.M., Hoelscher, H.E., 1957. Apparatus for preparation of very dilute gas mixture. *Anal. Chem.*, 29, 123.
115. ALTSHULLER, A.P., Cohen, I.R., 1960. Application of diffusion cells to the production of known concentrations of gaseous hydrocarbons. *Anal. Chem.*, 32, 802-810.
116. CHROMPACK - CP-4010 PTI/TCT User Manual, CHROMPACK, The Netherlands.
117. HP 5890 A Gas Chromatograph, 1986. *HP Reference Manual*. Vol. 1, section 10-5.
118. SANDRA, P.J.F., 1994. Gas Chromatography in *Ullmann's Encyclopedia of Industrial Chemistry*, executive editor Gerhartz, W., VCH. Vol. B5, 181-236.
119. SKOOG, D.A., Leary, J.J., 1992. An introduction to chromatographic separations in *Principles of Instrumental Analysis*. 4th Edition, Saunders College Publishing, Florida, U.S.A. 579-625.
120. POOLE, C.F., Poole, S.K., 1991. *Chromatography Today*. Elsevier, Amsterdam, 260-264.
121. BEREZKIN, V.G., Drugov, Y.S., 1991. Gas chromatography in air pollution analysis. *Journal of Chromatography Library* -Elsevier, Germany. Vol. 49, 28-29.
122. SCANLON, J.T., Willis, D.E., 1985. Calculation of flame ionization detector relative response factors using the effective carbon number concept. *J. Chromatogr. Sci.*, 23, 333-340.
123. TONG, H.Y., Karasek, F.W., 1984. Flame Ionisation Detector response factors for compound classes in quantitative analysis of complex organic mixtures. *Anal.chem.*, 56, 2124-2128.
124. YIERU, H., Qingyu, Q., Weile, Y., 1990. Characteristics of Flame Ionisation Detection for the quantitative analysis of complex organic mixtures. *Anal.chem.*, 62, 2063-2064.
125. SILVERSTEIN, R.M., Webster, F.X., 1998. Mass Spectrometry in *Spectrometric Identification of Organic Compounds*. 6th Edition, John Wiley & Sons, Inc, New York, U.S.A. 2-69.
126. SKOOG, D.A., Leary, J.J., 1992. Mass Spectrometry in *Principles of Instrumental Analysis*. 4th Edition, Saunders College Publishing, Florida, U.S.A. 420-459.

127. POOLE, C.F., Poole, S.K., 1991. *Chromatography Today*. Elsevier, Amsterdam, 848-850.
128. CANCELLA, D.A., Que-Hee, S.S., 1992. Review: O-(2,3,4,5,6-Pentafluorophenyl) methylhydroxylamine hydrochloride: a versatile reagent for the determination of carbonyl-containing compounds. *J. Chromatogr. A.*, 627, 1-16.
129. MUNCH, J.W., Munch, D.J., Winslow, S.D., 1998. A User's guide to aldehyde analysis using PFBHA derivatisation and GC-ECD detection : Avoiding the pitfalls. *Proc-Water Qual. Technol. Conf. [computer optical disk]*, 898-913.
130. SPITELLER, G., Kern, W., Spitteller, P., 1999. Review: Investigation of aldehydic lipid peroxidation products by gas chromatography-mass spectrometry. *J. Chromatogr. A.*, 843, 29-98.

Table 3.1 A comparison of various adsorbents [19,71-75,79,82]

	ADSORBENT	COMPOSITION	SURFACE AREA (m <sup>2</sup> /g)	PORE DIAMETER (nm)	APPLICATIONS	ADVANTAGES	DISDAVANTAGES
CARBON - BASED	Activated carbon Anasorb 747	Coconut/petroleum based charcoal	800-1000	2.0 / 1.8-2.2	Non-specific i.e. Most organic and inorganic compounds. Non-polar, polar, reactive and/or volatile. Mercury-vapour.	Cheap, efficient, permanent gases not adsorbed – H <sub>2</sub> , N <sub>2</sub> , O <sub>2</sub> , CO, CH <sub>4</sub> . Anasorb absorbs less H <sub>2</sub> O and desorption efficiencies for polar compounds are improved.	Polar compounds irreversibly adsorbed. Incomplete desorption. H <sub>2</sub> O reduces sorption of other compounds. Catalytic activity. Reacts with oxygen or sulphur derivatives.
	Graphitised carbon black Carbotraps	Pre-treated carbon black under vacuum and inert gas/ reductive atmosphere at 3000°C			Non-specific, as above.	No irreversible adsorption sites. No retention of H <sub>2</sub> O and low molecular mass compounds (CO <sub>x</sub> , CH <sub>4</sub> )	High desorption temperatures (400°C) required. Tiny particles of carbon can enter desorption unit.
	Carbon molecular sieves Carbosieves	Thermally decomposed polymer eg. polyvinyl chloride			Adsorption of hydrocarbons and low-boiling C1-C4 hydrocarbons, methyl formate and alkyl mercury compounds.	High capacity for small volatile molecules. Suitable for thermal desorption.	Inefficient retention of polar compounds. Solvent with high heat of adsorption required for displacement of adsorbates. H <sub>2</sub> O can block cryotrap.

<b>INORGANIC</b>	Silica gel	Si-OH groups on surface	100-800	2-4	Polar compounds from air. Amines, halogens, oxygen derivatives, organo-metallics, MeOH, HCHO and DMF. Silica gel is often used as a substrate for coating with derivatising reagents.	Cooling the sorbent allows trapping of C1-C4 hydrocarbons	Hydrophilicity decreases sorption capacity. Thermal desorption difficult. Silica gel retains H <sub>2</sub> O and CO <sub>2</sub>
	Aluminium oxide	Al <sub>2</sub> O <sub>3</sub>					
	Molecular sieves	Zeolites	Varied	Varied	Toxic inorganic compounds. Small conc. of H <sub>2</sub> S	Thermally desorbed at 240°C/extract with ice H <sub>2</sub> O	Organic compounds are irreversibly adsorbed excl. HCHO, acrolein and certain S-compounds. H <sub>2</sub> O block cryotrap
<b>POROUS POLYMERS</b>	Tenax	2,6-diphenyl-p-phenylene oxide	19	140	Organic bases, neutral and high boiling compounds. Chlorohydrocarbons. Support for derivatising reagents. Broad trapping range of compounds of varied molecular mass and polarity.	Tenax has a high thermal limit 350-400°C. Ideal for thermal desorption.	Not suited to solvent extraction due to low capacity for volatiles and is incompatible with many solvent systems.
	XAD-2 (Amberlite, Chromosorb 102)	Copolymer of 2,6-diphenyl-p-phenylene oxide in which one moiety is styrene or ethylvinylbenzene and the other monomer a polar vinyl compound.	300-400	8.5	Nitroso-compounds and polychlorinatedbiphenyls, aromatic, aliphatic nitro-compounds.	XAD's, Porapak and Chromosorbs come in wide ranges of polarity. Chromosorb	
	Porapak		600-650	7.5	Depending on polarity. Non-polar to polar compounds can be adsorbed. Chromosorbs adsorb inorganic compounds	106 greater capacity than tenax, suited to thermal desorption.	Polar Porapaks retain H <sub>2</sub> O and require great amount of energy to remove sorbates. Can't withstand high temp.
	Chromosorb101, 103, 104, 106, 108.		50 varied	300-400 varied			

## APPENDIX 2

### CALCULATION OF GAS CONCENTRATIONS

The gas standard in a dilution system provides a certain concentration of gas. The concentration,  $C$ , with units part-per-million volume/volume (ppm v/v) can be calculated from the following equation:

$$C = [f / (f + F)] \times 10^6 \quad (1)$$

Where  $f$  is the permeation/diffusion rate with units ml/min.  $F$  is the flow rate of the diluting gas in ml/min. Equation 1 can be simplified, since  $F \gg f$ , to:

$$C = (f / F) \times 10^6 \quad (2)$$

The permeation/diffusion rate, however, is usually determined gravimetrically in ng/min. It is important then to convert mass of gas to volume of gas, using the following equation:

$$f = (22.4 / M) \times (T / 273) \times (760 / P) \times r \times 10^{-6} \quad (3)$$

The molar gas volume is given as 22.4 L/mol.  $M$ , is the molecular mass of the compound in g/mol.  $T$ , is the absolute temperature in Kelvin (K) at which permeation/diffusion is occurring.  $P$ , is the pressure in mm/Hg, at which permeation/diffusion rate is measured and  $r$ , is the permeation/diffusion rate in ng/min.



Equation 3 is substituted into equation 2 resulting in:

$$C = (22.4 / M) \times (T / 273) \times (760 / P) \times (r / F) \quad (4)$$

At 25°C and atmospheric pressure (760mmHg), equation 4 reduces to:

$$C = (24.45 / M) \times (r / F) \quad (5)$$

From equation 4 and 5 it can be seen that the concentration of the standard is dependant on the diluting gas flow rate. The formaldehyde gas concentration, in an 80°C oven, will be worked out below using equation 4.

M (g/mol)	T (K)	P (mmHg)	r (ng/min)	F (ml/min)	C (ppm v/v)
30	353	760	1.333	10	0.1287

The acetaldehyde concentration at 25°C, is worked out similarly using equation 5.

M (g/mol)	r (ng/min)	F (ml/min)	C (ppm v/v)
44	40	10	2.218

To convert the units ppm (v/v) for a gas z, to  $\mu\text{g}/\text{m}^3$  ie. ng/L, the following method can be used:

$$1 \text{ ppm (v/v) } z = \frac{1 \text{ L } z}{10^6 \text{ L air}} \quad (6)$$

assuming the ideal gas law is valid under ambient conditions, 25°C and 760mmHg,  
then:

$$\begin{aligned} 1 \text{ ppm (v/v) } z &= \frac{(1 \text{ L } z / 22.4)}{(10^6 \text{ L})} \times M(z) \times 10^6 \mu\text{g/g} & (7) \\ &= 40.9 \times M(z) \mu\text{g/m}^3 \text{ or ng/L} \end{aligned}$$

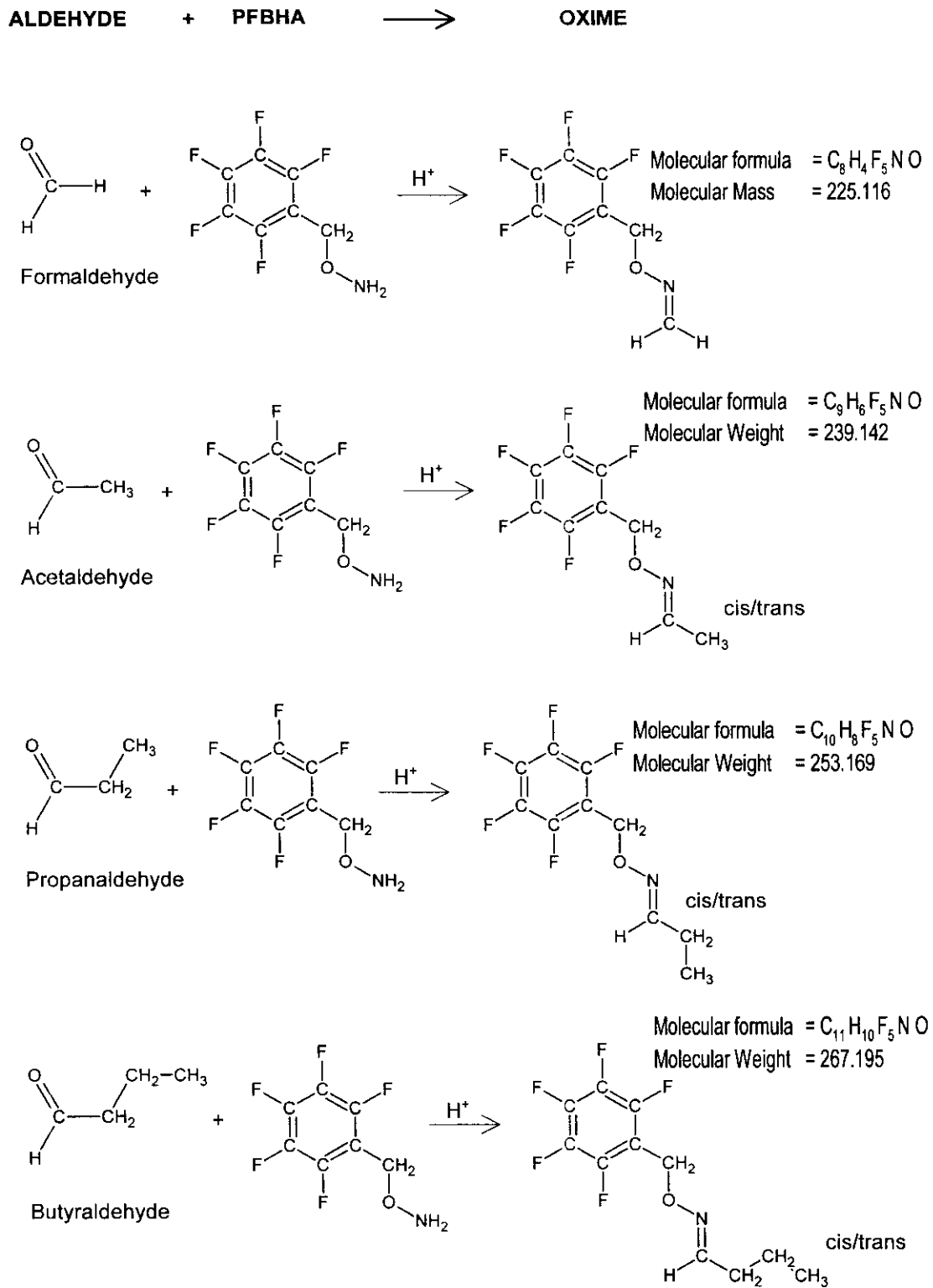
[1 m<sup>3</sup> = 1000 L]

For example, a 1 ppm (v/v) HCHO atmosphere is equivalent to 123 ng/L or 1.23 ng/ml.

With these units of measurement one can easily determine the concentration of the gas in an atmosphere, and if the collection volume is known, the mass of compound collected can also be determined.

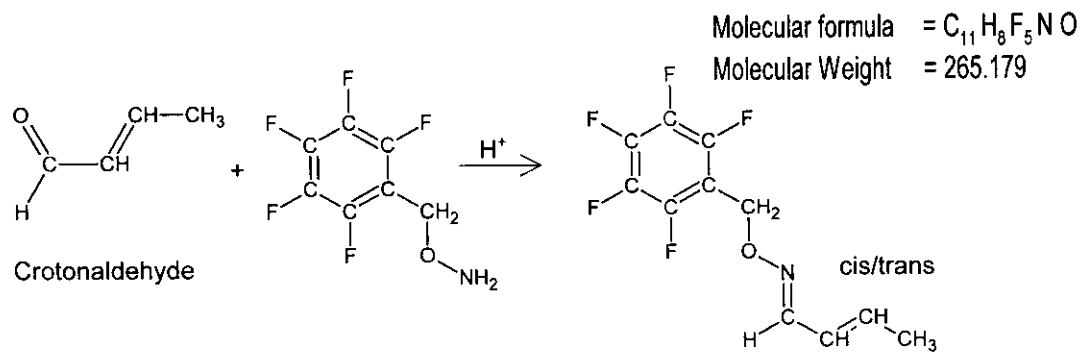
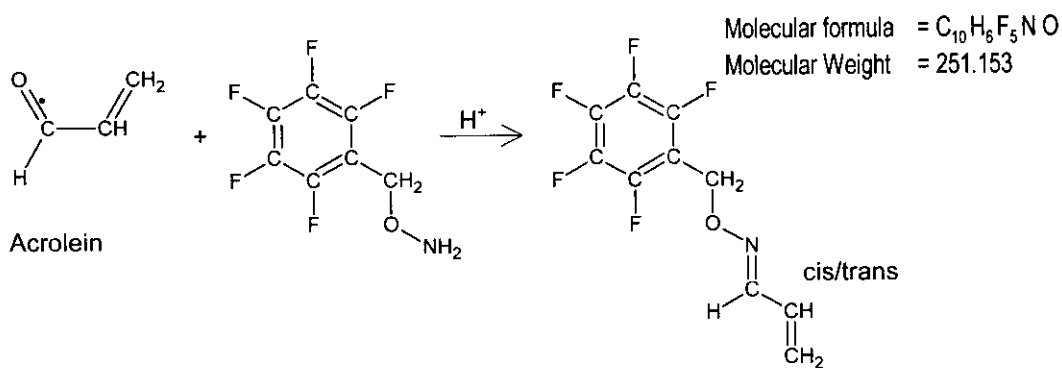
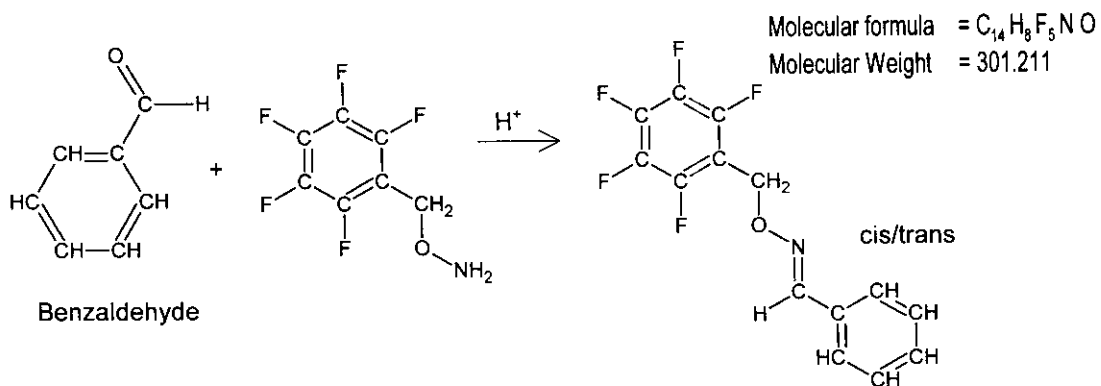
## APPENDIX 3

### PFBHA - ALDEHYDE REACTION SCHEMES



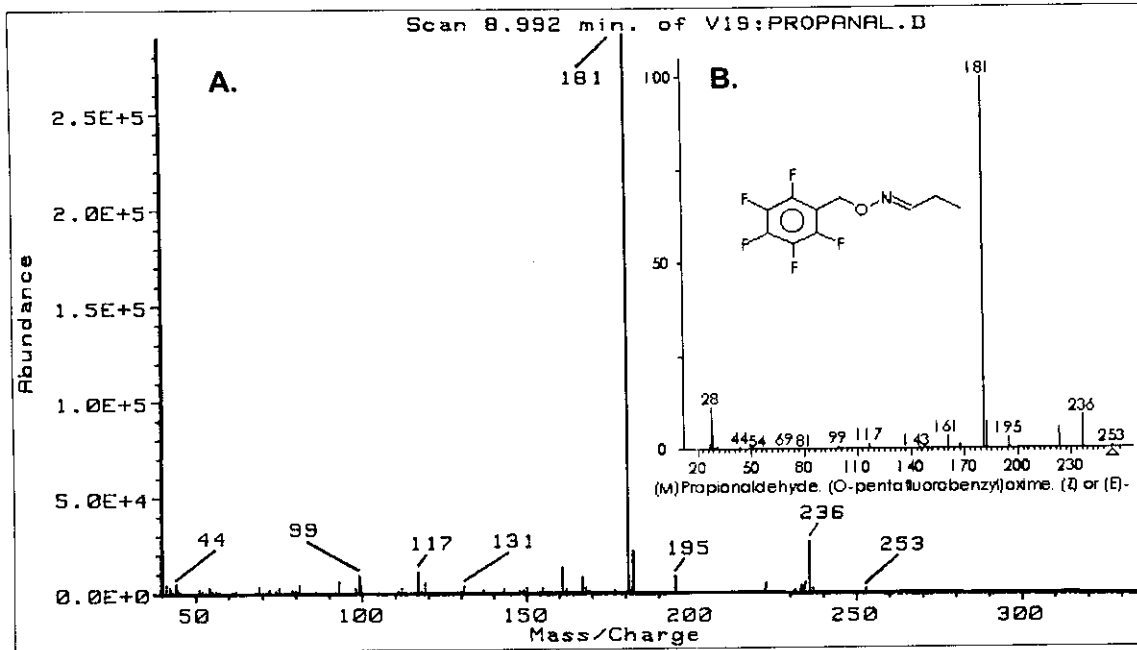
## APPENDIX 3

(continued)

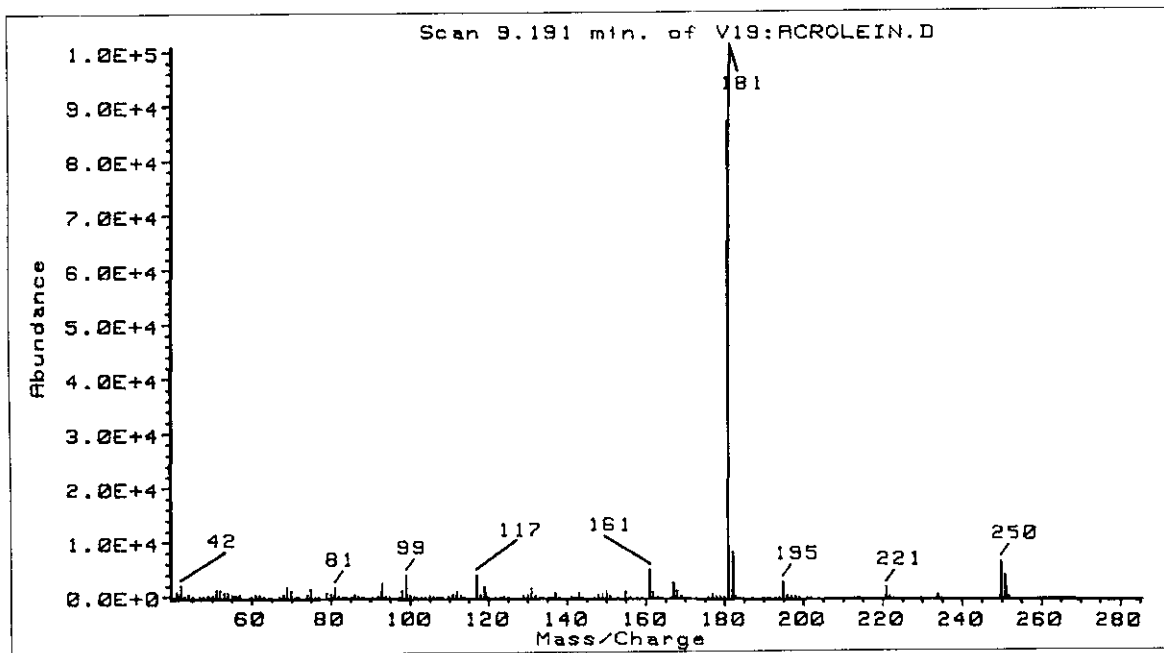


## APPENDIX 4

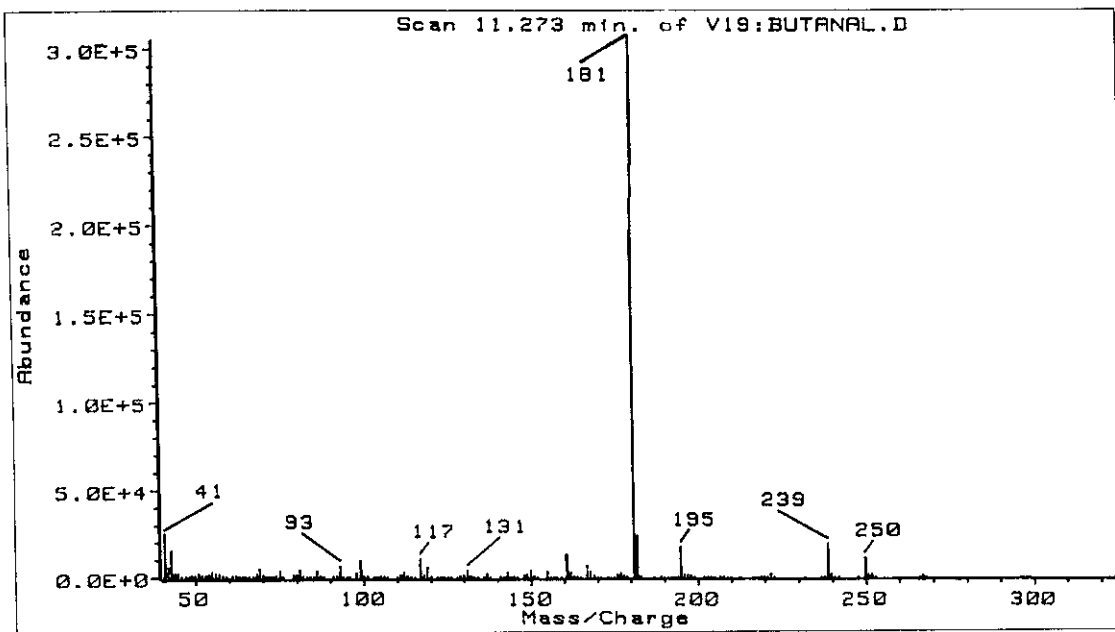
### EI-MASS SPECTRA OF PFBHA ALDEHYDE-OXIMES



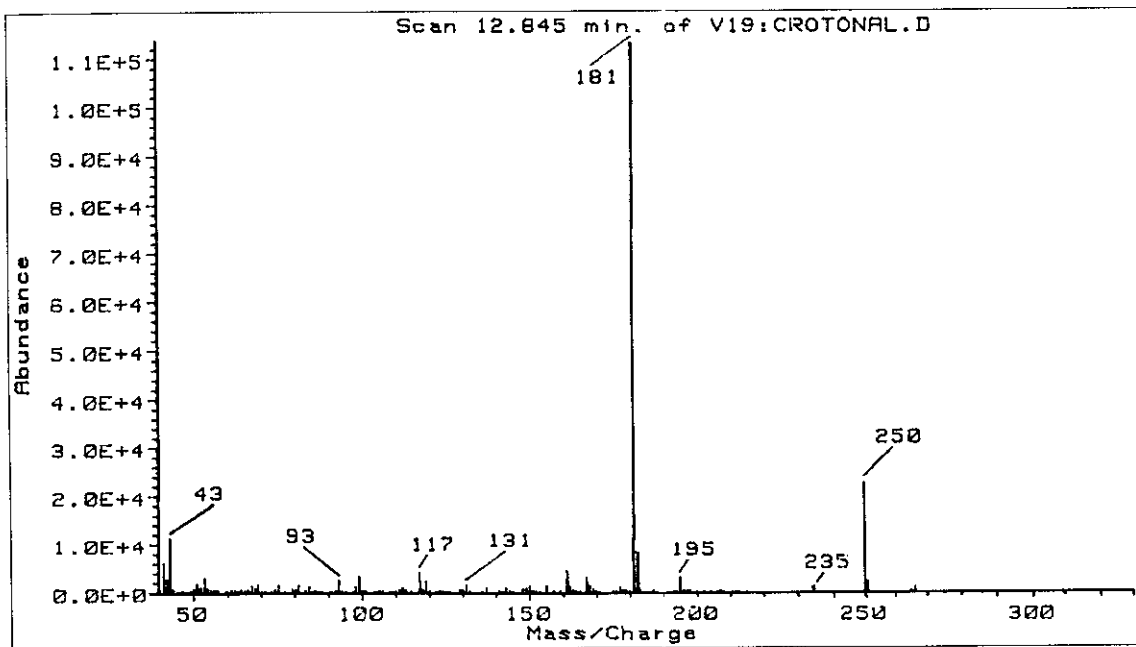
Appendix 4.1. **A.** Obtained EI-Mass spectrum of the propanal-oxime.  
**B.** NIST library EI-Mass spectrum of the propanal-oxime.



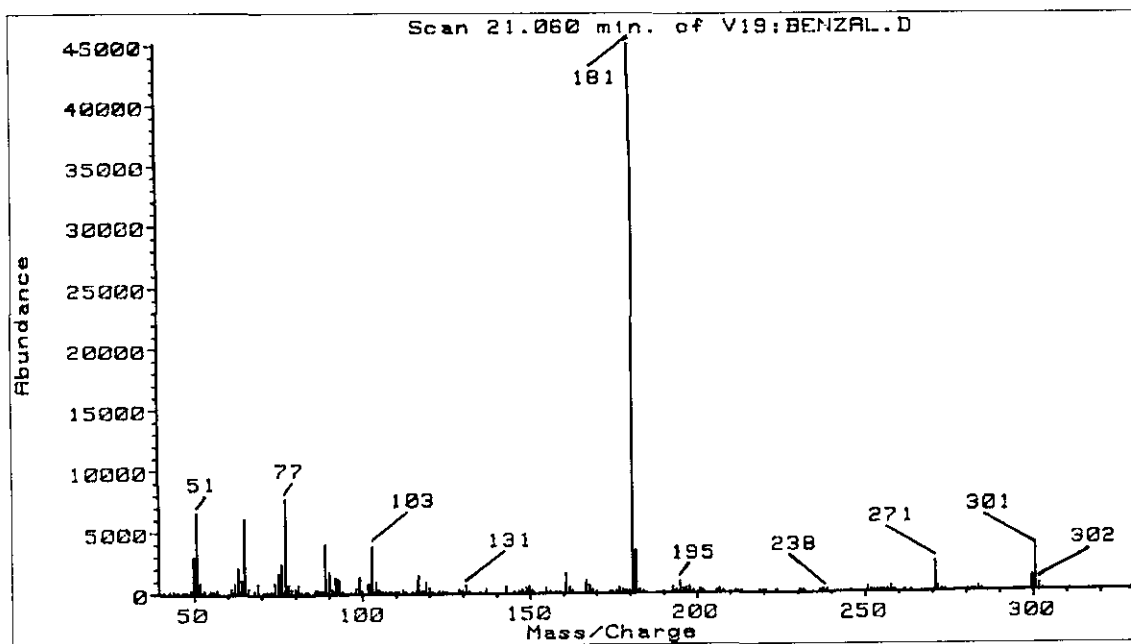
Appendix 4.2. Obtained EI-Mass spectrum of acrolein-oxime.



Appendix 4.3. Obtained EI-Mass spectrum of butanal-oxime.



Appendix 4.4. Obtained EI-Mass spectrum of crotonal-oxime.



Appendix 4.5. Obtained EI-Mass spectrum of the benzaldehyde-oxime.